CHALMERS

Installation of Allfa Europe Premium Stretcher

A Validation of a Stretcher for Search and Rescue Helicopters

Bachelor's Thesis within Mechanical Engineering

FRÖDELL LINA
HAMZA MEDIN
HELLMAN CASSANDRA
JOHANSSON DAVID
KARLSSON HENRIC
MAGNUSSON LISA

PPUX03-14-29
Department of Mechanical Engineering
Division of Product and Production Development
CHALMERS UNIVERSITY OF TECHNOLOGY
Gothenburg, Sweden 2014
Bachelor's Thesis 2014:1

Installation of Allfa Europe Premium stretcher
A validation of a stretcher for search and rescue helicopters
Bachelor's Thesis within Mechanical Engineering

FRÖDELL LINA
HAMZA MEDIN
HELLMAN CASSANDRA
JOHANSSON DAVID
KARLSSON HENRIC
MAGNUSSON LISA

Kandidatarbete/Institutionen för produkt- och produktionsutveckling,
Chalmers tekniska högskola 2014:1

Department of Mechanical Engineering
Division of Product and Production Development
Chalmers University of Technology
SE-412 96 Göteborg
Sweden
Telephone: + 46 (0)31-772 1000

Cover:
Allfa Europe Premium stretcher
(http://www.fernonorden.se/ferno/frontend/mediabank/676/allfa-eu-2008-med-ny-armst-d-jpg-cmyk˙ml.jpg)

Preface

This bachelor's thesis was initialised by the company Heli-One and carried out during the period January to May in 2014 at the division of Product and Production Development at Chalmers University of Technology.

We would like to thank Heli-One for giving us this opportunity to work with an actual project and at the same time improves our engineering competences. We are all very grateful for the welcoming in Stavanger and for the introduction of the project. We would specially like to thank Anders Pettersson and Cato Strandskog at Heli-One for their guidance and help throughout the project, it have been truly appreciated.

Our supervisor, Sara Caprioli, has been a big support for us and helped throughout the project and we thank her for her interest and dedication. We would also like to thank our examiner, Kristina Wärmefjord, for the guidance.

We appreciate the welcoming and participating from the manufacture Ferno Norden and for lending us the stretcher. We are also grateful to the ambulance staff in Sisjön and the helicopter ambulance staff in Säve for answering all our questions and demonstrate how they work with the stretcher. We would also like to thank a search and rescue contact for answering to our questions.

Finally, we would like to thank everyone who helped us during this project.

Gothenburg May 2014

Lina Frödell, Medin Hamza, Cassandra Hellman,
David Johansson, Henric Karlsson & Lisa Magnusson

Abstract

The aim of this project was to determine whether the stretcher Allfa Europe Premium would be able to meet the requirements in accordance to the regulations of European Aviation Safety Agency for installation in a search and rescue helicopter. To fulfil the regulations four different tasks had to be done; make a 3D-model of the stretcher, validation for certification, strength analysis and development of a concept for a fixation system. The 3D-model was created by using reverse engineering through disassembly and analysis of the stretcher. The computational model employed for strength analysis of the stretcher features only the load bearing part. To validate the trustworthiness of the numerical simulation handbook calculations based on linear elastic beam theory were performed. The results from the numerical simulation and handbook calculations show that the stretcher withstands the loads according to the regulations. Apart from the requirements on the loads, there are other requirements that the stretcher must fulfil. The paragraphs stating those requirements were investigated and formulated and are a basis for the certification. This combined with further analysis indicates that the stretcher would be able to fulfil certification requirements in the future. As a final task a fixation system for installation of the stretcher in a helicopter was developed.

Sammandrag

Projektets syfte var att undersöka huruvida båren Allfa Europe Premium uppfyller de krav som ställs av *European Aviation Safety Agency* för att kunna installera den i en *search and rescue*-helikopter samt att skapa en fullt dynamisk 3D-modell. Projektet omfattade fyra olika deluppgifter där samtliga genomfördes med hänsyn till regelverket. Uppgifterna var följande: Ta fram en 3D-modell av båren, genomföra en validering inför certifiering, utföra en hållfasthetsanalys samt utveckla ett koncept för en infästningsanordning. 3D-modellen togs fram med hjälp av *reverse engineering* genom att demontera och analysera en befintlig bår. Den lastbärande delen av 3D-modellen importerades till ett simuleringsprogram där en kontroll utfördes för att undersöka om strukturen klarar av de laster som krävs. Beräkningarna som utfördes i simuleringsprogrammet validerades med handberäkningar för att styrka trovärdigheten. Resultatet av beräkningarna visar att båren klarar av de påfrestningarna som anges i regelverket. Förutom reglerna om lastfallen tar regelverket upp flera andra paragrafer som båren måste klara av. Dessa undersöktes och lade grunden för en validering som senare kan utvecklas för att göra en certifiering av båren. Resultatet av valideringen indikerar att båren kommer klara en framtida certifiering. Vid sidan av detta togs ett förslag fram på ett infästningssystem för att kunna fästa båren i helikoptern.

Notations

This is a list of all the abbreviations and letters used in the thesis.

Abbreviations

ANSYS	Engineering simulation software
CAD	Computer-aided design
CES	Cambridge Engineering Selector
CS	Certification Specification
EASA	European Aviation Security Agency
Eurocode 9	DD ENV 1999-1-1:2000
FAA	Federal Aviation Agency
FEM	Finite element method
ISO	International Organization for Standardization
LCA	Life Cycle Assessment
MMPDS	Metallic Materials Properties Development and Standardization
RE	Reverse Engineering
SAR	Search and Rescue

Roman upper case letters

A	[mm^2]	Gross area of the cross section
E	[MPa]	Young's modulus
I	[mm^4]	Moment of inertia
K	[-]	Effective length factor
L	[mm]	Length of beam
L_{cr}	[mm]	Critical length
M	[Nmm]	Moment in general
N	[N]	Elastic critical load; axial force
N_{Ed}	[N]	Design value of the compressive force
W	[mm^3]	Section modulus

Roman lower case letters

b	[mm]	Width
d	[mm]	Height
ey	[mm]	Eccentricity in Y direction
ez	[mm]	Eccentricity in Z direction
f_0	[MPa]	Characteristic strength for bending and overall yielding in tension and compression
$f_{0.2}$	[MPa]	0.2% proof strength
f_a	[MPa]	Characteristic strength for the local capacity of a net section in tension or compression

f_u	[MPa]	Ultimate tensile strength
g	[mm/s^2]	Gravitational acceleration 9810
h	[mm]	Cross-sectional height
i	[mm]	Radius of gyration
r_i	[mm]	Cross section radius of gyration
t	[mm]	Thickness of cross section

Greek upper case letters

χ	[-]	Reduction factor

Greek lower case letters

α	[-]	Shape factor; Imperfection factor
β	[-]	Slenderness parameter
β_{ref}	[-]	Buckling factor
γ_{M1}	[-]	Partial safety factor
δ	[mm]	Deflection
ε	[-]	$\varepsilon = \sqrt{250/f_0}$
η	[-]	Efficiency
κ_f	[-]	Fitting factor
λ	[-]	Slenderness ratio
λb_0	[-]	Limit of the horizontal plateau
υ	[-]	Poisson's ratio
ξ	[-]	Factor of the distance to the deflection point
ρ	[kg/mm^3]	Density
σ	[MPa]	Stress
ϕ	[-]	Rotation; Slope; Ratio
ω	[-]	Beam columns without localized weld factor

Table of Contents

1 Introduction

For rescue operations in rough terrains where ambulances cannot access, a helicopter may be the only solution. The helicopter is therefore equipped with all required materials equivalent to an ambulance, such as a stretcher. Allfa Europe Premium, shown in Figure 1, is the most common stretcher in Swedish ambulances; it is therefore desirable to investigate its usage and adaptability in helicopters.

Figure 1. This is the Allfa Europe Premium in upright position.

1.1 Background

The project is a collaboration between students at Chalmers University of Technology and the companies Heli-One (Stavanger, Norway) and Ferno Norden (Trollhättan, Sweden). Heli-One is specialised in designing and maintaining parts for helicopters for clients worldwide, they are interested in making the stretcher Allfa Europe Premium a standard in their SAR helicopters. Ferno Norden is the manufacturer of the stretcher and is interested in expanding the area of usage for the stretcher. Ferno Norden does not possess enough background data to launch the stretcher in the SAR helicopter industry. The stretcher has not yet been tested with respect to the specification, CS 29, provided by EASA.

EASA regulates the standards for safety and environmental protection in civil aviation in Europe. This includes that everything in the aviation industry, from hot air balloons to large aircrafts and all of their components have to be certified according to EASA's regulation.

1.2 Aim

The aim of this bachelor's thesis is to develop a 3D-model with ergonomic attributes of the Allfa Europe Premium stretcher and determine whether the stretcher fulfils EASA's requirements in CS 29, for installation in SAR helicopters. Significant paragraphs for this project were provided by Heli-One, see Appendix B.

1.3 Assignment

In order to analyse the stretcher's suitability, the following tasks are covered:

- Development of a 3D-model of the stretcher with all its dynamic functions.
- Validation for certification of the stretcher according to EASA regulations.
- Strength analysis of the stretcher with respect to given ultimate static loads using finite element method. The analysis includes handbook calculations based on linear beam theory and numerical simulations.
- Identify and analyse different fixation systems and develop a final fixation system concept for the stretcher.

1.4 Limitations

The strength analysis does not take fatigue and wear issues or vibrational and dynamic loads into account. The model used for the numerical simulations features the load bearing part of the stretcher, see Figure 2.

Figure 2. The load bearing part

The development of the fixation system does not take the fixation between the system and the helicopter into account. By not taking a certain helicopter interface into account one expands the opportunity of system installation into several helicopter types.

1.5 Disposition

The project is divided into four sections, it has been appropriate to divide the report after these sections to make it as easy to read as possible. Every section has the same structure with its own introduction/theory, method, result and discussion. Finally, the report includes a discussion, conclusion and recommendation for the whole project.

The four sections are:

- Chapter 2 - 3D-Modelling
- Chapter 3 - Validation for Certification
- Chapter 4 - Strength Analysis
- Chapter 5 - Fixation System

1.6 Method

How to work with 3D-modelling is very different from how to perform a strength analysis therefore follows a short introduction of the methods below. A more detailed method is presented in each chapter.

1.6.1 3D-modelling

The 3D-model is developed through reverse engineering; a real full-scale stretcher provided by Ferno Norden was used as background material for sizes, shapes and functions of the stretcher to be represented in the model. The CAD software used for this was Autodesk Inventor 2014.

1.6.2 Validation for EASA

The validation of the stretcher is achieved by detailed studies of the EASA regulations chapter CS-29, Large Rotorcrafts, book 1 and book 2. Book 1 describes the paragraphs and book 2 describes how the paragraphs should be interpreted. FAA, which is the corresponding American version of EASA, is used as a complement.

1.6.3 Strength Analysis

According to EASA the stretcher has to withstand loads in several directions and in different conditions due to the different scenarios that the helicopter can be subjected to in case of crash landing or safety landing. The strength analysis includes handbook calculations as well as numerical simulations, following directives from Heli-One. Linear buckling analysis with respect to critical loads is also performed. The method for the calculations follows design practices according to linear beam theory and Eurocode 9[1]. The software used for the numerical stress-analysis was Autodesk Mechanical Simulations 2014.

1.6.4 Fixation System

In order to fulfil the EASA requirements in CS 29, the stretcher needs to be fastened inside the helicopter in order to not cause any injuries on occupants or damage to the surrounding structure. The fixation system is developed both by conventional engineering and reverse engineering, which includes both searching for existing products on the market and through generating new ideas. Conventional engineering and Reverse engineering were obvious chosen methods for this part of the project because they are commonly known for product development.

[1] British Standards Institution, *Eurocode 9*, DD ENV 1999-1-1:2000

2 3D – Modelling

The manufacturing company, Ferno Norden needs a 3D-model of the stretcher for demonstration to their customers. They also lack models of the individually components, which can be necessary when searching for spare parts and for maintenance. Heli-One develops the interior for the SAR helicopter and is therefore interested in implementing the 3D-model of stretcher in the SAR interior. This chapter describes the process of developing the 3D-model.

2.1 Method

A full-sized stretcher, lend by Ferno Norden was used as the base for creating the 3D-model. All different parts of the stretcher were constructed in the 3D-modelling program *Autodesk Inventor 2014* and then assembled to form a complete model.

The stretcher was disassembled to identify all the individual parts. As the stretcher consists of over 150 unique parts it required a system to keep track of all these. All of the individual parts obtained its own article number. The Bill of Material, BOM, illustrates a list of these parts. The list was created with the software BOM Tools Pro. Drawings of every single component except from screws, nuts and plates were made as a complement.

Each part was separately created in the 3D-model program and later assembled. Constrains were added to assemble the stretcher and make it fully dynamic. Information about materials for the critical components was provided by the manufacturer. For parts where no material information was provided, assumptions were made based on material properties. Measurements of the components were made by a calliper, which resulted in relatively large tolerance for the dimensions. This will be discussed in chapter 2.2. Working with this type of method is called reverse engineering and the philosophy behind this is described as below:

"In the fields of mechanical engineering and industrial manufacturing the term Reverse Engineering refers to the process of creating engineering design data from existing parts and/or assemblies. While conventional engineering transforms engineering concepts and models into real parts, in the reverse engineering approach real parts are transformed into engineering models and concepts."[2]

2.2 Tolerances

Tolerances are essential to the design data because it immediately affect the manufacturing of the part. The reverse engineering design will in most cases differ from the original part that was examined in the beginning, therefore the importance of tolerances. High geometrical and dimensional precision directly indicates higher quality to the product but

---

[2] Kaisarlis, George J. *A Systematic Approach for Geometrical and Dimensional Tolerancing in Reverse Engineering,* 2012

increases the cost.[3]

Two different types of tolerances had to be considered; manufacturing tolerance and measurement tolerance. ISO standard tolerances were not considered due to inaccessibility. When a vernier calliper and a steel rule were used, an accuracy of 1mm was achieved on non-critical dimensions. The critical dimensions, such as the cross sections on the beams, were measured with a dial calliper with an accuracy of 0.5mm.

The stretcher may contain components with a wider manufacturing tolerance than measurement tolerance. According to the manufacturer almost every manufacturing tolerance are narrower than the measurement tolerances, 1mm for non-critical components and 0.5mm for critical components.

2.3 Functions

The stretcher is versatile and has many different functions that facilitate for the paramedics and also make it more comfortable for the patient. Ergonomic attributes were included in the 3D-model and are described below. Pictures of the parts and functions are presented in Appendix A and Appendix H.

- Both the backrest and footrest are height adjustable so that the patient can sit and lay in different positions.
- Flywheels and assistant wheels are installed to make it easier to move and run the stretcher on rough ground.
- Adjustable handles both in front and back of the stretcher. They can be adjusted for every paramedic that is carrying the stretcher and thereby facilitate their work.
- A yoke is installed so that the paramedics easier can lift the stretcher when walking in staircases.
- Side handles used when the stretcher needs to be lifted by several people.
- Armrests for the patient.

2.4 Drawings

Drawings of all parts except nuts, screws and plates were made. They were extracted from the 3D-models according to ISO standard with guidelines from Heli-One. The dimensions of the drawings were made with baseline dimension.

2.5 Results

This part of the project resulted in a 3D-model including all of the functions described in

---

[3] Kaisarlis, George J. *A Systematic Approach for Geometrical and Dimensional Tolerancing in Reverse Engineering,* 2012

chapter 2.3. A movie with all the dynamic features was made based on the 3D-model. Figure 3 shows the complete 3D-model of the stretcher. The Bill of Materials in Appendix H includes pictures of every unique part of the stretcher.

Figure 3. The complete model without mattress and belts compared with the real life stretcher.

The drawings of the different parts are presented in Appendix I.

2.6 Discussion

Different callipers were used for measurement of the different parts of the stretcher. The main beams were measured with a steel rule because no calliper was long enough. The measuring instruments used and the human factors affect the accuracy of the 3D model. Every part of the stretcher was measured and mostly modeled for itself by different persons. When the parts and components later were assembled they did not always adapt correctly. Therefore some parts were altered to fit together while other parts were measured again. This means that the measures on the stretcher were regulated dependently on each other and not always dependently on the real life stretcher. The fewer people that works with the measurement and modelling; the more resembling result for the different parts. If a part would be measured several times, a mean value could be estimated and the measurement would be more accurate. Consequently the choice of method could interfere with the finishing result. Although the modification were minor and therefore the resulting 3D-model was still considered reliable.

3 Validation

The stretcher has to be certified according to the certification specification, CS, chapter 29 in EASA, in order to be installed in a helicopter. The certification has to be executed by the agency or by an authorized company such as Heli-One. This chapter provides a preliminary validation that could be used in a certification process.

3.1 Method

The paragraphs relevant for the stretcher are described in Appendix B. The selected paragraphs were carefully studied and construed using AC 29, Advisory Circular from FAA that describes how to interpret the paragraphs in CS 29. In order to ensure that all paragraphs were reviewed, a table was made where each paragraph can be ticked off if the requirement was met. The same requirements were fulfilled by different paragraphs in certain cases and were therefore referred to each other. The conclusions and recommendations can be used by the authorized company later in the certification process. Recommendations are implemented for cases when the stretcher does not qualify or need additional tests to ensure its suitability in the helicopter. The performed controls were to examine the material properties both analytically and with calculations to determine whether it is within the range of the requirements. Therefore it was necessary to use data from strength analysis, which is presented in chapter 4.

3.2 Paragraph Study

The paragraphs in EASA, CS 29, could sometimes be ambiguous and to determine how the paragraphs should be interpreted they were discussed in order to come to conclusions. Even regularly contact with Heli-One was held to make sure that the paragraphs was correctly interpreted. Daily discussions were held to make sure all calculations were performed properly and right forces were used according to the paragraphs.

3.3 Results

Table 1 summarises the validation result with respect to the strength analysis and discussions.

Table 1. Result of the validation

§	Amd.	Title	MC	Compliance Statement and/ or Doc. Ref.
C		**STRENGTH REQUIREMENTS**		
		GENERAL		
29.301	3	Loads	MC2 MC8	Calculations confirmed that the structure will withstand the static ultimate loads. The ultimate loads are described in CS 29.561b. For calculations see chapter 4

§	Amd.	Title	MC	Compliance Statement and/ or Doc. Ref.
29.303	3	Factor of safety	MC0	Calculations in chapter 4 used ultimate loads, which mean that the factor of safety was included.
29.305	3	Strength and deformation	MC2 MC8	The results show that the structure withstands the ultimate loads without significant plastic deformation.
29.307	3	Proof of structure	MC2 MC8	(a) Each critical loading condition was taken into account through calculations in chapter 4. All critical loads in this case were those mentioned in CS 29.561b.
		FLIGHT LOADS		
29.321	3	General	MC0 MC2	The loads used in calculations, see chapter 4, were assumed to act normal to the longitudinal axis, see Figure 7. The forces used were those mentioned in CS 29.561b.
29.337	3	Limit manoeuvring load factor	MC0	Since fatigue was not considered no calculations for these cyclic loads were made.
		EMERGENCY LANDING CONDITIONS		
29.561	3	General	MC2 MC8	Calculations with loads mentioned in part b in the paragraph were made and are presented in chapter 4. The calculations show that the structure can support the ultimate loads without failure.
D		**DESIGN AND CONSTRUCTION**		
		GENERAL		
29.601	3	Design	MC6	(a) Similar stretchers are already used in ambulance helicopters, see Figure 4, and therefore the structure has proved its reliability. (b) Since there were no questionable design features, no extra tests were necessary.
29.603	3	Materials	MC1	(a) The main part of the stretcher was made out of aluminium 6060, see Appendix E. Aluminium 60- series is a well-established material in aircrafts. (b) To ensure the strength properties of the structure calculations was made in chapter 4 with material data from CES. (c) The structure may be exposed to salt water and have to be corrosion resistant, which the aluminium parts complies since they are anodized or powder coated. Other environmental conditions such as temperature will not affect the stretcher because the service temperature is between -51°C and +35°C which is in the range of service temperature for aluminium.

§	Amd.	Title	MC	Compliance Statement and/ or Doc. Ref.
29.605	3	Fabrication methods	MC1 MC2	(a) One pair of the outer attachment was positioned on a welded part, see Figure 5 and could therefore be critical. (b) All the fabrication methods used to produce the stretcher, e.g. extruding, are well known.
29.607	3	Fasteners	MC2	(a) There is no single fastener in the constructions that can jeopardies the flight operation, which means that only one locking device is necessary. (b)The stretcher will be attached to the cabin floor, which means that it will be no rotating parts and therefore self-locking nuts may be used.
29.609	3	Protection of structure	MC1 MC2	(a) The bearing parts of the stretcher are anodized and the seat frame, see the blue parts in Appendix A, is powder coated. This is made to improve the corrosion resistance (b) Most of the structure is made in a way that prevents water accumulation. Two critical parts, 0024 and 0025, where water could be accumulated can be found in Appendix H.
29.613	3	Material strength properties and design values	MC0 MC2 MC8	(a) As mentioned in compliance with CS 29.603 all the materials used are well known and are suitable for their purpose. (d) All material data used in the calculations are given in Appendix E. (e) No materials are unknown for the helicopter industry and therefore no specimen tests were necessary.
29.619	3	Special factors	MC0	The only needed special factor was the fitting factor which is described in CS 29.625
29.621	3	Casting factors		There are no significant castings on the stretcher.
29.623	3	Bearing factors		The construction does not have any bearings.
29.625	3	Fitting factors	MC2	(d) The loads, from CS 29.561b, in the calculations in chapter 4 were multiplied by a fitting factor of 1.33 according to part d in the paragraph.
		PERSONNEL AND CARGO ACCOMMODATIONS		

§	Amd.	Title	MC	Compliance Statement and/ or Doc. Ref.
29.785	3	Seats, berths, safety belts and harnesses	MC1 MC2 MC3 MC5 MC8	(a) There are no sharp edges on the stretcher that could injure the occupants. (b-c) The stretcher is equipped with both seat belt and shoulder harness locked together with a single point release. It is also equipped with safety belts to fasten the legs, which could be a problem because they are not attached to the single point release. (d) Hand grips on each side of the stretcher are installed to comfort the patient but they are too low to be used for steadying the occupants using the aisle. (e) The stretcher does not contain any projecting object that can injure any person in the rotorcraft during normal flight conditions (f) Calculations in chapter 4 with inertial loads prescribed in CS 29.561b show that the structure supported the loads of a person with a weight of 77 kg. (g-h) No tests or calculations were made for the belts, harness or headrest. (i) The stretcher includes all equipment mentioned such as cushions and safety belts (restraint system). (j) CS 29.562 is not taken into account and therefore no conclusions for these conditions can be made. (k) The stretcher will be installed within 15° and the seat belts and shoulder harness will withstand the forward load reaction, therefore no extra padded endboard will be necessary.

3.4 Discussion

The paragraphs considered in this project are divided into two chapters; Subpart C that describes the strength requirements and subpart D that describes the design and construction requirements. For the paragraphs where no conclusions could be made or where the result indicated that it would not fulfil the requirements there were recommendations for the forthcoming certification process. The recommendations are presented separately for each chapter.

3.4.1 CS 29 Subpart C - Strength Requirements

The paragraphs in subpart C concerns strength requirements that applies to the rotorcraft and all its features. Subpart C contains both normal loading condition that could be expected during a flight and extreme loading condition that could occur in a crash or emergency landing.

General

The loads in EASA CS 29 are divided into two types; limit load and ultimate load. Limit load is the maximum expected load in service and ultimate load is limit load multiplied by a safety factor. If nothing else is prescribed the safety factor is 1.5. The calculations made in chapter 4 show that the structure can sustain the loads mentioned in these paragraphs.

Emergency Landing Conditions
This part describes the loading condition in the worst case scenario; a crash. All occupants and each item of mass should be restraint in a way that supports 4 g upwards, 16 g forward, 8 g sideward, 20 g downward and 1.5 g rearward in a crash. The structure has to be able to support these loading conditions without ultimate failures. The results of the calculations indicated that the structure would be able to withstand these emergency landing conditions. The numerical model features the load bearing part of the stretcher and does not take the interface between the stretcher and the surrounding into account. A draft of a fixation system for the interface is presented in chapter 5 but it has not been validated with respect to the strength requirements.

3.4.2 CS 29 Subpart D – Design and Construction

Subpart D includes information about the design features such as materials and fabrication methods. The paragraphs describe procedures to control the suitability of materials and new design features and also the safety factors that were used in the calculations.

General
Similar stretchers have been used before, both in rotorcrafts, see Figure 4, and regular ambulances without any problems and therefore no features were considered as hazardous or unreliable. All calculations and simulations show that the structure withstands the critical loads. However since the numerical model does not include the seat or the interface between the seat and the frame, see Figure 2. Therefore some additional test may be necessary in accordance with CS 29.601b.

Figure 4. Ambulance helicopter in Säve.

The stretcher is primarily made of aluminium and according to CES this material meets all requirements. For example Al 6060, which the load bearing part is made of, has good corrosion properties for the expected environments such as salt water and moist. CES is not a database provided by EASA and it is therefore necessary to control the material properties in MMPDS, which is a book with specifications for metallic materials. It also meets the requirement of service temperature from -51 ˚C to +35 ˚C. A full material specification can be found in Appendix E. Another argument that verifies the suitability for this material is that similar aluminium alloys are commonly used in rotorcrafts with good results. Although aluminium 6060 meets the material requirements, it will be appropriate to control the structure at every service time to ensure that the material has not deteriorated.

One pair of the outer attachment is attached to a welded part see Figure 5, this part requires therefore special care with respect to a more accurate fatigue analysis. It is also important to notify the manufacturer to perform the welds in accordance to CS 29.605. Note that all calculations were made with the assumption that the welded part is solid.

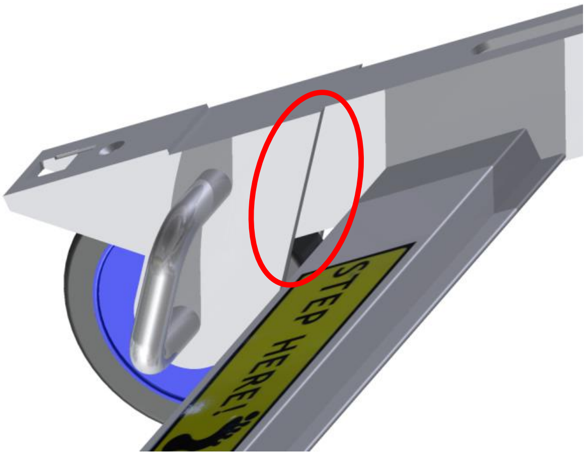

Figure 5. This part is welded

The stretcher was considered as a feature that had no effect on the flight characteristics even if a fastener would come loose it would not affect the ability to manoeuvre the rotorcraft safely. How the stretcher could withstand the critical forces with a loose fastener was not considered in this paragraph.

As mentioned above, the material has good corrosion properties but according to CS 29.609b some extra drain holes may be necessary in parts 0024 and 0025, see Appendix H, to prevent water accumulation. Note that these parts are included in the bearing structure and extra holes can affect the strength properties. Otherwise the structure was estimated to be of a kind where water easily could drain, see Figure 6.

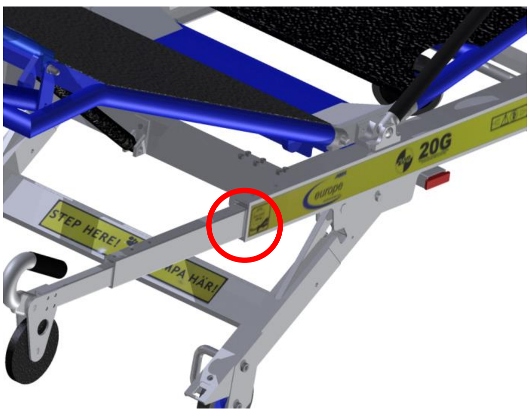

Figure 6. This gap could cause water accumulation in 0024 and 0025

Personnel and Cargo Accommodation
The paragraph in this part of Design and Construction describes how a seat or in this case a berth needs to be designed and what it needs to be equipped with to be classified as a safe structure. For some sections under the paragraph it was easy to determine if the berth is safe or not but for those that could not be established future actions are presented below.

As prescribed in Table 1 the stretcher is equipped with seat belt, shoulder harness and two separate belts for the legs. Since only the seat belt and shoulder harness are combined with a single point release the structure for the legs may be controlled or replaced to a belt that is easier to handle.

The calculations show that only the supporting structure of the stretcher withstands the loads of an occupant that weights at least 77 kg. Therefore it is necessary to control the belts and harnesses according to CS 29.785f and the headrest according to CS 29.785h.

The stretcher will be installed within 15°, see Figure 7, of the longitudinal axis of the rotorcraft and the seat belts and shoulder harness will withstand the forward load reaction. This depends on if the fixation system is installed within 15° of the longitudinal axis of the rotorcraft. An investigation of that has not been implemented during the project because one part of the project was to develop a draft of the actual fixation system.

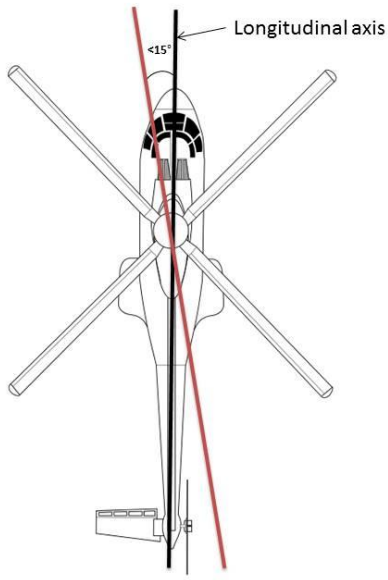

Figure 7.[4] 15 ° from longitudinal axis.

3.5 Conclusion

There are no signs of a failure for the stretcher in a forthcoming certification based on the result and discussion.

---

[4]http://www.armyrecognition.com/europe/France/helicopteres/Super_Puma_AS332/Super_Puma_AS332_avions_helicopter_France.htm

4 Strength Analysis

To become certified by EASA, there are requirements on the stretcher's strength that must be met. This part of the project focused on proving that the stretcher would meet these requirements and withstand various loads in different directions. The strength analysis is based on handbook calculations and numerical FEM simulations. It was discussed whether the stretcher would be approved for use in helicopters or if adjustments are needed.

The paragraphs CS 29.301, CS 29.561 and CS 29.625 in EASA are relevant for structural analysis. According to CS 29.301 limit load and ultimate loading conditions have to be considered. Under limit loading conditions, the structure shall not undergo plastic deformation and under ultimate loading conditions the structure shall not buckle or undergo ultimate failure. The ultimate loads are the maximum loads that the beam can be subjected to. Therefore only the ultimate load is considered for the strength analysis. If the structure would show plastic deformation for ultimate loads the case would have to be studied for whether the beam would buckle or be subjected to ultimate failure and checked against any plastic deformation when subjected to limit loads.

According to CS 29.561 the stretcher must be designed to handle ultimate inertial load factors in a crash landing, see Figure 8. The directions of the loads are shown in Figure 9, Figure 10 and Figure 11. The stretcher will not be subjected to the loads at the same time and the figures only describe the direction.

CS 29.561 (b)
The structure must be designed to give each occupant every reasonable chance of escaping serious injury in a crash landing when:

(1) Proper use is made of seats, belts, and other safety design provisions;
(2) The wheels are retracted (where applicable); and
(3) Each occupant and each item of mass inside the cabin that could injure an occupant is restrained when subjected to the following ultimate inertial load factors relative to the surrounding structure:

(i) Upward 4 g
(ii) Forward 16 g
(iii) Sideward 8 g
(iv) Downward 20 g, after the intended displacement of the seat device
(v) Rearward 1.5 g

Figure 8. The paragraph CS 29.561, section (b)

According to CS 29.625 the inertia forces prescribed in CS 29.561b must be multiplied by a fitting factor of 1.33 (κ_f). See equation (7).

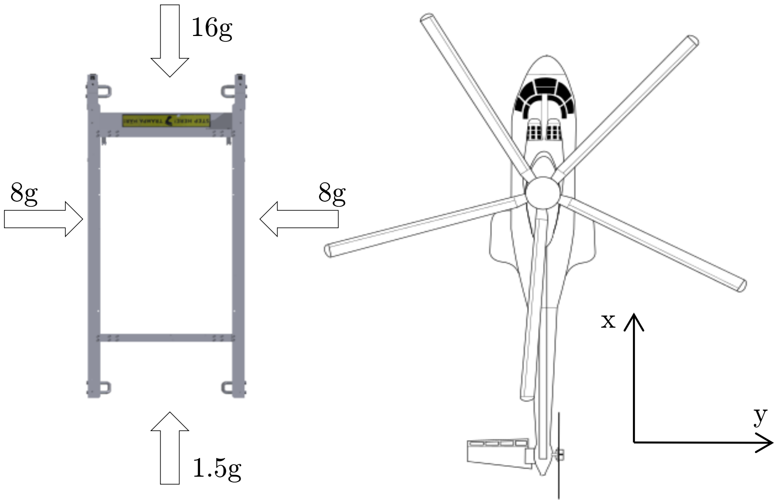

Figure 9[5]. The helicopter and stretcher in direction x,y

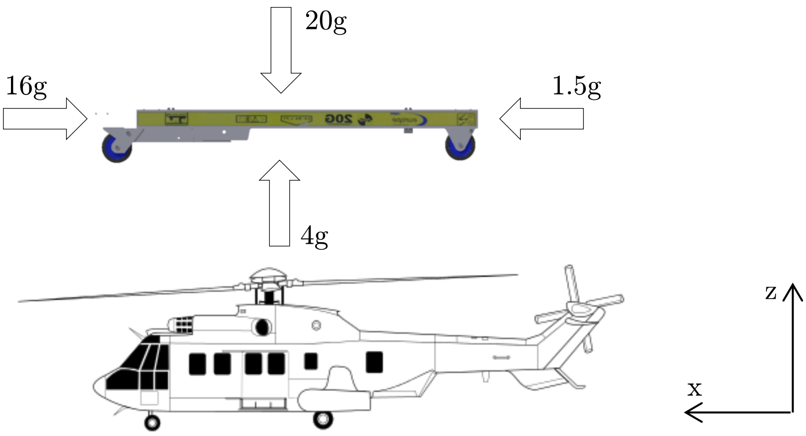

Figure 10[6]. The helicopter and stretcher in direction z,x

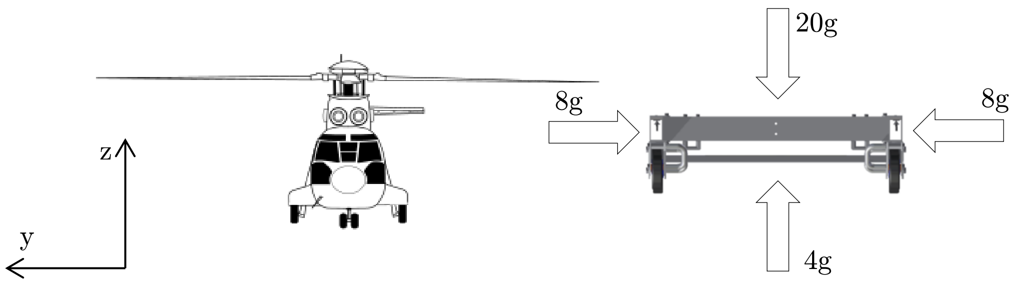

Figure 11[6]. The helicopter and stretcher in direction z,y

---

[5]http://www.armyrecognition.com/europe/France/helicopteres/Super_Puma_AS332/Super_Puma_AS332_avions_helicopter_France.htm

4.1 Theory

FEM is a method to compute differential equations and is used to perform the strength analysis when calculating the numerical simulations. For each load case, the equivalent von Mises stress is compared with the yield stress of the material, 170 MPa to identify areas plastic deformation.

A loaded material will begin to deform plastically when it reaches a level of stress; the yield stress σ_y. The von Mises stress is used to predict yielding of materials under any loading conditions[6].

The yield criteria can be defined as

$$\sigma_e = \sigma_y \tag{1}$$

When the equivalent stress σ_e is equal to the yield stress σ_y, the material is subjected to plastic deformation.

The equivalent stresses can be defined as main stresses

$$\sigma_e = \sqrt{\frac{1}{2}[(\sigma_1 - \sigma_2)^2 + (\sigma_2 - \sigma_3)^2 + (\sigma_3 - \sigma_1)^2]} \tag{2}$$

4.2 Method

Given the rather simple geometry of the load bearing part of the stretcher, see Figure 12, the structural properties under given loading conditions could easily be estimated by linear beam theory handbook cases. The handbook analysis and the numerical FEM simulations were based on linear-elastic material response. Deflections, displacement, von Mises stress and normal stress were evaluated. The displacements from the numerical simulation are compared to the deflections from the handbook calculation with respect to that the displacement is the magnitude of the deflection vectors. The normal stress was calculated to have an estimation of the order of magnitudes for the stresses that should be expected in the FEM simulations. The mass of the computational model has been adjusted in order to take into account the mass of the missing components of the stretcher and the mass of the person lying on it.

The load cases that were used in the calculations are:

- Uniformly distributed load
    - Load case 1 – 20g downward
    - Load case 2 – 8g sideward
    - Load case 3 – 4g upward
    - Load case 4 – 16g forward

[6] Lundh Hans, *Grundläggande hållfasthetslära*, 2000

- One point load
    - Load case 5 – 20g downward

Figure 12. The bearing part of the stretcher that is examined.

It was necessary to perform calculations that study how the stretcher is affected by axial loads and it was therefore important to study buckling. The linear buckling analysis was based on design practice according to linear beam theory following Grundläggande Hållfasthetslära[7] and Eurocode 9 since Euler's buckling cases would be non-conservative. The load cases for buckling are:

- One point load
    - Load case 6 – 16g forward
    - Load case 7 – 8g sideward

The numerical simulations were made in Autodesk Simulation Mechanical 2014 and include a mesh sensitivity analysis, various optimisation processes and discussion of possible sources of errors.

4.2.1 Mass of the Stretcher

The mass of the stretcher with all its components was measured to 36.2 kg. Due to precision issues, it was rounded to 37 kg. The computational model features only the load bearing part of the stretcher and therefore its density had to be scaled in order to compensate for the missing parts up to 37 kg.

4.2.2 Cross Section for Handbook Calculations

The cross section of the beam and its dimensions for I_y and I_z are presented in Table 2 and calculated in Appendix D.

---

[7] Lundh Hans, *Grundläggande hållfasthetslära*, 2000

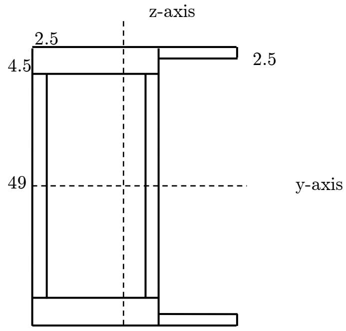

Figure 13. The cross section of the main beam divided in parts.

$$I_{tot} = \sum I_{y,i} + a_i{}^2 A_i \tag{3}$$

$$I_i = \frac{bh^3}{12} \tag{4}$$

$a_i = distance\ from\ center\ of\ mass\ of\ part\ to\ center\ of\ mass\ of\ cross\ section$
$A_i = area\ of\ part$

The cross-section of the joist is given in Figure 14.

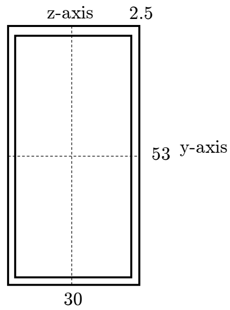

Figure 14. The cross section of the joist

$$I_y = I_z = \frac{bh^3 - b_{in}h_{in}{}^3}{12} \tag{5}$$

Table 2 summarises cross-sectional data and material properties.

Table 2. Materials and cross sections for main beam and joist.

	Main beam	Joist
Cross section	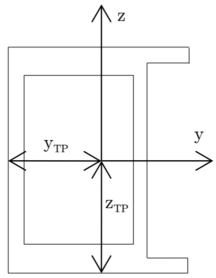 $y_{TP} = 17.46mm$ $z_{TP} = 29mm$ $I_y = 2.9592 \cdot 10^5 mm^4$ $I_z = 9.5987 \cdot 10^4 mm^4$	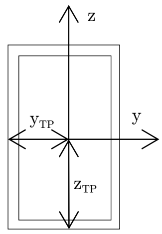 $y_{TP} = 15mm$ $z_{TP} = 26.5mm$ $I_{joist} = 7.7054 \cdot 10^4 mm^4$
Material	SAPA EN AW 6060 T6	SAPA EN AW 6060 F22.T6
E-modulus	$E = 70\ GPA$	$E = 70\ GPA$
Poisson's ratio	$\upsilon = 0.33$	$\upsilon = 0.33$

4.3 Deflection, Normal Stress and Buckling According to Linear Beam Theory

In most cases when the stretcher is used, there is a patient laying on it. The stretcher was therefore in these cases dimensioned with the addition of the human body mass. The human's mass is 77kg according to CS 29.785g. The most ideal case would be if the patient lies down on the stretcher, see Figure 17. However, depending on the situations, patients may be seated in different ways on the stretcher which might require a seated position, raised head or raised legs. Therefore an analysis of implying different loading conditions on the load bearing part was made. There are many options on seating positions that patients can require but only two positions were analysed. The first position is when the patient is lying down on its back and the load is uniformly distributed on the entire stretcher. The other position is when the patient is sitting on the stretcher and can be assumed to affect it with a point load. The point load affects the stretcher most because all force is centered to one point. Consequently this means that the main beams was subjected to a point load while the joist was subjected to a uniformly distributed load but only for joist beneath the buttocks. If the main beams could handle a point load and the joist could handle uniformly distributed load from a human; then they could handle any type of seating position.

The stretcher can be attached inside the rotorcraft in two different ways, one with the head first and the other with the feet first. This means that the stretcher has four attachment points, two on each beam, in the positions shown in Figure 18 and Figure 20. These were calculated as two separated cases named attachment 1 and 2.

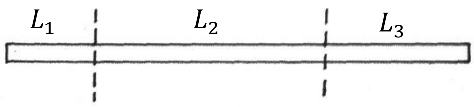

Figure 15. Split of main beam

$L_{tot} = 1185mm$	$L_1 = 170mm$	$L_2 = 785mm$	$L_3 = 230mm$

The beam was split up in three parts, as seen in Figure 15, Figure 19 and Figure 21, because of the joists that work as support for the main beams. This affected the calculations and the choice of the handbook cases. As the stretcher was divided into three parts the mass of the stretcher needed to be distributed for each part as (6) shows. This was because none of the parts takes up the entire mass and therefore the percentage was awarded based on the lengths.

$$m_{ALLFA,i} = \frac{L_i}{L_{tot}} \cdot 37kg \qquad i = 1,2,3 \qquad (6)$$

$$m_{body,i} = \frac{L_i}{L_{tot}} \cdot 77kg \qquad i = 1,2,3 \qquad (6)$$

$$m_{total,i} = m_{ALLFA,i} + m_{body,i}$$

4.3.1 Deflection and Normal Stress of Main Beam due to Load Case 1

The load can be modeled as a constant load uniformly distributed along the beam, shown in Figure 16.

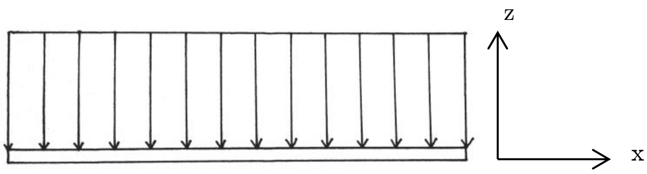

Figure 16: The beam is uniformly distributed a constant load.

The load was equally distributed between the two main beams of the stretcher. Therefore the load was divided in two. The load for the human body mass and the stretchers mass was considered in the calculations and composed the total load.

$$Q_{ALLFA,i} = \frac{m_{ALLFA,i} \cdot ultimate\ load \cdot \kappa_f}{2} \qquad (7)$$

$$Q_{body,i} = \frac{m_{body,i} \cdot ultimate\ load \cdot \kappa_f}{2} \qquad (7)$$

$$Q_{total} = Q_{body,i} + Q_{ALLFA,i}$$

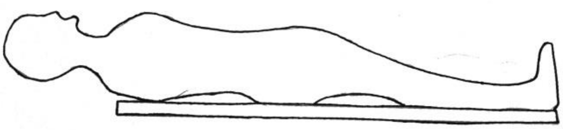

Figure 17. The patient in the most optimal position

Attachment 1

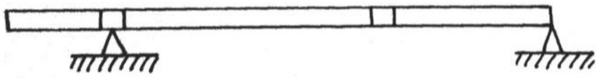

Figure 18. The first attachment

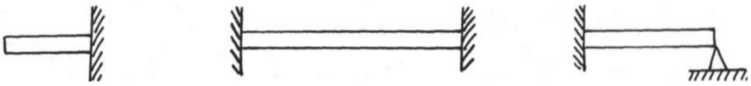

Figure 19. The beam in its different parts with different handbook cases.

For the deflection of the beam, the following applications are relevant in this following order in Table 3:

Table 3. These are the handbook cases for the different parts of the beam

Attachment 1		
Part 1: Cantilevered beam 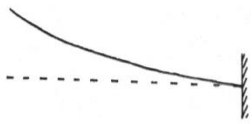	$m_{total,1} = \frac{L_1}{L_{tot}} 114kg$ (6) $Q_{total,1} = \frac{m_{total,1} \cdot 20g \cdot \kappa_f}{2}$ (7) $\delta_{1.1}(\xi) = \frac{Q_{total,1} L_1^3}{24EI_y}(\xi^4 - 4\xi + 3)$ (8) $M_{max,1.1} = \frac{Q_{total,1} L_1}{2}$ (9) $\lvert\sigma_{x,1.1}\rvert = \frac{\lvert M_{max,1.1}\rvert}{I_y} \cdot \max(\lvert z_{min}\rvert, \lvert z_{max}\rvert)$ (10)	$m_{total,1} = 16.35\ kg$ $Q_{total,1} = 2133.8\,N$ $\lvert\sigma_{x,1.1}\rvert = 17.77\,MPa$
Part 2: Fixed beam 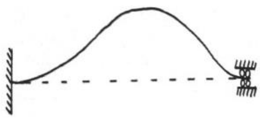	$m_{total,2} = \frac{L_2}{L_{tot}} 114kg$ (6) $Q_{total,2.1} = \frac{m_{total,2} \cdot 20g \cdot \kappa_f}{2}$ (7) $\delta_{2.1}(\xi) = \frac{Q_{total,2} L_2^3}{24EI_y}(\xi^2 - 2\xi^3 + \xi^4)$ (11) $M_{max,2.1} = \frac{Q_{total,2.1} L_2}{12}$ (12) $\lvert\sigma_{x,2.1}\rvert = \frac{\lvert M_{max,2}\rvert}{I_y} \cdot \max(\lvert z_{min}\rvert, \lvert z_{max}\rvert)$ (10)	$m_{total,2} = 75.51\ kg$ $Q_{total,2} = 9853\,N$ $\lvert\sigma_{x,2.1}\rvert = 13.79\,MPa$
Part 3: Fixed beam - sliding membered beam 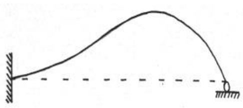	$m_{total,3} = \frac{L_3}{L_{tot}} 114kg$ (6) $Q_{total,3.1} = \frac{m_{total,3} \cdot 20g \cdot \kappa_f}{2}$ (7) $\delta_{3.1}(\xi) = \frac{Q_{total,3} L_3^3}{48EI_y}(2\xi^4 - 3\xi^3 + \xi)$ (13) $M_{max,3.1} = \frac{Q_{total,3} L_3}{8}$ (14) $\lvert\sigma_{x,3.1}\rvert = \frac{\lvert M_{max,3}\rvert}{I_y} \cdot \max(\lvert z_{min}\rvert, \lvert z_{max}\rvert)$ (10)	$m_{total,3} = 22.12\ kg$ $Q_{total,3} = 2886\,N$ $\lvert\sigma_{x,3.1}\rvert = 6.01\,MPa$

Attachment 2

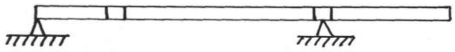

Figure 20. The second attachment

Same as for the attachment 1, the beam was split into three parts as shown in Figure 21

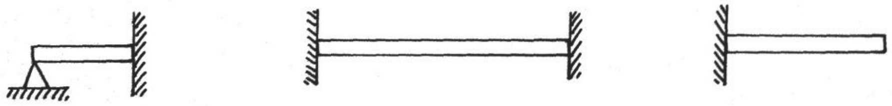

Figure 21. The beam in its different parts and handbook cases.

The same handbook cases as for attachment 1 apply with different lengths for each beam part, see Table 4.

Table 4. These are the same handbook cases as in attachment 1 but on different parts.

Attachment 2		
Part 1: Fixed beam - sliding membered beam 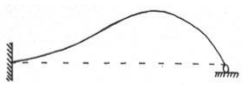	$\delta_{1.2}(\xi) = \frac{Q_{total,1}L_1^3}{48EI_y}(2\xi^4 - 3\xi^3 + \xi)$ (13) $M_{max,1.2} = \frac{Q_{total,1}L_1}{8}$ (14) $\lvert\sigma_{x,1.2}\rvert = \frac{\lvert M_{max,1.2}\rvert}{I_y} \cdot \max(\lvert z_{min}\rvert, \lvert z_{max}\rvert)$ (10)	$\lvert\sigma_{x,1.2}\rvert = 4.44\ MPa$
Part 2: Fixed beam 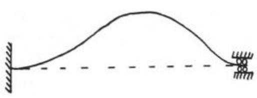	*This calculation and answer is the same as in Attachment 1 – Part 1.*	
Part 3: Cantilevered beam 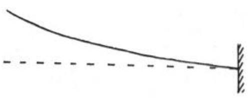	$\delta_{3.2}(\xi) = \frac{Q_{total,3}L_3^3}{24EI_y}(\xi^4 - 4\xi + 3)$ (8) $M_{max,3.2} = \frac{Q_{total,3}L_3}{2}$ (9) $\lvert\sigma_{x,3.2}\rvert = \frac{\lvert M_{max,3.2}\rvert}{I_y} \cdot \max(\lvert z_{min}\rvert, \lvert z_{max}\rvert)$ (10)	$\lvert\sigma_{x,2.2}\rvert = 24.04\ MPa$

4.3.2 Deflection and Normal Stress of Joist due to Load Case 1

There are two joists that are attached between the main beams and hold these together. When subjected to loads downward they will eventually bend. Since they are held between the two main beams it can be assumed that they are fixed. However, the fixed points could differ depending on how the fixation system looked like but the assumption was made that the joist was fixed as shown in Figure 22.

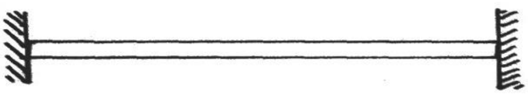

Figure 22. Joist

The length and mass of the joist

$$L_{joist} = 495\ mm$$
$$m_{joist} = 0.5 \cdot (37 + 77)\ kg$$

The mass for the whole stretcher is 37kg and the joists would in reality not alone be subjected to the entire mass. The load would be distributed over both the joists and the main beams. For these calculations the two joists were subjected to loads calculated with half of the mass since it would be closer to the maximum loads they supposed to manage. The calculations for the deflection of the joist are shown in Table 5.

Table 5. The deflection of the joist

Joist			
Fixed beam 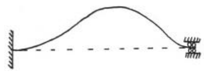	$Q_{joist} = \frac{m_{joist} \cdot ultimate\ load \cdot \kappa_f}{2}$ $\delta_{joist}(\xi) = \frac{Q_{total} L_{joist}^3}{24 E I_y}(\xi^2 - 2\xi^3 + \xi^4)$ $M_{max,joist} = \frac{Q_{total} L_{joist}}{12}$ $\lvert\sigma_{xjoist}\rvert = \frac{\lvert M_{max,joist}\rvert}{I_y} \cdot \max(\lvert z_{min}\rvert, \lvert z_{max}\rvert)$	 (11) (12) (10)	$Q_{joist} = 7437\ N$ $\lvert\sigma_{x,joist}\rvert = 105\ MPa$

4.3.3 Deflection and Normal Stress of Main Beam due to Load Case 2

For the deflection of the beam sideward, the handbook cases are the same. The difference was that the cases considered bending round the z-axis. For this case, the direction of the load is sideward and is described in Figure 9 and Figure 10. Figure 23 below shows the principle for how the beam is subjected to the load. The different calculations are presented in Table 6 and Table 7.

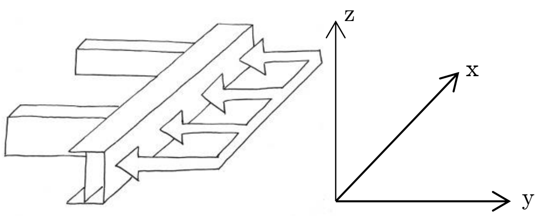

Figure 23. A simplified sketch for the direction of the load.

Attachment 1

Table 6. The handbook cases for the beam in attachment 1

Attachment 1 - sideward			
Part 1: Cantilevered beam 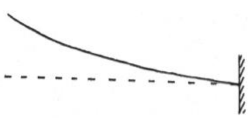	$Q_{SIDE,1} = \frac{m_{total,1} \cdot 8g \cdot \kappa_f}{2}$ $\delta_{S1.1}(\xi) = \frac{Q_{SIDE,1} L_1^3}{24 E I_z}(\xi^4 - 4\xi + 3)$ $M_{max,s1.1} = \frac{Q_{SIDE,1} L_1}{2}$ $\lvert\sigma_{x,s1.1}\rvert = \frac{\lvert M_{max,1.1}\rvert}{I_z} \cdot max(\lvert y_{min}\rvert, \lvert y_{max}\rvert)$	(7) (8) (9) (10)	$Q_{SIDE,1} = 853\ N$ $\lvert\sigma_{x,s1.1}\rvert = 13.2\ MPa$
Part 2: Fixed beam 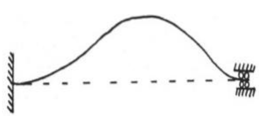	$Q_{SIDE,2} = \frac{m_{total,2} \cdot 8g \cdot \kappa_f}{2}$ $\delta_{S2.1}(\xi) = \frac{Q_{SIDE,2} L_2^3}{24 E I_z}(\xi^2 - 2\xi^3 + \xi^4)$ $M_{max,s2.1} = \frac{Q_{SIDE2.1} L_2}{12}$ $\lvert\sigma_{x,s2.1}\rvert = \frac{\lvert M_{max,2}\rvert}{I_z} \cdot \max(\lvert y_{min}\rvert, \lvert y_{max}\rvert)$	(7) (11) (12) (10)	$Q_{SIDE,2} = 3941\ N$ $\lvert\sigma_{x,s2.1}\rvert = 46.89\ MPa$

Part 3: Fixed beam - sliding membered beam 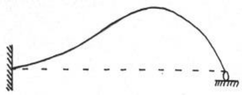	$Q_{SIDE,3.1} = \frac{m_{total,3}\cdot 8g \cdot \kappa_f}{2}$ (7) $\delta_{S3.1}(\xi) = \frac{Q_{SIDE,3}L_3^3}{48EI_z}(2\xi^4 - 3\xi^3 + \xi)$ (13) $M_{max,s3.1} = \frac{Q_{SIDE,3}L_3}{8}$ (14) $\lvert\sigma_{x,s3.1}\rvert = \frac{\lvert M_{max,3}\rvert}{I_z} \cdot \max(\lvert y_{min}\rvert, \lvert y_{max}\rvert)$ (10)	$Q_{SIDE,3} = 1154\ N$ $\lvert\sigma_{x,s3.1}\rvert = 6.04\ MPa$

Attachment 2

Table 7. The differences for attachment 2

Attachment 2 - sideward		
Part 1: Fixed beam - sliding membered beam 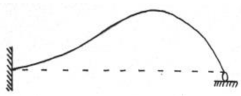	$\delta_{1.2}(\xi) = \frac{Q_{SIDE,1}L_1^3}{48EI_z}(2\xi^4 - 3\xi^3 + \xi)$ (13) $M_{max,1.2} = \frac{Q_{SIDE,1}L_1}{8}$ (14) $\lvert\sigma_{x,1.2}\rvert = \frac{\lvert M_{max,1.2}\rvert}{I_z} \cdot \max(\lvert y_{min}\rvert, \lvert y_{max}\rvert)$ (10)	$\lvert\sigma_{x,1.2}\rvert = 13.2\ MPa$
Part 2: Fixed beam 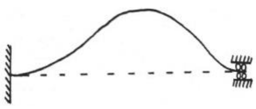	*This calculation and answer is the same as in attachment 1.*	
Part 3: Cantilevered beam 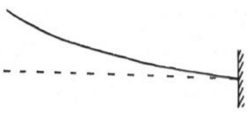	$\delta_{3.2}(\xi) = \frac{Q_{SIDE,3}L_3^3}{24EI_z}(\xi^4 - 4\xi + 3)$ (8) $M_{max,3.2} = \frac{Q_{SIDE,3}L_3}{2}$ (9) $\lvert\sigma_{x,3.2}\rvert = \frac{\lvert M_{max,3.2}\rvert}{I_z} \cdot \max(\lvert y_{min}\rvert, \lvert y_{max}\rvert)$ (10)	$\lvert\sigma_{x,2.2}\rvert = 24.15\ MPa$

4.3.4 One Point Load due to Load Case 5

In this case the patient would sit with the head and legs raised from the seat, see Figure 24. The weight from the human is centered at one point, at the buttocks. This is the worst case when the beam is loaded in only one place. This case was studied for both the main beam and the joist. The case with the joist was calculated with the assumption that the loads from the human and the stretcher itself were subjected to it as a uniformly distributed load, but only for the joist beneath the buttocks. In reality the joist is not directly underneath the buttocks, and was scaled as described below. If the deflection is non-critical it would show that the joist withstands any kind of seating because in reality it would never be subjected to such loads.

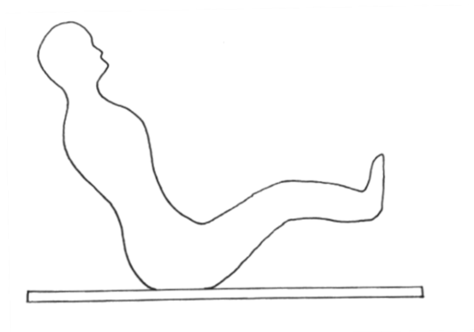

Figure 24. The patient in the worst scenario case.

Main beam

The point load was only affecting part 2 of the main beam and was therefore the only part that was analysed. The calculations are presented in Table 8.

Table 8. Handbook case for the part of the main beam that is affected by the one point load

One point load		
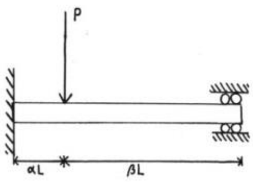	$P = \frac{m_{body} \cdot ultimate\ load \cdot \kappa_f}{2}$ (15) $\alpha = \frac{0.185}{L_2}$ $\beta = \frac{0.6}{L_2}$ $\xi = \alpha$ $\delta_{tot}(\xi) = \frac{PL_2^3}{6EI}\beta[(1-\alpha-\alpha\beta-\beta^2)\xi + (\alpha+\alpha\beta)\xi^2 - \xi^3] + \delta_{2.1,m_{ALLFA}}(\xi)$ (16) $M_{max,point} = \frac{PL_2}{12}$ (12) $\lvert\sigma_{xmax}\rvert = \frac{\lvert M_{max,point}\rvert}{I_y} \cdot \max(\lvert z_{min}\rvert, \lvert z_{max}\rvert) + \lvert\sigma_{x,2.1,m_{ALLFA}}\rvert$ (8)	$P = 10\ 046.4\ N$ $\lvert\sigma_{xpoint}\rvert = 71.06\ MPa$

Joist

The calculation for the joist is similar to the ones in chapter 4.3.2 but with modifications. Since the point load is applied to the main beams and is not applied directly to the joist, the force that affects the joist is not the total load. The load from the human is applied 0.185m from the joist and therefore the weight can be scaled to a lesser value. The assumption was made that it could be reduced with 50%. As this case is special because of the indirect load, the mass of the stretcher has been scaled 1/6. This is because it would be too much to apply the whole deadweight onto one single joist as for the earlier cases. The calculations are presented in Table 9.

Table 9. Handbook case for the joist that is affected by the one point load

Joist – Uniformly distributed load		
Fixed beam 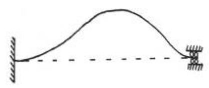	$Q_{joist,body} = \left(\frac{m_{ALLFA}}{6} + 0.5 \cdot m_{body}\right) \cdot 20g \cdot \kappa_f$ (7) $\delta_{joist,body}(\xi) = \frac{Q_{joist} L_{joist}^3}{24EI_y}(\xi^2 - 2\xi^3 + \xi^4)$ (11) $M_{max,joist,body} = \frac{Q_{joist} L_{joist}}{12}$ (12) $\lvert\sigma_{xjoist,body}\rvert = \frac{\lvert M_{max,joist}\rvert}{I_y} \cdot \max(\lvert z_{min}\rvert, \lvert z_{max}\rvert)$ (10)	$Q_{joist,body} = 11656\ N$ $\lvert\sigma_{x,joist,body}\rvert = 165\ MPa$

4.3.5 Buckling

According to EASA, CS 29, it is required that the beams will not buckle when they are subjected to ultimate loads. To show that the beams are suitable, the critical load - P_k had to be calculated by using Euler's buckling cases and then compared to the ultimate loads. The loads are assumed to be one point loads affecting the center of gravity. If these were greater than, P_k, the beam would buckle which is not acceptable.[8] It must be taken into account that the beam will normally buckle earlier in reality than what linear buckling predicts. Therefore, design practices that compensate for this must be followed.

These calculations were made with the total mass of 114kg with the forward acceleration 16g, affecting the main beams, and for the sideward acceleration 8g, affecting the joists.

Buckling for the Main Beams due to Load Case 4

To determinate that the requirements were met it was compulsory to study three different buckling cases that depended on the attachment. Given that the fixation system was not developed it was necessary to study each of these three cases and not only the worst.

The calculations were only made for attachment 1, see Figure 18. This was because if the calculations show that the beams will not buckle for these cases the other cases for attachment 2, see Figure 20, is similar enough that the assumption could be made that these would not buckle either.

The procedure for design practice on how P_k was determined is as follows:

The force that occurs from the acceleration 16g on the main beams is

$$P = \frac{16g \cdot m_{total} \cdot \kappa_f}{2} = 11900\ N \qquad (7)$$

Buckling stress for plastic deformation is defined as

[8] Lundh Hans, *Grundläggande hållfasthetslära*, 2000

$$\sigma_k = \frac{P_k}{A} \tag{17}$$

The free buckling length for Euler buckling is defined as

$$L_{f,rek} = \beta_{rek} L \tag{18}$$

The free buckling length $L_{f,rek}$ takes the elasticity of the fixed attachments into consideration and can be found in table 6[9]. Free buckling length of the Euler buckling $L_{f,rek}$ differs for different Euler cases. β_{rek} can also be found in the same table.

The slenderness ratio must be found to determinate the buckling stress σ_k. The slenderness ratio is defined as:

$$\lambda = \frac{L_{f,rek}}{r_i} \tag{19}$$

Where r_i is the cross section radius of gyration is given by:

$$r_i = \sqrt{\frac{I}{A}} \tag{20}$$

$$r_i = 12.8mm$$

Cross section area

$$A = 5.835 \cdot 10^2\ mm^2$$

Moment of Inertia

$$I_z = 9.5987 \cdot 10^4 mm^4$$

σ_k is found in figure 17.3[10] with the slenderness ratio λ for aluminum alloy.

$$\sigma_k \cdot A = P_k \tag{21}$$

To show that buckling does not occur for the case this must apply:

$$P \leq P_k \tag{22}$$

---

[9] Lundh Hans, *Grundläggande hållfasthetslära*, 2000

[10] Sundström, Bengt. *Handbok och Formelsamling i hållfasthetslära*, 1998

Table 10. Buckling load case 4

Buckling for main beam	
Euler 1 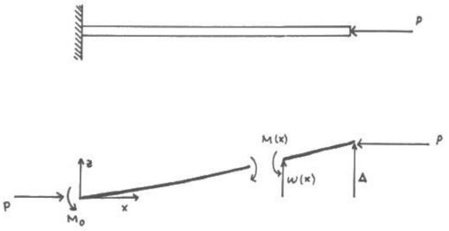	$L_{1f,rek} = 2.1L_1 = 357mm$ $r_i = 12.8mm$ (20) $\lambda = 27.89$ (19) $\sigma_k = 130\ {}^{N}/_{mm^2}$ (21) $P_K = 75.86\ kN$ (21)
Euler 3 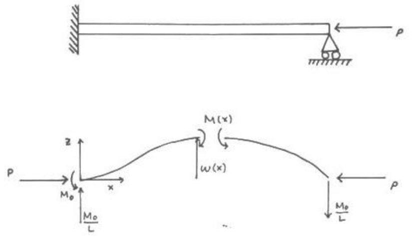	$L_{3f,rek} = 0.8L_3 = 184mm$ $\lambda = 14.375$ (19) $\sigma_k = 180\ N/mm^2$ (21) $P_K = 105.03\ kN$ (21)
Euler 4 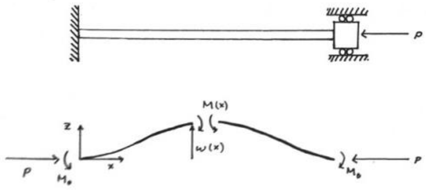	$L_{2f,rek} = 0.6L_2 = 471mm$ $\lambda = 36.8$ (19) $\sigma_k = 125\ N/mm^2$ (21) $P_K = 72.93\ kN$ (21)

Buckling for Joist due to Load Case 5

This acceleration affects the joists axial and it is therefore necessary to study a buckling case for these as well as the main beams, see Table 11.

$$P = \frac{8g \cdot m_{total} \cdot \kappa_f}{2} = 5949\ N \tag{7}$$

Table 11. Buckling for load case 5

Buckling for joist	
Euler 4 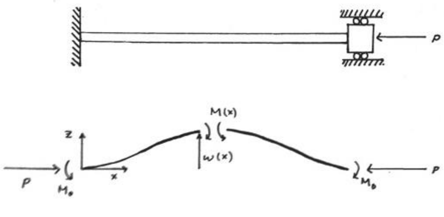	$L_{joist\ f,rek} = 0.6L_{joist} = 297mm$ $\lambda = \frac{L_{joist\ f,rek}}{r_i} = 21.13$ (19) $r_i = \sqrt{\frac{I_{y,joist}}{A_{joist}}} = 0.014$ (20) $\sigma_k = 128\ N/mm^2$ (21) $P_K = 49.92\ kN$ (21)

4.4 Buckling According to Eurocode 9

When a strength analysis is performed, it is essential to look at how loads will affect the design and how it will meet the requirements that are set. Eurocode 9 was used to check the various buckling cases. This is useful when studying how flexural buckling and lateral torsional buckling influence the beam. What differ these calculations from the previous ones is the additional use of factors that take into account the imperfections that occur in aluminum structures. These cases consider checking members that are subjected to a combination of axial force and major axis or minor axis bending. [11]

Eurocode 9 describes how to perform a buckling check. This indicates whether a specific value is greater or lesser than one, if the value is greater than one the stretcher is considered unsafe but if the value is lesser than one; it is considered safe. At first the cross section was classified, by defining a beta factor that depends on the length and thickness of the cross sections. Some factors compensate for whether the material is heat-treated or welded. Considering members that are subjected to compressive forces may have reduced resistance because of local buckling of slender elements. It is therefore important to calculate reductions factors that increased with flexural buckling and lateral-torsional buckling. All of this was then used in the buckling check that determined if the stretcher was safe or not:

$$\left(\frac{N_{Ed}}{\chi_{min} \cdot \omega_x \cdot N_{Rd}}\right)^{\psi_c} + \frac{1}{\omega_0}\left(\left(\frac{M_{y,Ed}}{M_{y,Rd}}\right)^{1.7} + \left(\frac{M_{z,Ed}}{M_{z,Rd}}\right)^{1.7}\right)^{0.6} \leq 1.00 \tag{23}$$

A buckling check for the main beam and the joist is presented in Appendix D.

4.5 Numerical Simulation

Below follows a step by step description on how the numerical simulations were done and which assumptions that were made.

4.5.1 3D-Model

The computational model, see Figure 25, features only the load bearing part of the stretcher with the most necessary parts. Parts that do not contribute to stiffness properties were removed from the load bearing part to make the simulations more effective.

[11] British Standards Institution, *Eurocode 9,* DD ENV 1999-1-1:2000

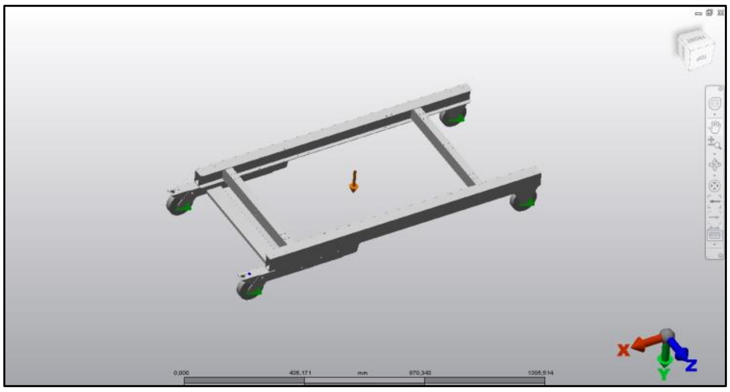

Figure 25. 3D-dummy model

4.5.2 Loads and Boundary Conditions

The densities of the different materials were increased with a factor so that the models mass was equal to the mass of the stretcher with all its components including the person mass. The calculations below show how the density of the computational model was scaled to take into account missing parts and person mass.

$$\rho = \frac{m}{V} \qquad (24)$$
$$\rho_1 = \frac{m_{model}}{V}$$

ρ_1 is the density without humans mass.

$$\rho_2 = \, factor \cdot \rho_1 = \frac{m_{model} + m_{body} + (m_{stretcher} - m_{model})}{m_{model}} \cdot \frac{m_{model}}{V} \qquad (25)$$

ρ_2 is the new density with the factor of ρ_1

$$factor = \frac{m_{model} + m_{body} + (m_{stretcher} - m_{model})}{m_{model}} = 15.2$$

For the case with one point load the main beams were loaded with nodal forces as seen in Figure 26.

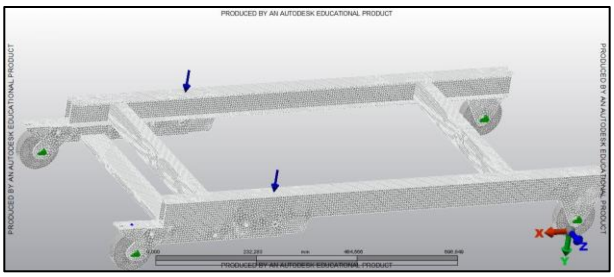

Figure 26. The arrows show where the nodal forces were applied.

Another assumption was that the boundary conditions were set as fixed on the joints that go through the wheels of the stretcher, see Figure 27. This is not how it looks like in reality because these four points will never be attached on the fixation system. This assumption was made mainly because it was hard to take the fixation system into the simulation. The aim was to attach the stretcher in a similar way that hardly would affect the calculations; consequently the joints were fixed in all directions.

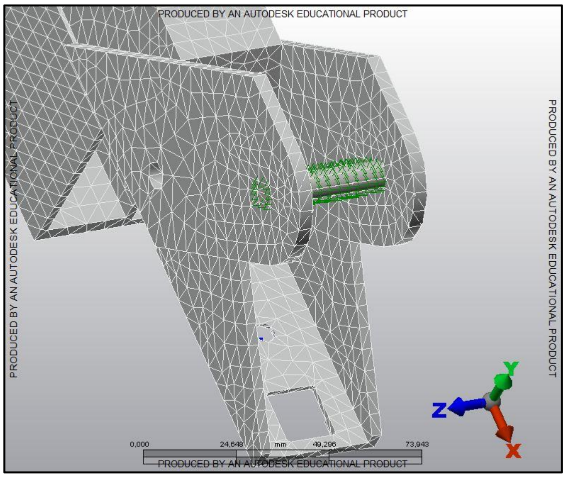

Figure 27. The stick in the picture is the joint that goes through the wheel.

4.5.3 Element Definition

Quadratic tetrahedral elements were used. This was to ease the mesh especially at radii and transition edges.

4.5.4 Mesh Convergence Study

The mesh convergence study was performed on the size of the elements where three levels of refinement were applied. The first coarser mesh was refined by decreasing the element size by 30% and then by decreasing it further by 20%. Below follows an example of the mesh analysis due to load case 1.

Mesh 1

Nodes	217226
Mesh size	4.47-11.1 mm
Elements	113229
Parts	27

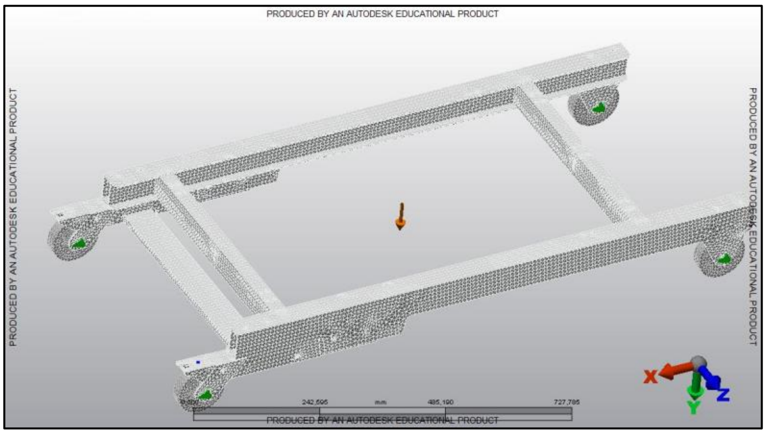

Figure 28. Mesh plot

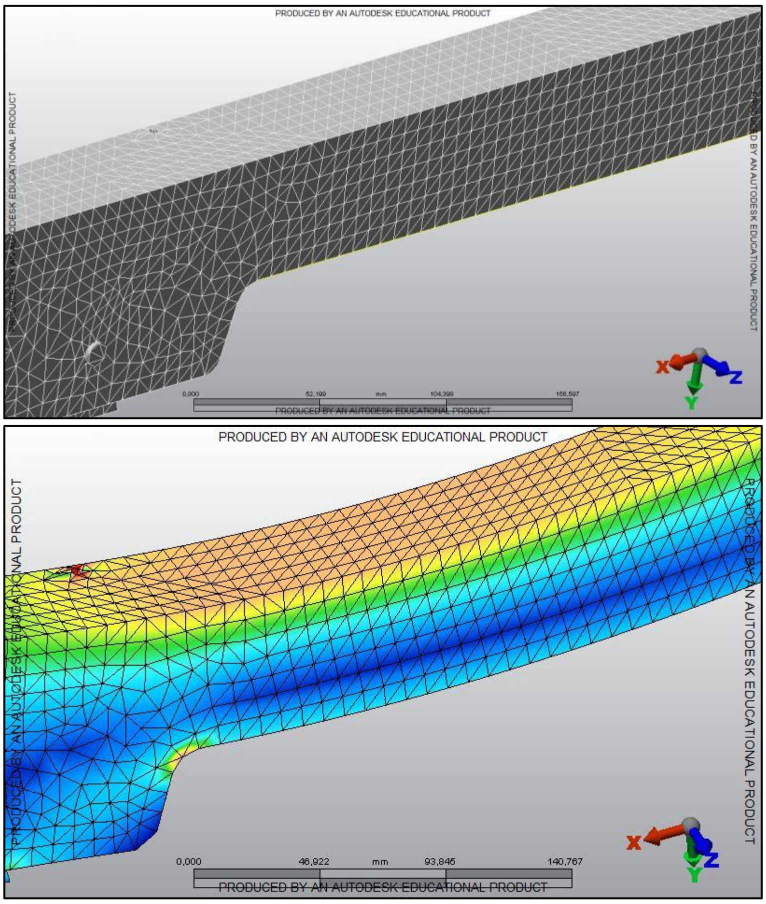

Figure 29. Detail of mesh plot with and without displacement results.

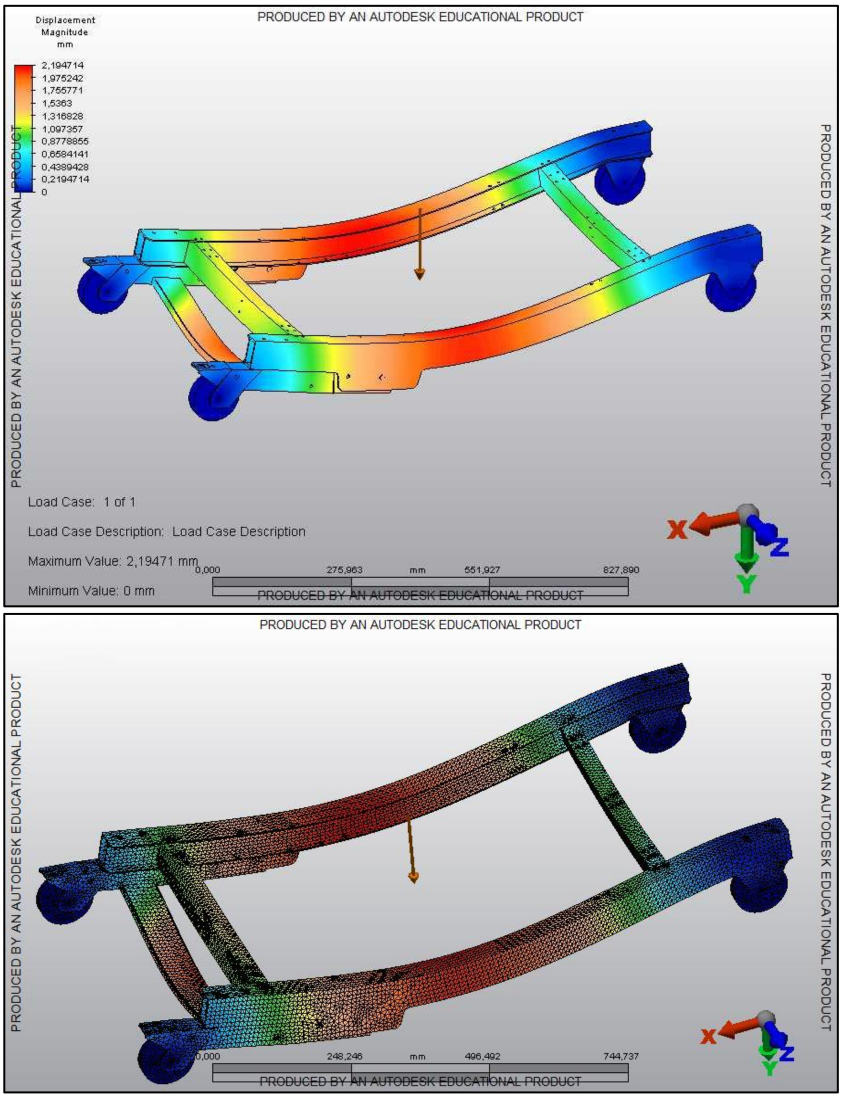

Figure 30. Displacement plot

Maximum displacement: 2.19mm at the main beams.

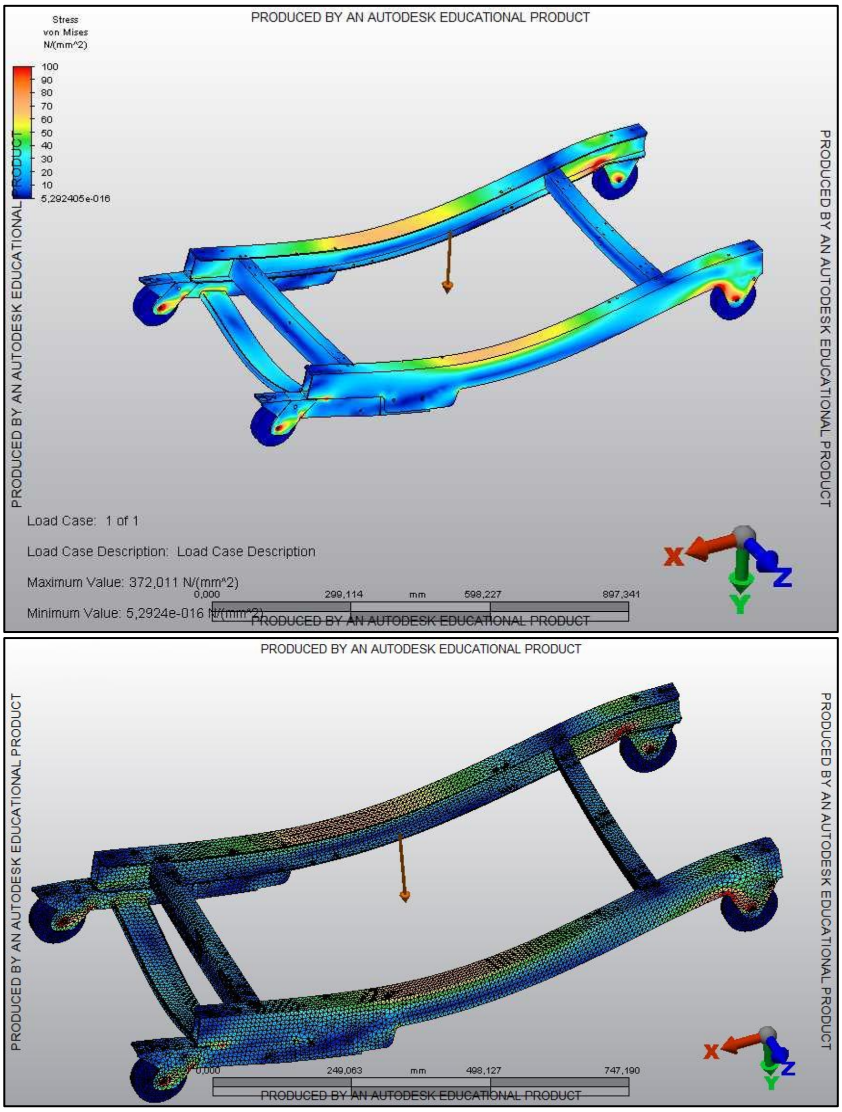

Figure 31. Stress plot

Stresses at the main beams show values from 30 to 70MPa. Other areas show values below 30MPa.

Mesh 2

Nodes	326124
Mesh size	4.0-9.1 mm
Elements	170834
Parts	27

The elements have now increased with 30% from previous mesh.

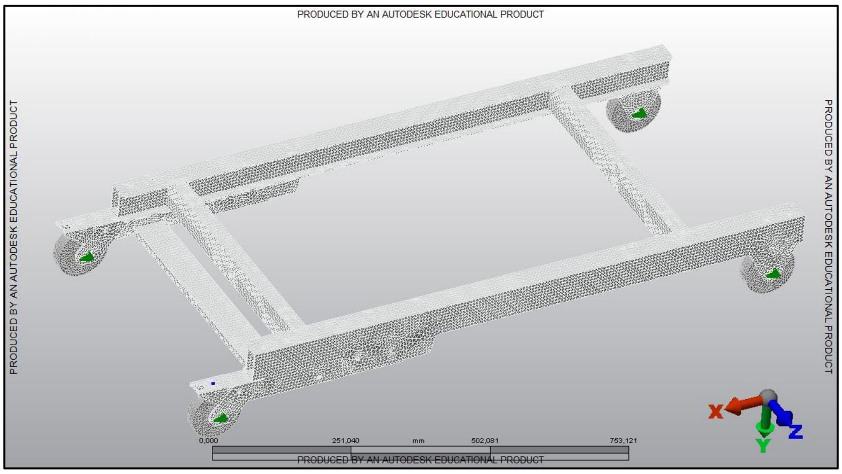

Figure 32. Mesh plot

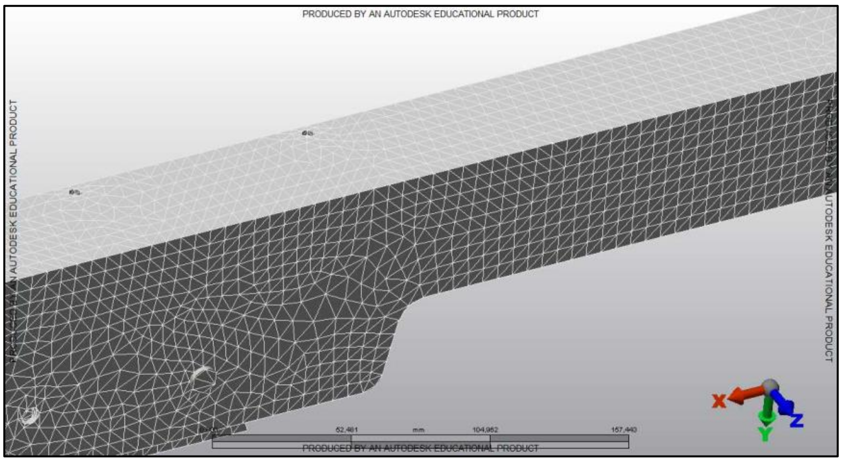

Figure 33. Detail of mesh plot

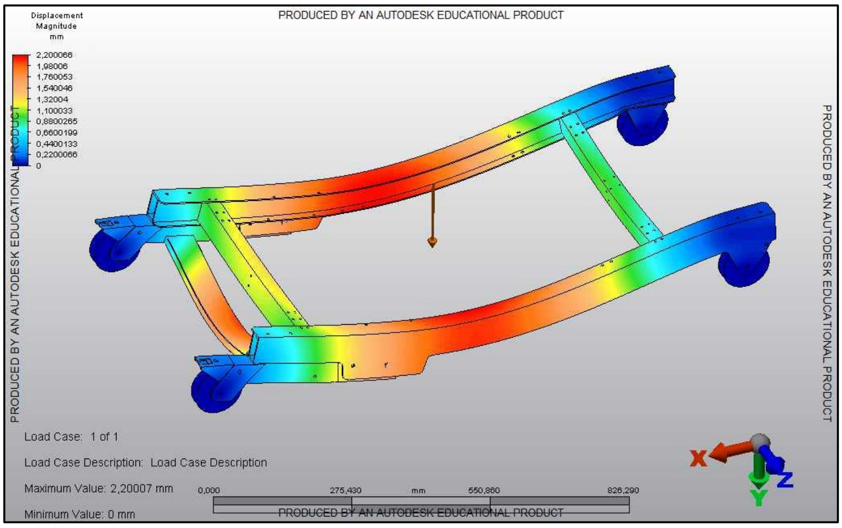

Figure 34. Displacement plot

The maximum displacement has increased to 2.2mm

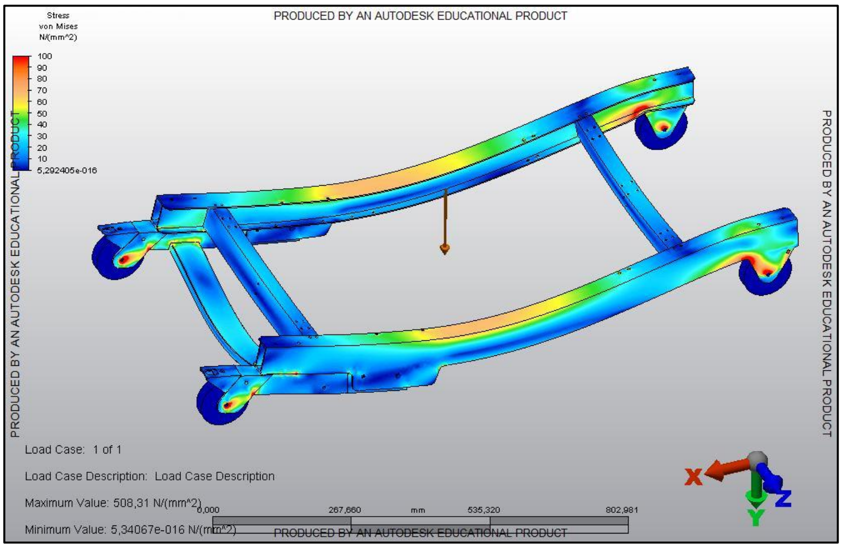

Figure 35. Stress plot

The green area at the main beams shows stress with values from 40 to 80MPa. Other areas show values below 30MPa.

Mesh 3

Nodes	423133
Mesh size	3.48-7.77 mm
Elements	222273
Parts	27

The elements have almost doubled its amount from the first mesh.

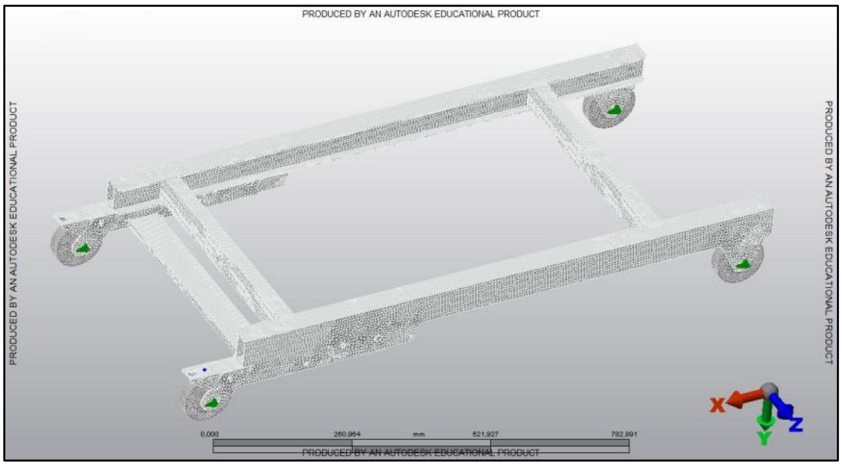

Figure 36. Mesh plot

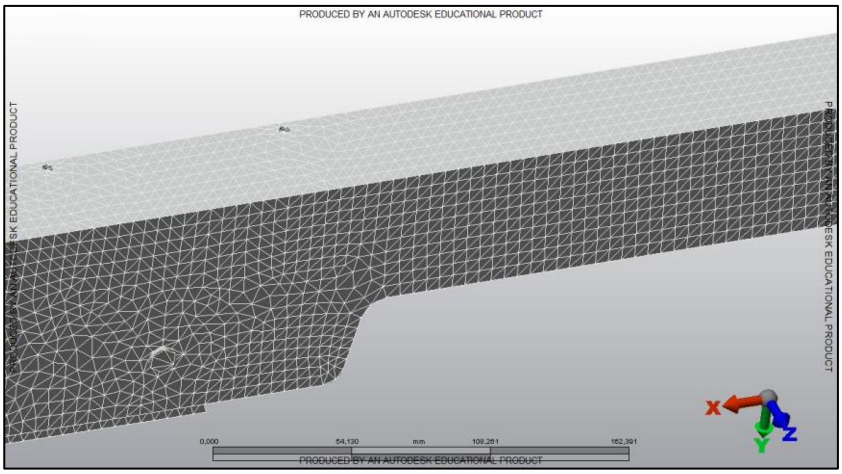

Figure 37. Detail of mesh plot

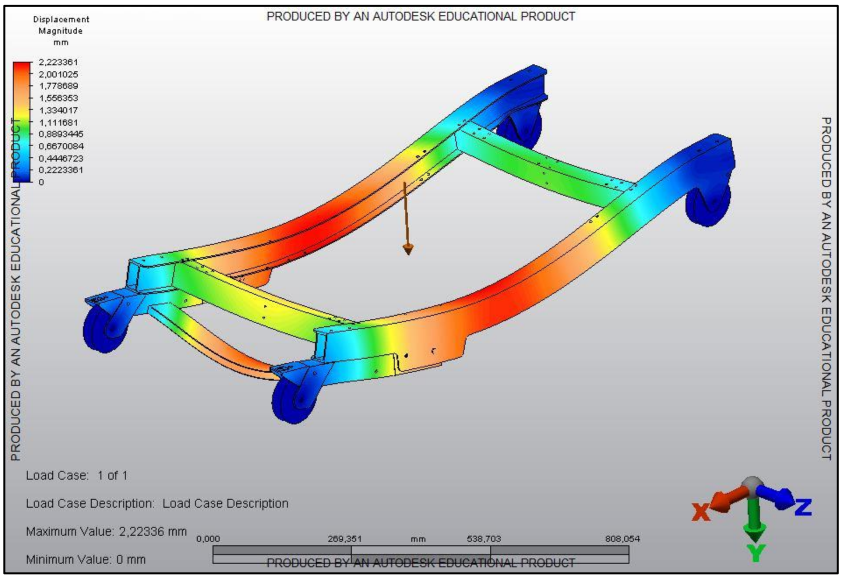

Figure 38. Displacement plot

The maximum displacement has increased to 2.22mm which is a 1.37% increase from the first mesh. This shows that the values converged.

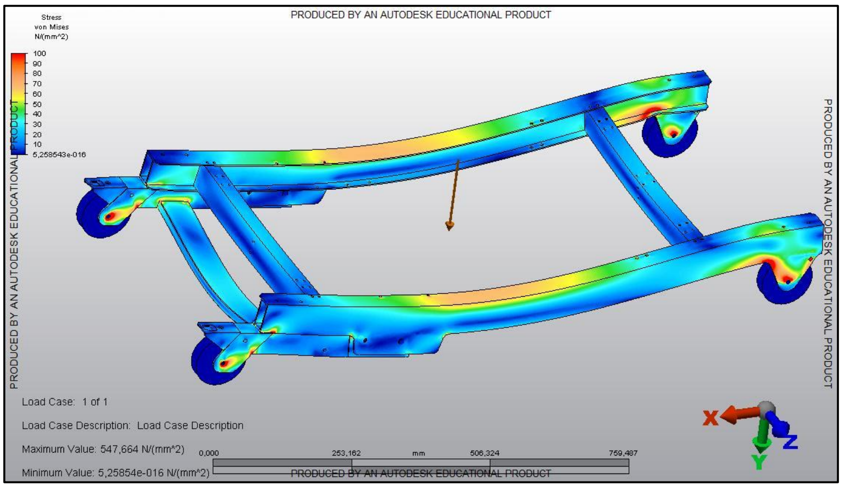

Figure 39. Stress plot

The stress plots showed almost exactly the same values for all three discretisations. The values at the main beams had hardly changed from the first mesh, which means that it had converged and that this mesh was confidently to work with. A further element increase would not affect the results. Mesh 3 was then used for all the simulations with the different loads.

4.5.5 Choice of Materials

This project studied a linear elastic material behaviour of the load bearing part of the stretcher. The materials that are used for the simulation are presented in Appendix E. All materials that were chosen for the different parts were correct according to actual stretcher except for the wheels. The wheels contain a bearing at the centre and hard rubber at the edges but the main material is plastic and was therefore chosen as the material for the wheels. The main reason for this assumption was to simplify the model and this did not affect the result much because the wheels were not the interesting part to analyse.

4.5.6 Interpreting the Results

The requirements from EASA are that the stretcher does not undergo significant yielding. The only values that were calculated are deflection and von Mises stress. The main part of the model is made of aluminium with yield strength of 170MPa which is presented in Appendix E. Areas for which stress levels exceeds the yield limit were further analysed.

4.6 Results

4.6.1 Deflection, Normal Stress and Buckling According to Linear Beam Theory

To make it easier to analyse the influence and the essential values for the deflection the results are presented in Table 12, Table 13 and Table 14. Comparing the maximum deflections can provide conclusions considering the stiffness of the structure. The stresses are presented for comparison with the numerical simulation analysis.

The results for buckling are presented in data tables. For buckling according to linear beam theory the value for P_k is the greatest value allowed before the beam would buckle. The value P is the calculated load that the beam is subjected to. Comparing these to each other show if P_k is greater than P, and if that is the case, it would be safe against buckling.

To illustrate the maximum deflection of the handbook calculations which occurred due to load case 2 for attachment 2 in Part 2, fixed beam, it is presented in Figure 40.

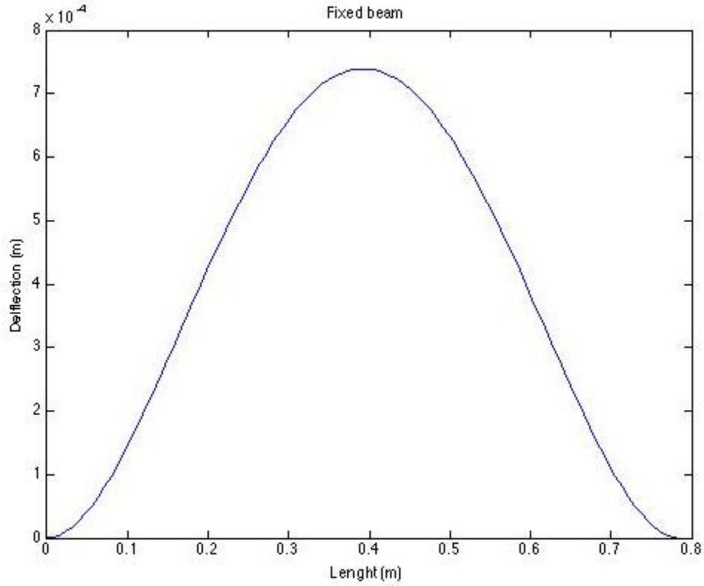

Figure 40. Maximum deflection for handbook calculation.

Table 12. Deflection and Normal Stress due to Load Case 1

Main Beam	Deflection and normal stress
Attachment 1 - Part 1: Cantilevered Beam	$\delta_{max} = 6.3262 \cdot 10^{-2} mm$ $\lvert\sigma_{x,h1.1}\rvert = 17.77\ MPa$
Attachment 1 - Part 2: Fixed Beam	$\delta_{max} = 0.599\ mm$ $\lvert\sigma_{x,h2.1}\rvert = 13.79\ MPa$
Attachment 1 - Part 3: Fixed Beam – Sliding Membered Beam	$\delta_{max} = 9.1836 \cdot 10^{-3} mm$ $\lvert\sigma_{x,h3.1}\rvert = 6.01\ MPa$
Attachment 2 – Part 1: Fixed Beam – Sliding Membered Beam	$\delta_{max} = 2.7409 \cdot 10^{-3} mm$ $\lvert\sigma_{x,h1.2}\rvert = 4.44\ MPa$
Attachment 2 – Part 2: Fixed Beam	$\delta_{max} = 0.599\ mm$ $\lvert\sigma_{x,h2.2}\rvert = 13.79\ MPa$
Attachment 2 – Part 3: Cantilevered Beam	$\delta_{max} = 0.212\ mm$ $\lvert\sigma_{x,h3.2}\rvert = 24.04\ MPa$

Joist	**Deflection and normal stress**
	$\delta_{max} = 0.435\ mm$ $\lvert\sigma_{x,joist}\rvert = 105\ MPa$

Table 13. Deflection and Normal Stress due to Load Case 2

Main Beam	**Deflection and normal stress**
Attachment 1 - Part 1: Cantilevered Beam	$\delta_{max} = 7.80 \cdot 10^{-2} mm$ $\lvert\sigma_{x,s1.1}\rvert = 13.2\ MPa$
Attachment 1 - Part 2: Fixed Beam	$\delta_{max} = 0.738\ mm$ $\lvert\sigma_{x,s2.1}\rvert = 46.89\ MPa$
Attachment 1 - Part 3: Fixed Beam – Sliding Membered Beam	$\delta_{max} = 0.113\ mm$ $\lvert\sigma_{x,s3.1}\rvert = 6.04\ MPa$
Attachment 2 – Part 1: Fixed Beam – Sliding Membered Beam	$\delta_{max} = 3.38 \cdot 10^{-3}\ mm$ $\lvert\sigma_{x,s1.2}\rvert = 13.2\ MPa$
Attachment 2 – Part 2: Fixed Beam	$\delta_{max} = 0.738\ mm$ $\lvert\sigma_{x,s2.1}\rvert = 46.89\ MPa$
Attachment 2 – Part 3: Cantilevered Beam	$\delta_{max} = 0.261\ mm$ $\lvert\sigma_{x,s2.2}\rvert = 24.15\ MPa$

Table 14. One Point Load due to Load Case 5

Main beam	**Deflection and stress**
	$\delta_{max} = 0.399\ mm$ $\lvert\sigma_{xpoint}\rvert = 71.06\ MPa$
Joist	**Deflection and stress**
	$\delta_{max} = 0.682\ mm$ $\lvert\sigma_{x,joist,body}\rvert = 165\ MPa$

Buckling

Table 15. The table shows if $P<P_k$

	$\boldsymbol{P}$	$\boldsymbol{P_k}$	$\boldsymbol{P < P_k}$
Main beam - Euler 1	$11.9\ kN$	$75.86\ kN$	Yes
Main beam - Euler 3	$11.9\ kN$	$105.03\ kN$	Yes
Main beam - Euler 4	$11.9\ kN$	$72.93\ kN$	Yes
Joist - Euler 4	$5.95\ kN$	$49.92\ kN$	Yes

As shown in Table 15 there is no risk for buckling for any of the cases.

4.6.2 Eurocode 9

Buckling

For buckling according to Eurocode 9 a buckling check was performed. The value in Table 16 is the value calculated from the buckling check. If the value is greater than or equal to one the beam is considered unsafe but if the value is less than one the beam is considered safe.

Table 16. The table shows if the beam is safe or unsafe.

	Value	Safe?
Main beam - Euler 1	0.55	Yes
Main beam - Euler 2	0.55	Yes
Main beam - Euler 3	0.7	Yes
Joist - Euler 4	0.48	Yes

4.6.3 Numerical Simulation

The results of the numerical simulations are presented here. Equivalent von Mises stress values are compared with the yield strength of the material, 170Mpa.

Displacement and Stress due to Load Case 1

Table 17. Applied force

Acceleration due to body force	9814.56 mm/s^2
X multiplier	0
Y multiplier	26.60
Z multiplier	0

The multiplier is defined as: $ultimate\ load \cdot \kappa_f = 26.60$

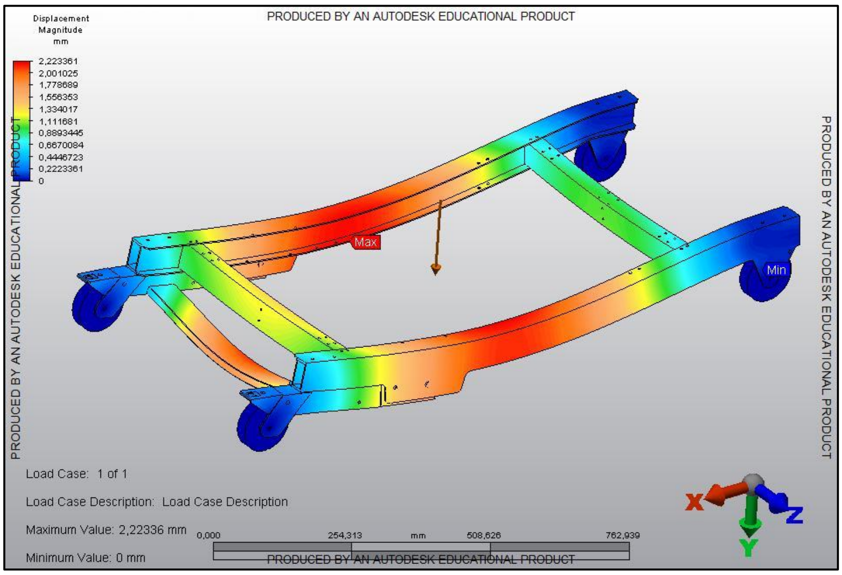

Figure 41. Displacement plot

Maximum displacement: 2.22mm at the main beams.

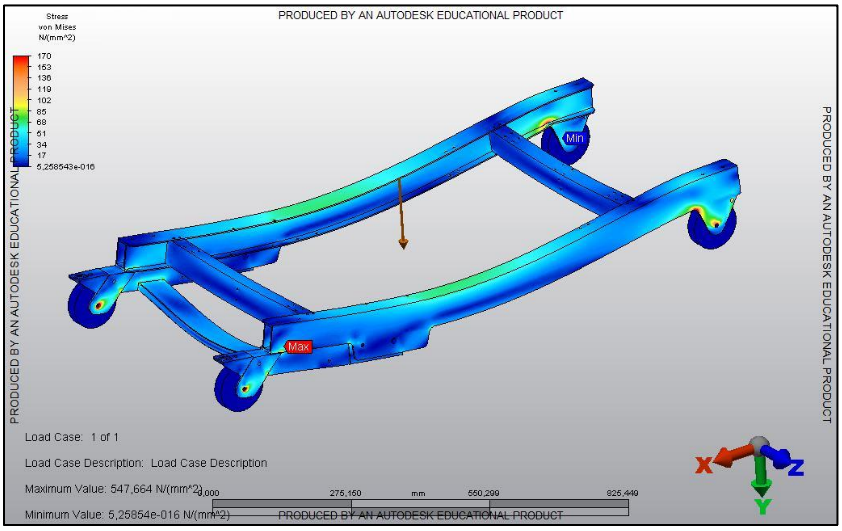

Figure 42. Stress plot

The von Mises stress in the structure is mainly between 30 and 80Mpa. Stress concentration areas (in which the equivalent von Mises stress exceeds the yield limit) appear in the following locations:

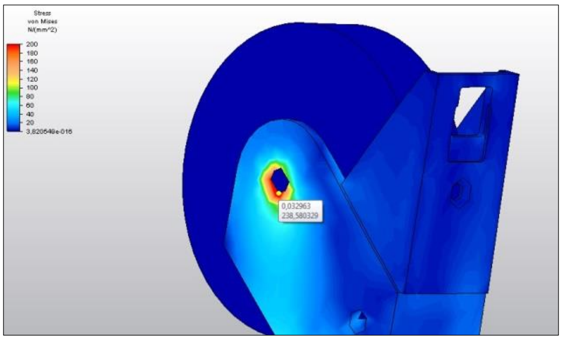

Figure 43. The stress around the hole is 255MPa

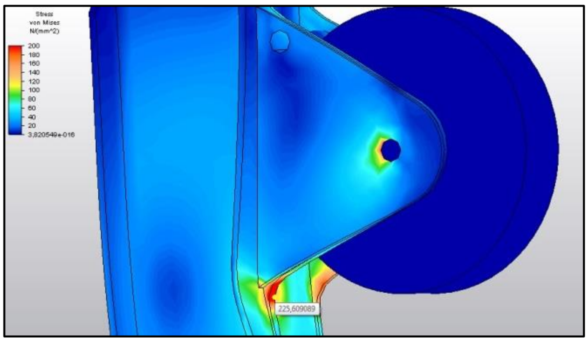

Figure 44. The stress at the sharp edges is 312MPa

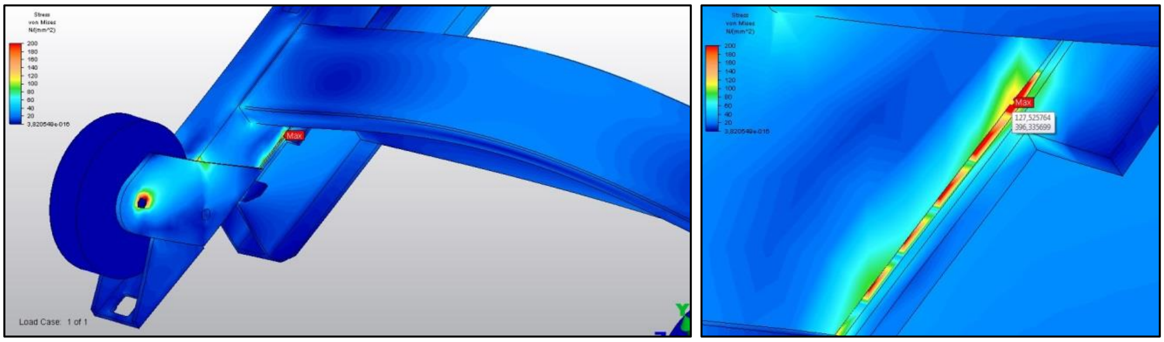

Figure 45. There are trails that run through the bottom of the main beams. The stress values at these trails are near 550MPa.

Displacement and Stress due to Load Case 2

Table 18. Applied load

Acceleration due to body force	9814.56 mm/s^2
X multiplier	0
Y multiplier	0
Z multiplier	10.64

The multiplier is defined as: $ultimate\ load \cdot \kappa_f = 10.64$

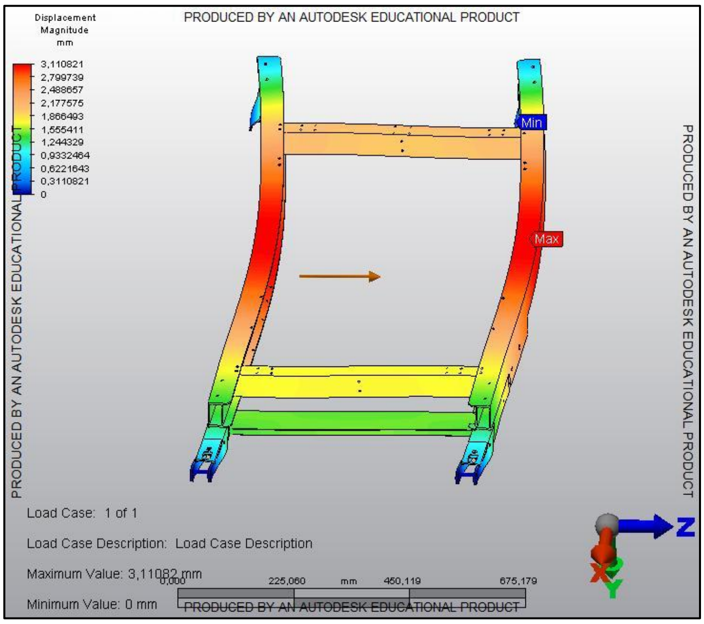

Figure 46. Displacement plot

Maximum displacement: 3.11mm at the main beams.

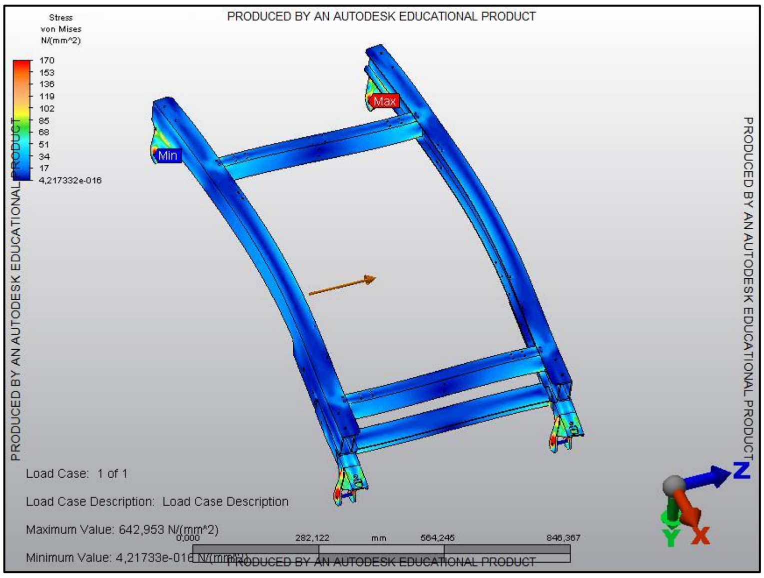

Figure 47. Stress plot

The von Mises stress in the structure is mainly between 20 and 60Mpa. Stress concentration areas appear in the following locations:

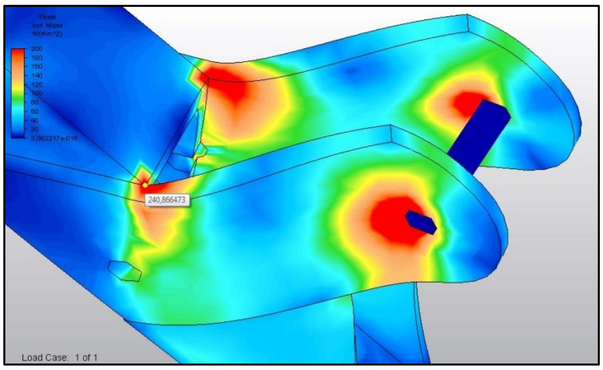

Figure 48. The area around the holes has stress values up to 643MPa. The area around the edges has values around 320MPa

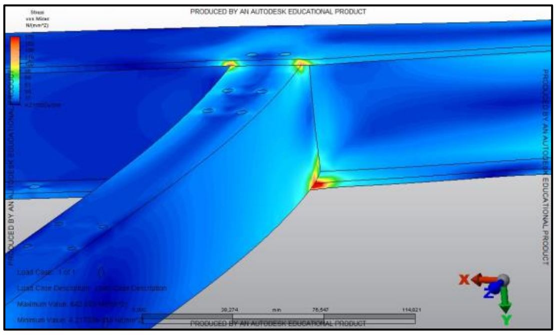

Figure 49. This is the edge between a joist and a main beam. The stress is 260MPa.

Displacement and Stress due to Load Case 3

Table 19. Applied load

Acceleration due to body force	9814.56 mm/s^2
X multiplier	0
Y multiplier	-5.32
Z multiplier	0

The multiplier is defined as: $ultimate\ load \cdot \kappa_f = 5.32$

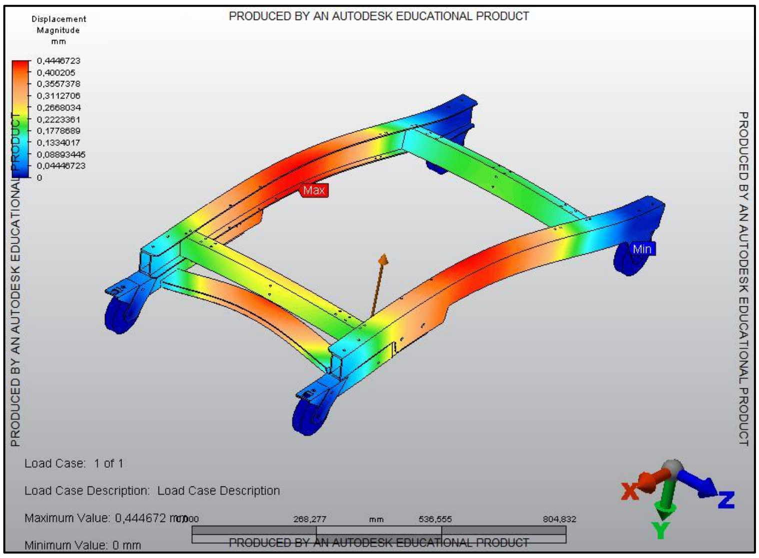

Figure 50. Displacement plot

Maximum displacement: 0.44mm at the main beams.

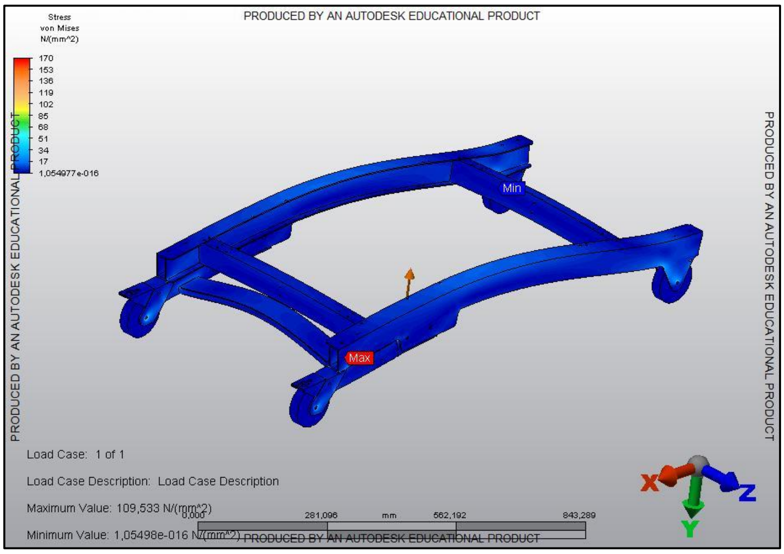

Figure 51. Stress plot

The von Mises stress in the structure is mainly between 5 and 20Mpa. The maximum stress is 109.5MPa and appears at the trails, the same way as for load case 1.

Displacement and Stress due to Load Case 4

Table 20. Applied load

Acceleration due to body force	9814.56 mm/s^2
X multiplier	21.28
Y multiplier	0
Z multiplier	0

The multiplier is defined as: $ultimate\ load \cdot \kappa_f = 21.28$

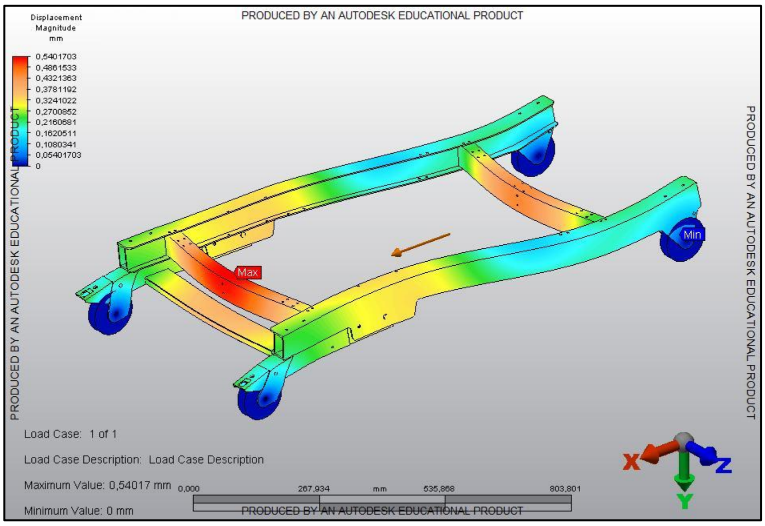

Figure 52. Displacement plot

Maximum displacement: 0.54mm at the front joist.

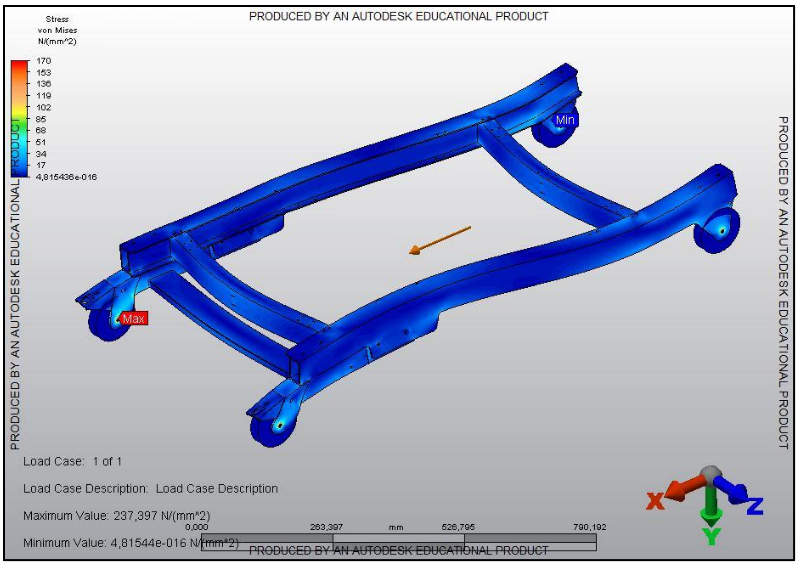

Figure 53. Stress plot

The von Mises stress in the structure is mainly between 5 and 30Mpa. Stress concentration areas appear in the following locations:

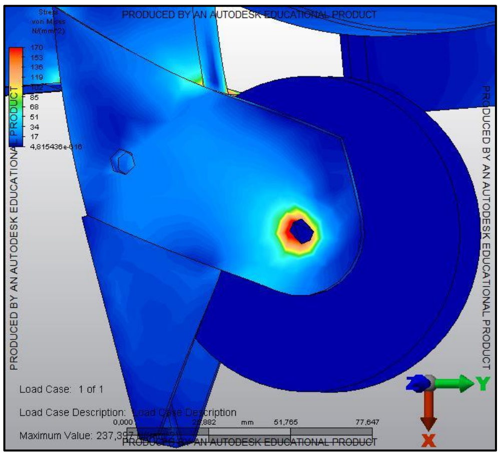

Figure 54. The stress around the hole is 234MPa, which is the maximum stress value for the whole model.

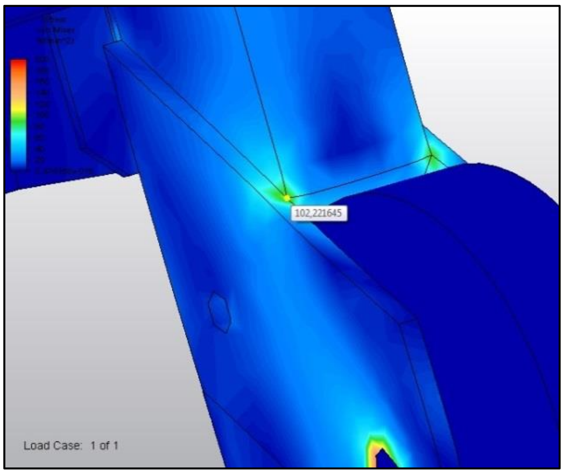

Figure 55. The stress at the edges is around 120MPa

One Point Load due to Load Case 5

In this case, the load was applied differently and only the greatest load which depends on 20g acceleration was studied. The forces that are applied are calculated the same way as in chapter 4.3.4 one point load.

$$P = \frac{m_{body} \cdot ultimate\ load \cdot \kappa_f}{2} = 10\ 046.4\ N \quad (15)$$

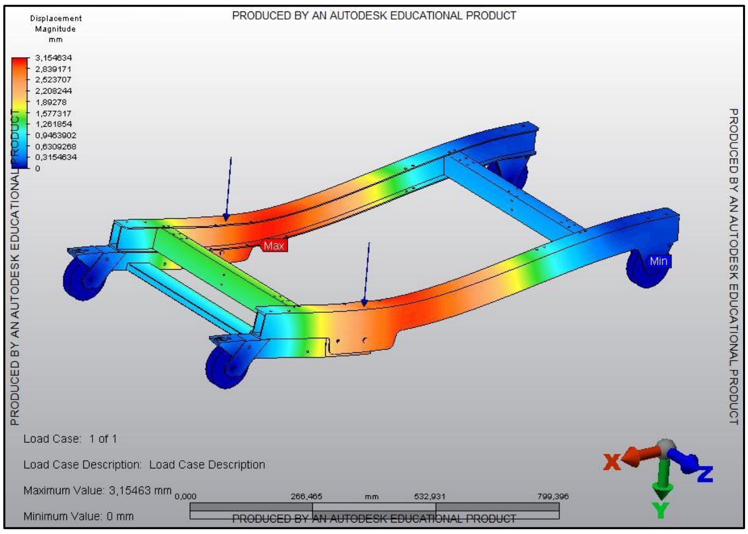

Figure 56. Displacement plot. The arrows show where the point load is applied.

Maximum displacement: 3.15mm at the main beams where the force is loaded.

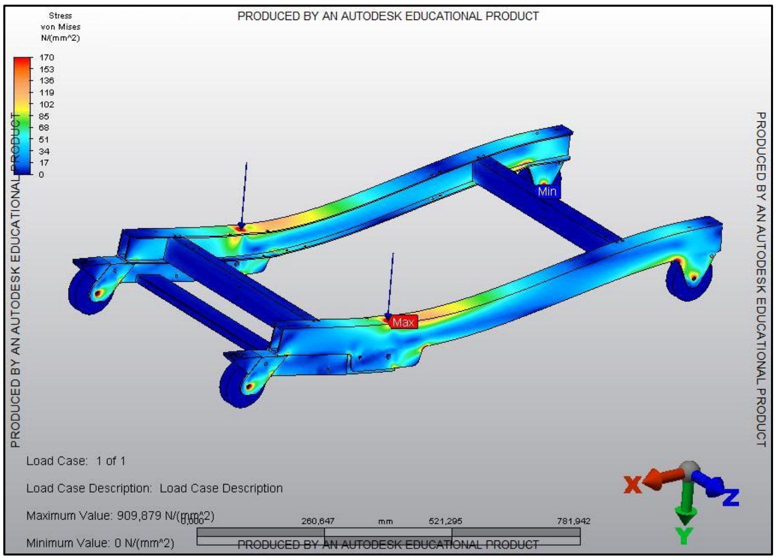

Figure 57. Stress plot

The beams are more affected than before. The area near where the load is applied shows stress values from 60 to 120MPa. The area where the load is applied shows stress values up to 910MPa. Other stress concentrations appear in the same way as in load case 1.

4.7 Discussion

The normal stress is calculated for comparison between numerical simulation and handbook calculations. The normal stresses should have similar values within reasonable limits and thereby validate the calculations. The values in the results show that this is true and the specific stresses for each case did not differ significantly between the numerical simulation and the handbook calculations. The stress values range between 4 and 120 MPa for all cases in both calculations. The normal stress for the handbook case when the joist is subjected to a one point load differs significant from the others. However it can be discussed whether this case would ever come near to reality since the stretcher will never be subjected to this kind of load and neither will the joist. Even though the weight and the load were scaled it is still far from reality. The same case shows that the stress at the joist is much lower in the numerical simulation and has no critical impact. That is why this case is not reliable and can therefore be considered as unimportant.

However, the stresses do differ between the numerical simulation and handbook calculations. This is because of the different assumptions that were made. For the handbook calculations the structure was separated into individual beams and then subjected to different load cases. For the numerical simulation the whole load bearing part was subjected to the load cases and therefore the results between the two methods will differ. Nevertheless since the calculations show similar result they validate each other and through this the strength of the stretcher.

The displacement and the deflection differ between the handbook calculation and the numerical simulation. This depends on the fact that the handbook calculations only consider the deflections in the same direction as the load direction while the displacement from the numerical simulations consider the magnitude of the deflection vectors. If the corresponding vector value for the same vector as in the handbook calculations would have been examined, more similar results would probably have been achieved.

4.7.1 Handbook Calculations

The mass of the stretcher with all its components was included in all calculations. Since the main beams are attached with joists, that can be assumed to be fix, the beam was divided into three parts to consider the boundary conditions that appeared. Assumptions regarding how the masses were divided for these parts of the beam were made, using the relation between length and mass of the stretcher. In reality the distribution of the weight is too complicated to calculate by hand. To compensate for this, the assumptions were made with greater loads than the load bearing part should manage. This gave yet another margin of safety that showed that the beams can handle larger loads without critical deflection or buckling.

As seen in the results in chapter 4.6.1, the values for deflection are not high or critical. The extent of the deflection can be used when determining the stiffness properties. The loads that are considered for these calculations represent the loads during a crash landing and are therefore assumed to be substantial. Since the deflections were very small for this structure it showed that the beams have good stiffness properties, which seem reasonable since the beams are made of aluminum.

The assumption regarding the relation between the stretchers weight and length is only a theory developed for this project. This means that to strengthen or validate the handbook calculations it could be investigated how this assumption could have been made differently and more accurate. Although since these handbook calculations are validated by numerical simulation calculations this is not necessary.

Buckling
Only attachment 1 was taken into consideration as mentioned previously. Because of the deflection results that show that the difference between attachment 1 and 2 are negligible and if the stretcher can handle the loads for attachment 1, it would undoubtedly handle the loads for attachment 2 as well. It was therefore no idea to calculate buckling for attachment 2.

The values in the results according to linear beam theory are far below the critical values, which show that there is no risk of buckling rather that the forces could be much larger without any significant impact. The calculations from Eurocode 9 shows similar results, which also indicates that all the beams are safe from buckling and they are also far below the critical values. These results are perfectly reasonable considering the forces acting on the stretcher.

The two methods differ in quite a few ways but they are both based on the same principle. This principle compensates for the fact that predictions based on the analytical critical load according Euler's buckling cases are non-conservative. Both methods therefore treat buckling analysis from a more practical perspective and also the material, aluminum, is taken into account. However the main differences are the various factors used for the calculations. In the buckling check according to Eurocode 9 many different factors were taken into account, for example factors for welding and imperfection. This is what makes the method more precise and accurate. Linear beam theory on the other hand looks at practical calculations as well but does not use as many safety factors. However it uses a table to find the tension and since this is the maximum tension allowed before buckling it can be used to calculate the critical load. It is therefore difficult to know which type of factors that are included in the table and if they can represent those that are used in Eurocode 9.

4.7.2 Numerical Simulation

The results from the simulation show values in all cases as the stress of the main part of the model barely gets higher than 100MPa. It could therefore be established that the structure does not present significant yielding. However, as the results show, it appeared a few stress concentrations at certain points. These can be neglected in the stress calculations since a static strength analysis is performed. Local plastic deformation will take place in these areas and the stress will redistribute. This does not impact the static strength but these stress concentrations can be misleading in the results, it is therefore important to analyse and discuss why they emerge.

Stress concentrations at the trails on the bottom of the main beams

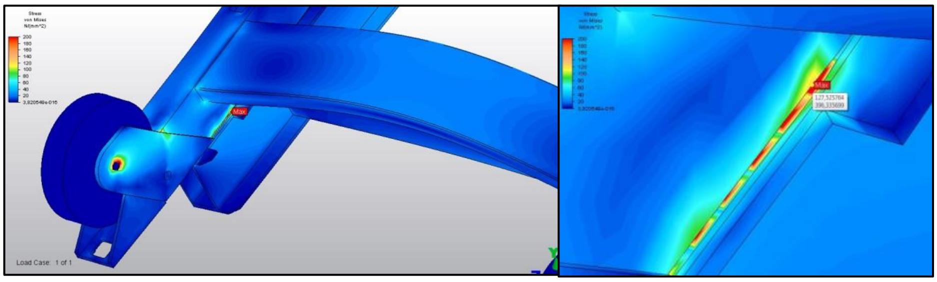

Figure 58. Stress concentrations at the trails

There are trails that run through the bottom of the main beams as shown in Figure 59. These are made as protection when the support part, on which the wheels are assembled to, collides with the beams. The trails have a thickness of 1mm and are meant to be slowly worn out due to aging. The stress values at these trails were near 550MPa.

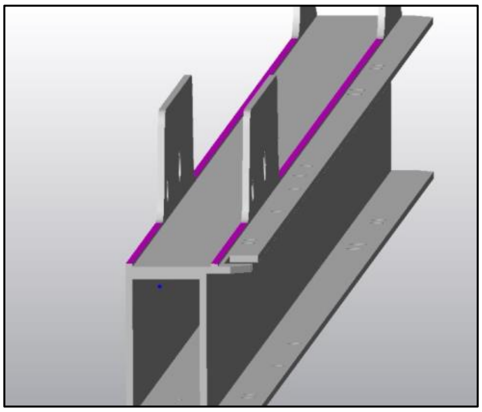

Figure 59. The trails are marked with purple

An analysis was done where these trails were removed from the model to make sure that the stress concentrations appeared because of the trails; and it showed to be true. Worth noting is that these stresses only occurs from loads in y-direction, in other words, upwards and downwards. Another main reason why this area got high values is because of the mesh quality in this area. However, these values do not matter since the area is not critical.

Stress concentrations around the holes at the wheels

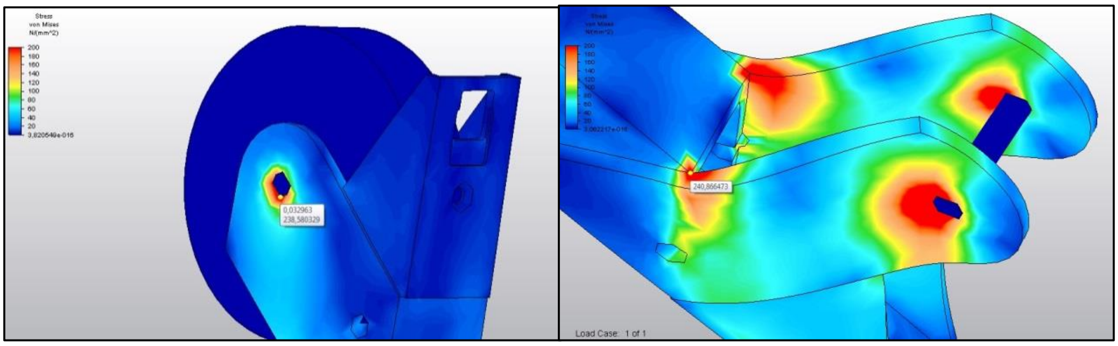

Figure 60. Stress concentration around the holes

These areas showed to be critical for loads in all directions. In Figure 60, the picture to the right is the stress plot from the 8g load which shows very high stresses around the holes where the wheels are attached. The main reason for this is that the boundary condition is set at the joint that holds up the wheel, the blue stick in the right picture. As mentioned before, this is not how it will work in reality. The wheels are attached in a different way, as seen in Figure 61 below, this means that the stretcher will have four attachment points. This concludes that the area around the wheels will not be subjected with as much load as the results show. Therefore further studies together with fixation system is needed.

Figure 61. This is how it looks like in reality. The outer attachment will be fixed in the fixation system which does not allow the stretcher to move.

Stress concentrations at the edges

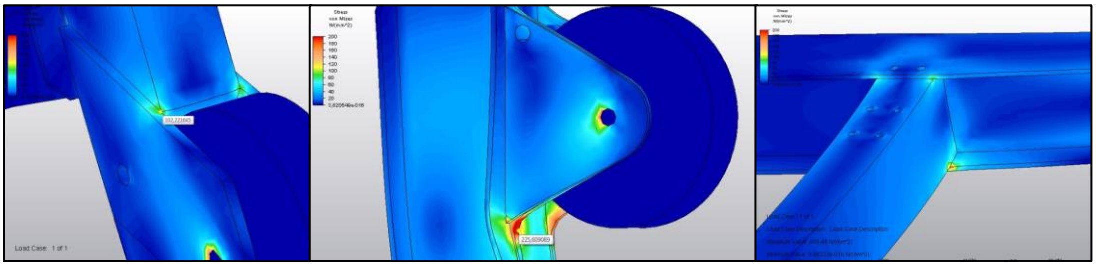

Figure 62. Stresses at the edges

These stress concentrations are typical for edged structures. The edges are more rounded in reality compared to the edges in the 3D-model which explains the high stresses at these areas in the simulations. If the requirements were to consider fatigue issues, the stresses concentration factors at radii would be interesting.

One Point Load
First of all the g forces will never act as a point load. There will be a distributed load over an area even if a person sits in a position as shown in Figure 24. The stresses, 910MPa that occur right at the point loads can be ignored because the load would never be applied as one point in reality.

4.8 Conclusion

The conclusion is based on both handbook calculations and numerical simulations that together verify overall similar results. Based on these aggregated results, it concludes that the stretcher withstands the required ultimate loads that are imposed by EASA.

4.9 Optimisation

An optimisation process was made to examine if it is possible to simplify the structure by reducing material without affecting structural and stiffness properties. This would make the stretcher cheaper and lighter, although it is important to consider whether these changes are operable in practice.

The thickness of the cross-section of the beams which constitute the computational model has been reduced as shown in Figure 63.

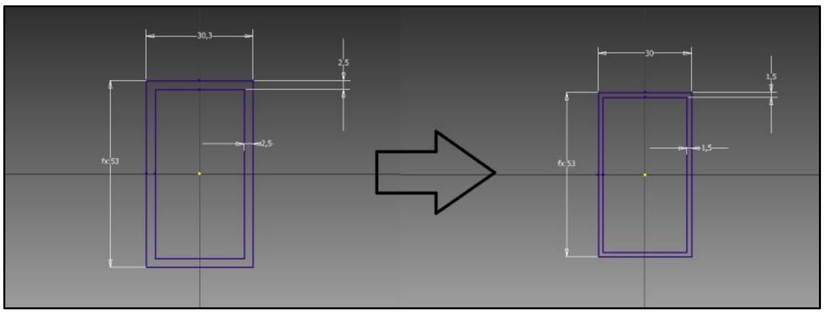

Figure 63. The thickness of cross section at the joists is thinner

Another detail that was easy to reduce at the same time was the pedal in the support part to see if it was necessary to have such a big pedal as before. The comparisons of the pedals are seen in Figure 64.

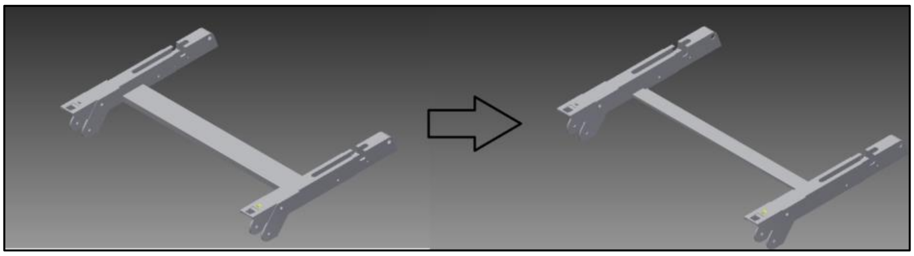

Figure 64. The pedal to the right is narrower

The old pedal had a volume of 368706mm^3 and the new one have a volume of 102201mm^3. The new mass of the model is 5.85kg which is a material reduction by 22%.

Displacement and Stress due to Load Case 1

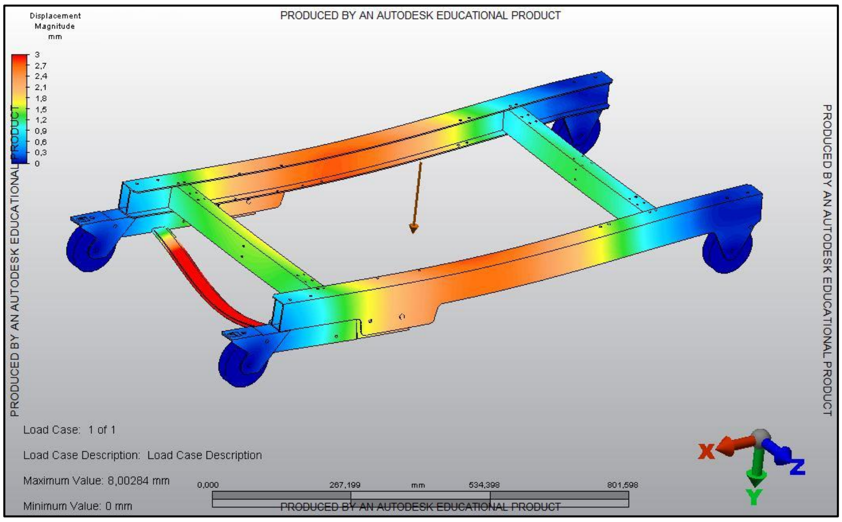

Figure 65. Displacement plot

Maximum displacement: 8mm at the pedal, see Figure 65.

The displacement at the main beams is approximately 2.6mm. The beams were bent similar to the original while the pedal was bent much more now when it is smaller.

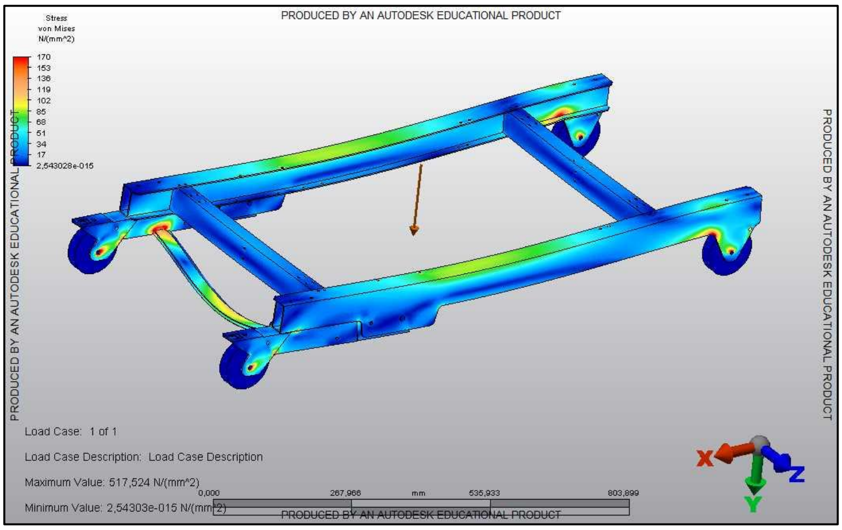

Figure 66. Stress plot

Unlike the previous model the beams are subjected to higher stresses, in this case around 30 to 90 MPa. It also appears stress concentrations at a new area, which is shown in Figure 67.

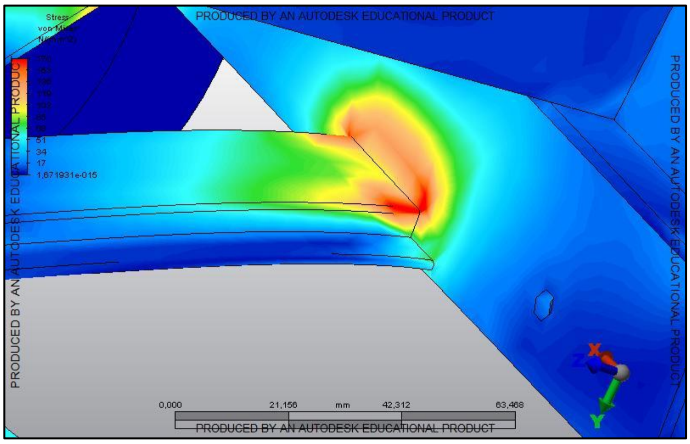

Figure 67. This is the area where the pedal is welded to the main beams.

As can be seen in Figure 67; the stresses reach values of 230MPa. However, it can be discussed whether this is true because the part is welded and the 3D-model does not have rounded edges as in reality.

Other stress concentrations occur at the same areas as for the original model and shows approximately the same stresses. The values differ with 20-40MPa.

Displacement and Stress due to Load Case 2

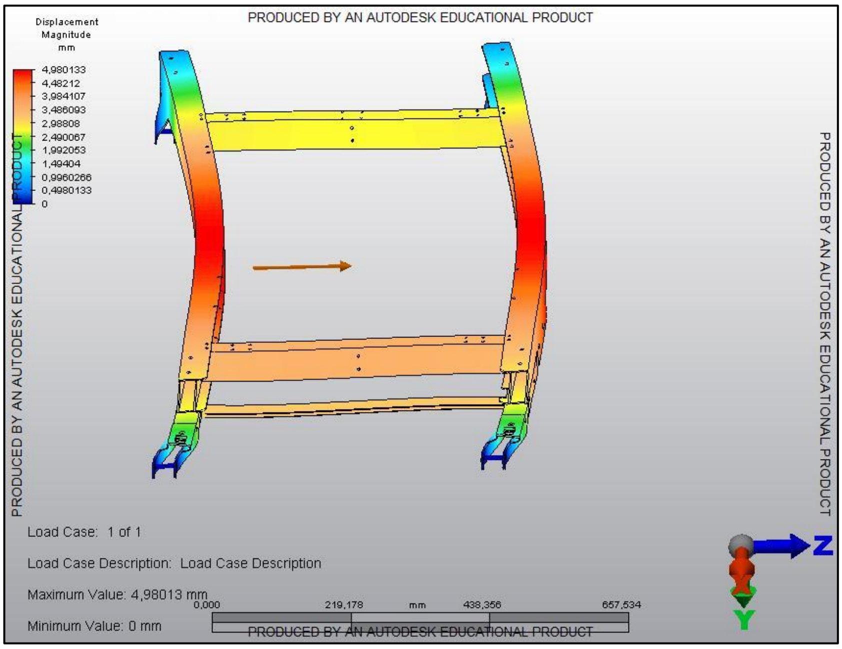

Figure 68. Displacement plot

Maximum displacement: 4.98mm at the main beams - an increase with 2.74mm from the original model.

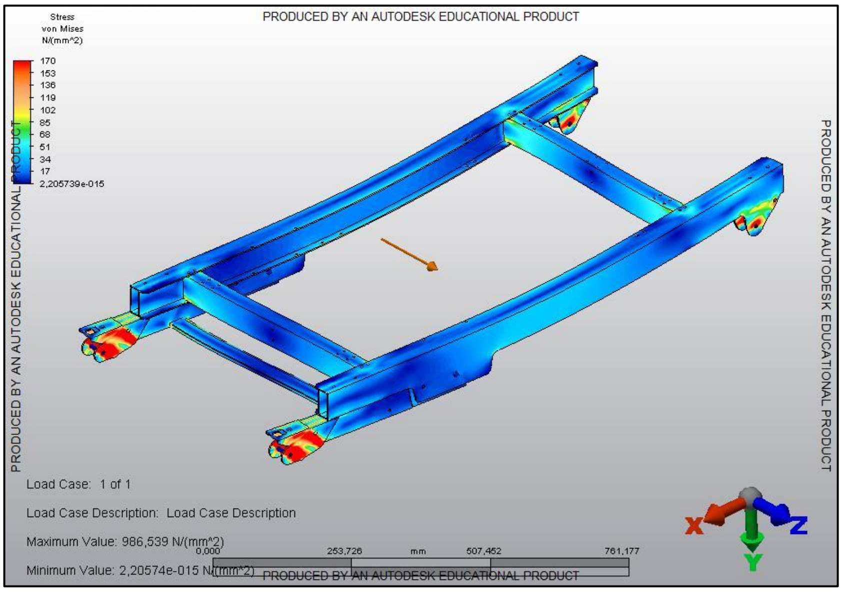

Figure 69. Stress plot

The plot shows the same values on the beams as for the original model. The same stress concentrations appears but with higher values. The stresses near the joints for the wheels have values up to 987MPa, and other edges have values around 350MPa.

Displacement and Stress due to Load Case 3

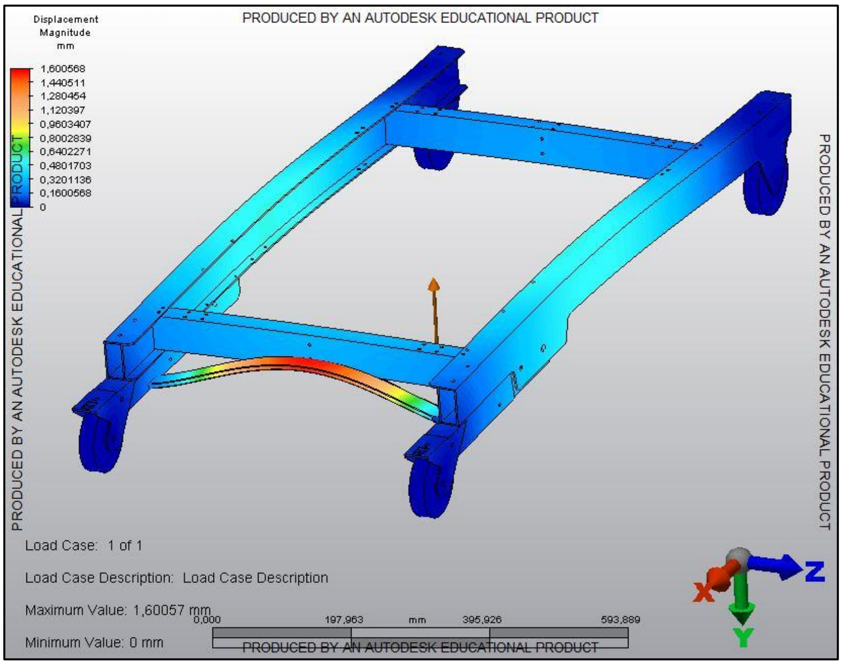

Figure 70. Displacement plot

Maximum displacement: 1.6mm at the pedal. The displacement at the beams is the same as for the original model, around 0.53mm.

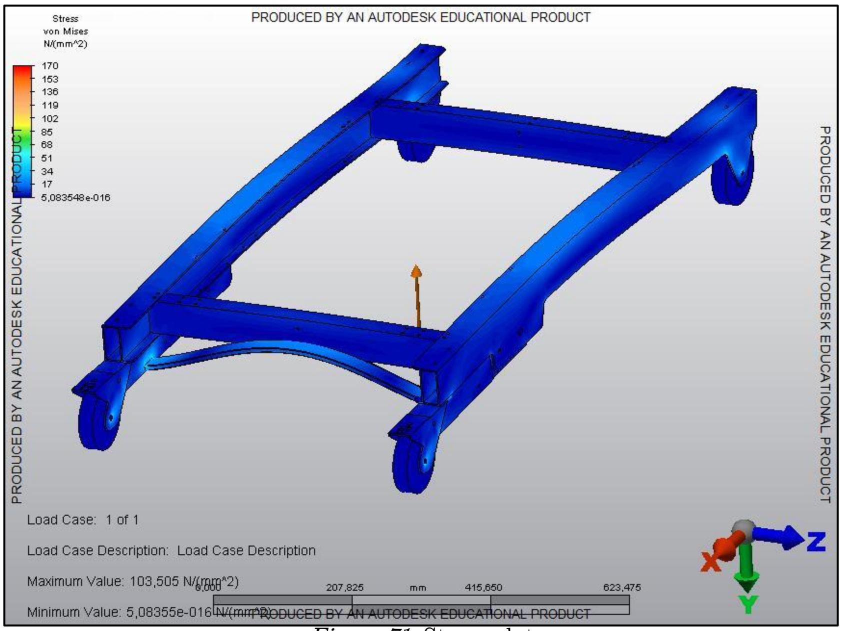

Figure 71. Stress plot

The stress plot in Figure 71 shows almost the same results as for the original model.

Displacement and Stress due to Load Case 4

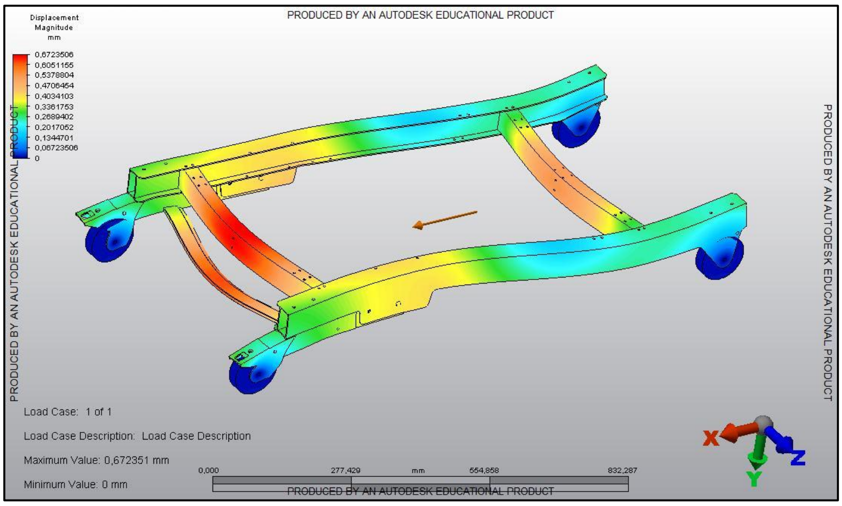

Figure 72. Displacement plot

Maximum displacement: 0.67mm at the front joist and at the pedal. The deflection has increased with about 0.28mm from the original.

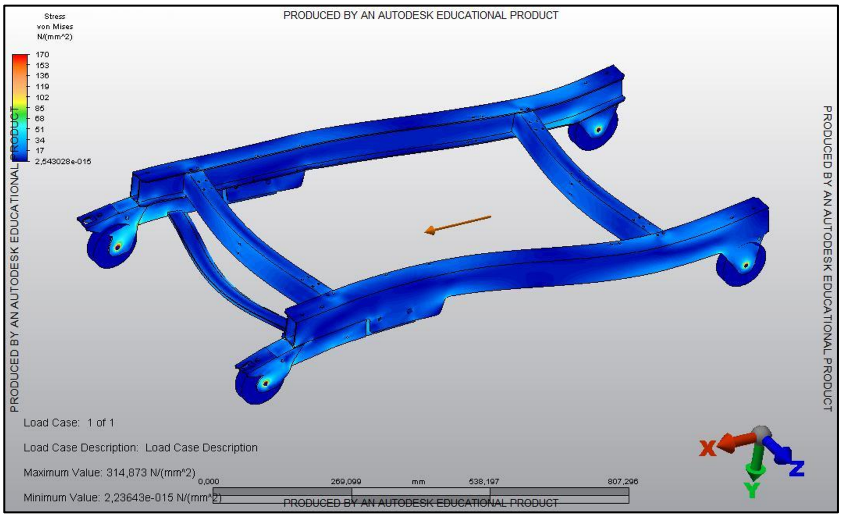

Figure 73. Stress plot

No noticeable difference from the original model was observed which indicates that there is no major difference between the results where the stresses at the main beams are between 5 to 30MPa. The same stress concentrations occur as for the original model.

One Point Load due to Load Case 5

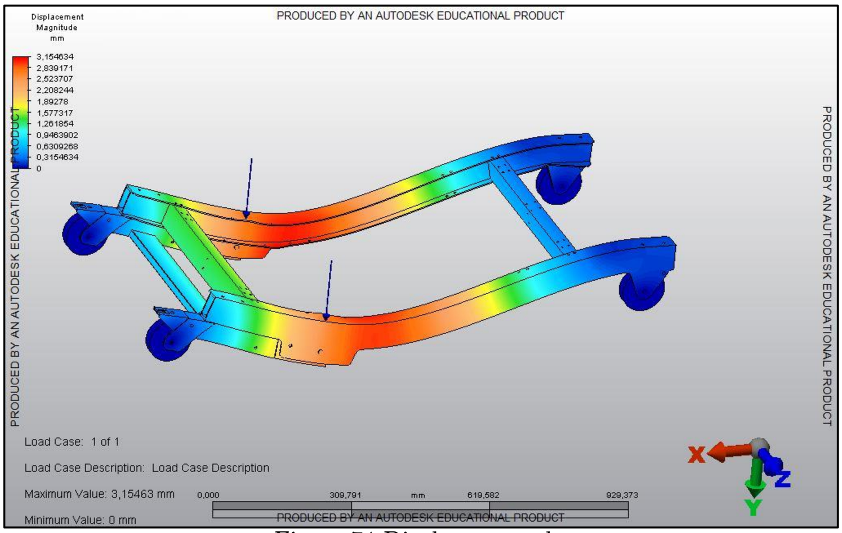

Figure 74. Displacement plot

Maximum displacement: 4.09mm at the main beams where the force is loaded; an increase with 0.99mm from the original model.

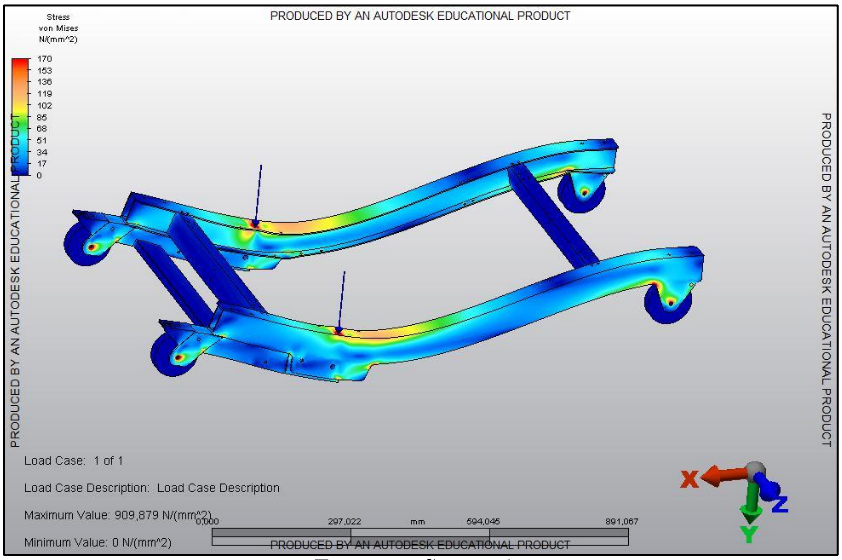

Figure 75. Stress plot

As the plot can tell, there are very high stress values where the force is placed; almost three times higher than the original. This is obviously because of the thickness decrease at the beams.

Discussion

The result for the optimisation shows higher stress and displacement values than the original model. When analysing the whole structure it would still be allowed to reduce the materials and still get acceptable results. But there are some areas that might get critical when they are made thinner. These areas are where the pedal is welded when applying 20g downward and the area around the holes at the wheels when applying 8g sideward. The stiffness at these areas is clearly reduced. However it may be discussed how important the pedal is to stiffness property for the load bearing part. It is also hard to determinate if the area around the hole would be able to stand against failure or undergo significant yielding because in reality, the boundary values are set in a different way. But to be sure, it is not recommended to make these areas that thin and non-linear simulations could therefore be an interesting future approach to further study weight reduction.

However it is a question about the manufacturing restrictions and user friendliness for the customer. When reducing the material of a product it is important to check the manufacturing restrictions that may be a hold back for the new construction, especially when it comes to such thin constructions. The material reduction might also give negative effect on the user friendliness for the customer. For example, the reason for the size of the pedal may be made because it will be easier for the staff to use the stretcher and making it smaller might cause problems.

5 Fixation System

The stretcher is the tool that helps the paramedics to carry an injured person in and out from the helicopter, it is therefore important to make it as easy as possible for the paramedics to attach and detach it in the helicopter. The stretcher is placed preferably where the orange parts are located in Figure 76. As the figure shows, the stretcher is surrounded by objects in the helicopter that gives limited access to manage it. When the stretcher is unnecessary for the helicopter operation it is desirable to use its space for cargo. Consequently it is convenient to design the fixation system to be as low as possible to not take up unnecessary space. This also reduces the different ways the attachment can be designed and all the concepts in 5.4 are taking these limitations into account. In this chapter the developing process is shown and a final concept is presented.

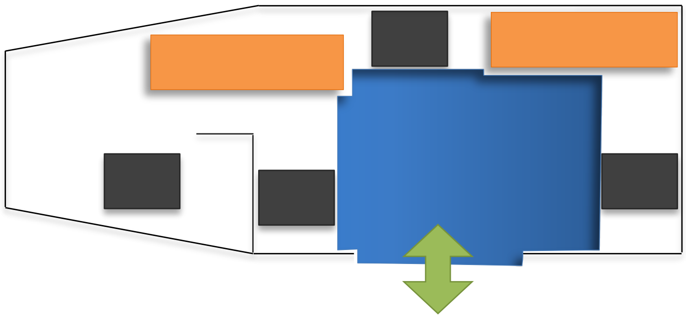

Figure 76. Interior of the helicopter.

5.1 Method

Several tools were used to develop the fixation system for the stretcher. First of all a requirement specification was produced, based on that concepts for both positioning and locking were generated through brainstorming. All concepts were compiled to a morphological matrix and an evaluation process was made. The first step was to make an elimination matrix to eliminate the concepts that for different reasons were not realisable. The next step in the process was to rank the concepts. This was done by making two Pugh matrices, which were based on the requirement. By considered the result in both matrices a final concept was developed. To evaluate the material and manufacturing method of the final concept a LCA was performed with several assumptions. These are presented in the following list:

- Traveling distance of 240km/day.
- 365 flight days/year.
- The same construction of the fixation system was used for both titanium and aluminium.

To enhance the understanding of working with the stretcher in reality and how it is used, study visits at the ambulance helicopter base in Säve, the ambulance division at Sahlgrenska University Hospital and the stretcher manufacturer Ferno Norden were organised. The choice of the visits was made to get diverse input from different users. To find out what the SAR crew thought about working with the Allfa Europe Premium stretcher an interview was held.

5.1.1 Attachments

Further on, the following names are used to describe the different attachments on the stretcher: The inner attachment and the outer attachment. See Figure 77 and Figure 78.

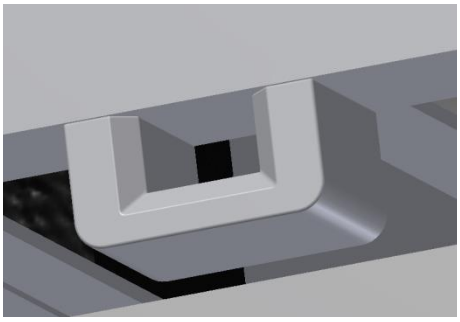

Figure 77. The inner attachment.

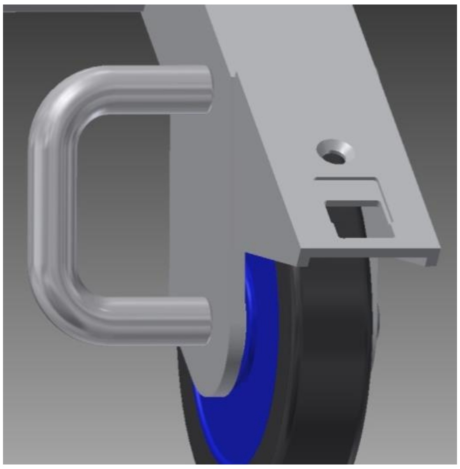

Figure 78. The outer attachment

5.2 Black Box and Function Structure

In the beginning of the development process a hypothetic black box, Figure 79, and function structure, Figure 80, were made. The hypothetic black box and the function structure are tools which help to develop the fixation system in an open-minded way without the influence of existing products[12]. The black-box describes inputs and outputs to the fixation system and the function structure describes more in detail the assumed steps for the function of the fixation system.

[12] Söderberg, Rikard. *Produktarkitektur*, lecture 2013-10-28

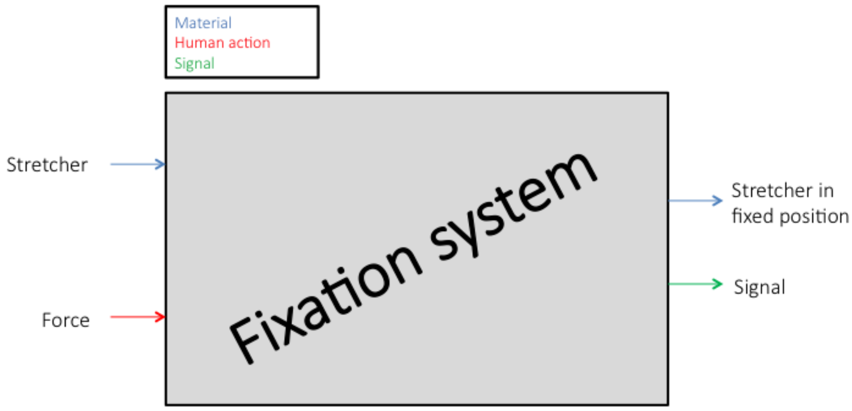

Figure 79. Black box fixation system.

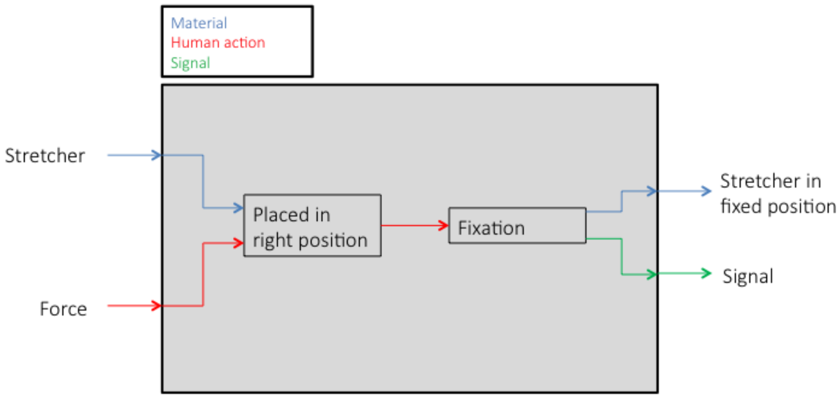

Figure 80. Hypothetical function structure

After visiting the ambulance helicopter base in Säve, a function structure for an existing product was developed. The fixation system used in the ambulance helicopter is shown in Figure 81. These function structures were later used to define necessary functions for the fixation system.

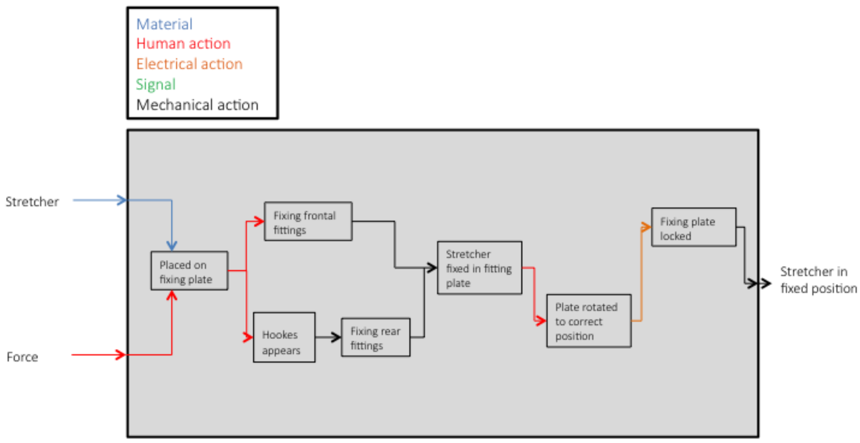

Figure 81. Function structure of the fixations system in the Ambulance helicopter.

5.3 Requirement Specification

The specification contains requirements and requests that define the groundings for the product. To define these, requirements from EASA, CS 29, and information from Heli-one, paramedics and helicopter crew from Gothenburg were considered and the requests were graded based on significance on a scale from 1 to 5, where 5 is the most significant. A description on the control method for the requests and requirements was also presented. The result can be seen in the Table 21.

Table 21. The table shows the requirements and the requests that the fixations system must have.

Requirement Specification				
Requirement/request	**Control method**	**Value**	**Requirement/Request**	**Weight**
EASA				
Comply with certification requirement (EASA CS 29)	Calculation, test	-	Requirement	-
Size				
Weight	Calculation	40 kg	Requirement	-
Weight	Calculation	20 kg	Request	4
Time between service	Calculation, test	1 year	Requirement	-
Maximum height	Calculation	200mm	Requirement	-
Time				
Installation time for stretcher	Evaluation	15s	Requirement	-
Installation time for stretcher	Evaluation	5s	Request	2
Demount of stretcher	Evaluation	20s	Requirement	-
Demount of stretcher	Evaluation	7s	Request	2
Service life	Calculation, test	10 years	Requirement	-
Environment				
Ability to separate materials at disposal	Evaluation	95%	Request	1
Number of components	Calculation	20	Request	2
Maximum number of different materials	Calculation	5	Request	1
Features				
Possibility to strap cargo	Evaluation	-	Requirement	-
Possibility to place the stretcher in two directions	Evaluation	-	Requirement	-
Possibility to place the stretcher in two locations	Evaluation	-	Requirement	-

Requirement/request	Control method	Value	Requirement/Request	Weight
Number of people needed to locate the stretcher in right position	Evaluation	2	Requirement	-
Safety				
No risk of injury	Evaluation	-	Requirement	-

5.4 Brainstorming

To generate concepts for the fixation system a brainstorming was used to get as many ideas as possible. In the following sections all of the generated concepts are described. Concept A-G is the actual fixation and concept 1-5 is how to locate the stretcher in right position.

5.4.1 Concept A – Ambulance Fixation

The concept in Figure 82 is the most commonly used in Swedish ambulances. The left claw is grabbing the fixation point on the stretcher when the stretcher is pushed into the fixation system. The right claw is fixed and prevents the stretcher to move forward and upward.

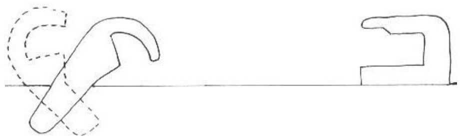

Figure 82. Sketch for concept A

5.4.2 Concept B – The Pinball

The fixation system has a function that can bend downwards but not upwards, as shown in Figure 83. When the stretcher is pushed into the system the attachments will push the blocks apart and thereafter attach. If a force affects the stretcher upwards, the blocks will stop it. The concept works similar to a reversed pinball machine.

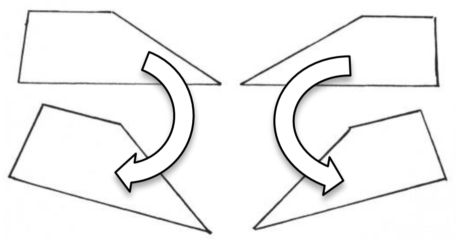

Figure 83. Sketch for concept B.

5.4.3 Concept C – The Sideway

This concept looks like concept B but with the difference that the blocks are separated sideways instead. Figure 84 shows the sequence.

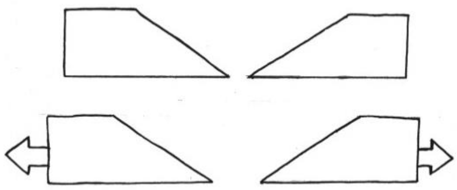

Figure 84. Sketch for concept C.

5.4.4 Concept D – The Pit

The function of this concept is shown in Figure 85. The attachment is inserted in a cavity and is blocked in five directions. To stop the movement in the direction upwards a plate is pushed though the loop.

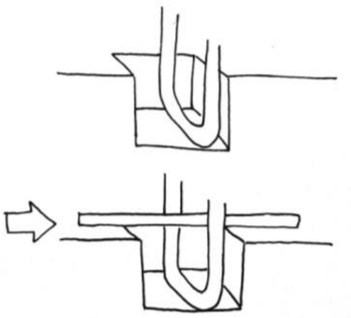

Figure 85. Sketch for concept D.

5.4.5 Concept E – The Taxi

Some taxis are equipped with stretcher attachments to enable patient transportation. In these taxis, there is a fixation system that may be useful for this application. The system is currently too heavy to be installed into the helicopter and needs to be further developed. The concept can be seen in Figure 86

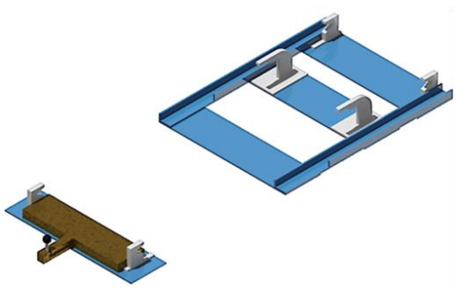

Figure 86. The Taxi attachment.

5.4.6 Concept F – The Claw

This concept is based on the same principle as a carabineer. When the stretcher is pushed into position all four claws grabs at the same time as shown in Figure 87. To release the stretcher manual operation is needed.

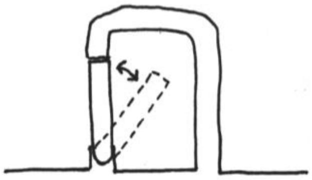

Figure 87. Sketch for concept F.

5.4.7 Concept G – Helicopter Fixation

The fixation system in one of the ambulance helicopters at Säve has the following functions. The first fixation, see Figure 88, is similar to concept F with the same principle as a carabineer. The second fixation is the same as in concept A and E, with the exception that it can be pushed down under the floor to make room for the rest of the stretcher. See Figure 89.

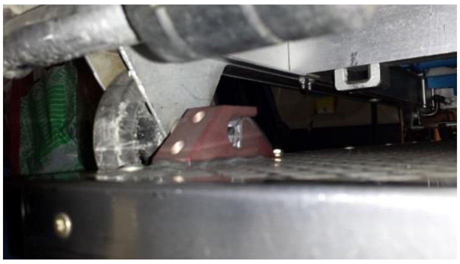

Figure 88. The stretcher attached to the fixation system.

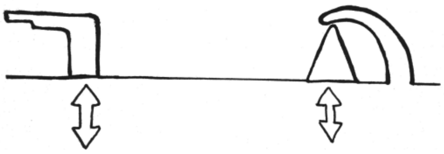

Figure 89. Concept for fixation system

5.4.8 Concept 1 – The Lift

The position of the stretcher makes it difficult for the paramedics to roll or drag it on the floor in the helicopter. The blue container, see Figure 76, is blocking the path from entrance or exit to the stretcher's attachment position. The container is surrounded by high edges and consequently the stretcher must be lifted over the edges and thereafter be lowered down into the fixation system vertically, see Figure 90.

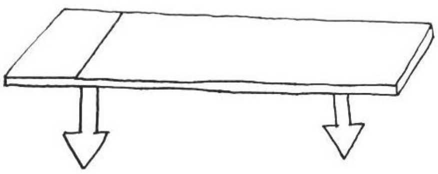

Figure 90. Sketch for concept 1.

5.4.9 Concept 2 – The Slide

Due to limited space in the helicopter the stretcher accessibility is limited from different directions. The paramedics need the space in front and in the back of the stretcher to carry it and put it in place. The stretcher is shoved into the right position. The concept is sketched in Figure 91.

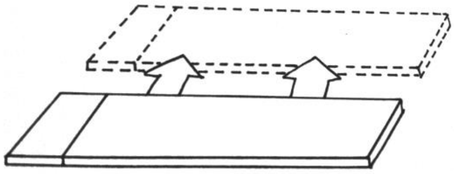

Figure 91. Sketch for concept 2.

5.4.10 Concept 3 – The Rail

This concept is based on opinions from paramedics working within *Västra Götalandsregionen*. They think that the Allfa Europe Premium stretcher is heavy and not user-friendly. The implementation in a helicopter would not make things easier. To minimize the trouble of handling the stretcher, a rail can be placed on the floor of the helicopter, see Figure 92.

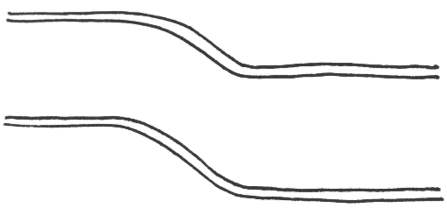

Figure 92. Sketch for concept 3.

5.4.11 Concept 4 – The Rotation

To facilitate the fastening of the stretcher to the fixation system it is convenient to work from one direction since the stretcher is placed in a corner. This concept is based on the idea of a rotation to fixate the stretcher as seen in Figure 93. The following list describes the procedure of the concept.

1. The stretcher is inserted straight into the fastening point.
2. It is attached on the first point that can rotate.
3. The stretcher rotates 90 degrees into final position.
4. It is attached on the second point that holds the stretcher in a fix position.

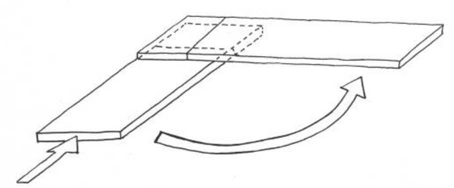

Figure 93. Sketch

5.5 Matrices

Morphological Matrix

A morphological matrix is a commonly used tool to illustrate how to combine the different sub concepts into full concepts[13]. In Table 22 all the earlier described concepts are presented in a morphological matrix. How these concepts can be combined is shown in Appendix F, where "x" means that the concepts can be combined.

Table 22. Morphological Matrix.

MORPHOLOGICAL MATRIX					
Positioning			Locking		
1	The Lift		A	Ambulance attachment	
2	The Slide	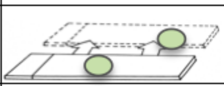	B	The Pinball	
3	The Rail	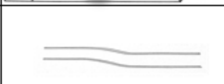	C	The Sideway	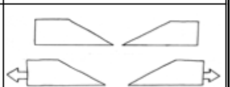
4	The Rotation	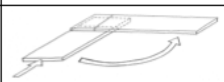	D	The Pit	
			E	The Taxi	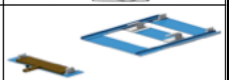
			F	The Claw	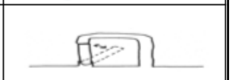
			G	Helicopter attachment	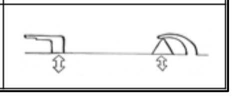

Elimination Matrix

The elimination matrix is used to eliminate unrealisable concepts, or those concepts that clearly would not meet all requirements.[14] The first step in the elimination process was to use an Elimination matrix, which can be found in Appendix F. The reasons why some concepts were eliminated are presented in "Comments". After the elimination, 8 concepts were remaining.

[13] Lindstedt, Per and Burenius, Jan ; *The Value Model*, 2003.
[14] Lindstedt, Per and Burenius, Jan ; *The Value Model*, 2003.

Pugh Matrix
A Pugh matrix is used to compare the concepts. One of the generated concepts is used as a reference and the other concepts are compared with it. There are two types of Pugh matrices that are commonly used; one where all the compared specifications are weighted and one where they are not. To be sure that the result is consistent the matrix is often made several times with different reference concept[15]. In the Pugh matrix, which can be seen in Appendix F, concepts were graded relatively to each other. Two matrices with different references were produced to get a more accurate result. The criteria were based on the requirement specification earlier presented. As seen in Appendix F the two Pugh matrices both gave the same result. The combined concept A2, F2 and G2 obtained exact the same score and these three were therefore kept for further development.

5.6 Results

By combining the three remaining concepts, one final concept was produced. To lock the stretcher in the front, the same fixation point that was used in A2 was selected. This is a non-moving part that uses the inner attachment to lock the stretcher. In the back the karabiner, presented in F2 and G2, is used to lock the outer attachment. To simplify the procedure of installing the stretcher and the complexity of the construction, the outer attachment is reversed compared to G2. These fixation points are not removable like they are in the concept G2 due to its direction. Therefore the stretcher has to be placed with its first wheels in front of these points otherwise the stretcher will stop at fixation point 2. To make it easier to place the stretcher at right position a steering device was developed. The stretcher is removed by first unlock fixation point 2 and then slide it out of fixation point 1. The following picture, Figure 94, shows the three different components and their positions relatively to each other.

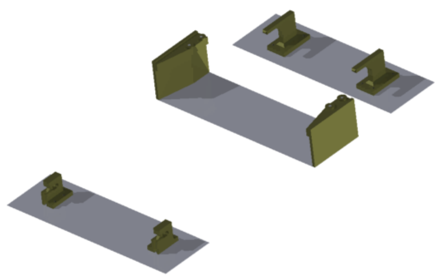

Figure 94. Fixation system – all components.

5.6.1 Fixation Point 1

As seen in Figure 86 fixation point 1 locks the stretcher by the inner attachment. It is wedge-shaped to make it easier to position the stretcher. The front of the fixation point is extended, compared to G2, to meet the request of the possibility to install the stretcher in two directions. The extension is necessary because the distance between the inner attachment and the outer attachment differs by about 10 mm depending on which ends of

---

[15] Lindstedt, Per and Burenius, Jan ; *The Value Model*, 2003.

the stretcher that goes first into the helicopter. The following two pictures, Figure 95 and Figure 96, show what fixation point 1 looks like and where it should be attached.

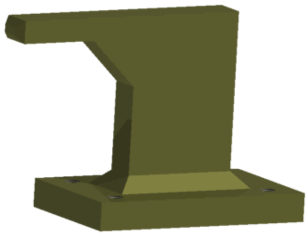

Figure 95. Fixation point 1.

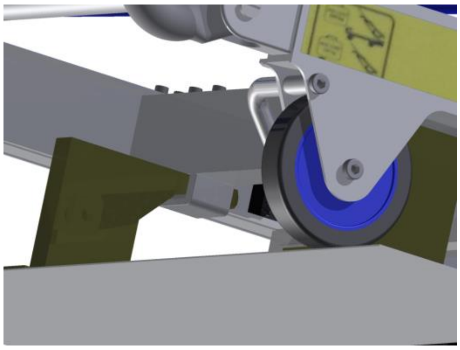

Figure 96. Fixation point 1 – in use.

5.6.2 Fixation Point 2

Fixation Point 2 is based on the function of a karabiner. When the stretcher slides in the fixation it automatically locks the stretcher. To be able to unlock the fixation and remove the stretcher it has to be a gap of a few millimetres between the outer attachment and Fixation Point 2 when the stretcher is in the locked position. Otherwise the locking pin will clash with the attachment when opened. That makes it easy to unlock the fixation system while carrying out the stretcher. A pedal is linked to both locking pins at Fixation Point 2. By lowering the pedal the locking pins are also lowered and the stretcher can be removed. The following pictures, Figure 97, Figure 98 and Figure 99, show fixation point 2 in unlocked state, locked state and with the stretcher attached.

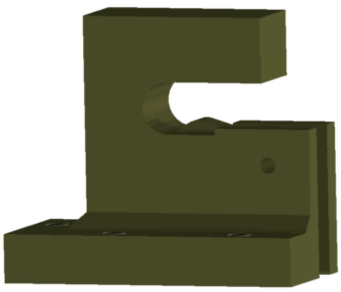

Figure 97. Fixation point 2 – unlocked.

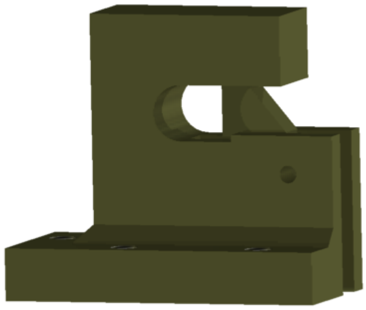

Figure 98. Fixation point 2 – locked.

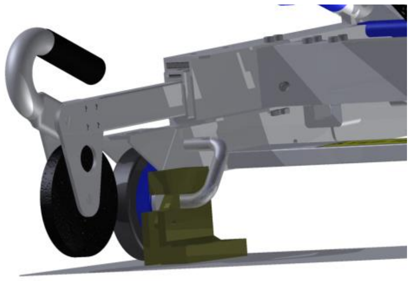

Figure 99. Fixation point 2 – in use.

5.6.3 Steering Device

If the fixation points should be able to lock the stretcher it has to be in the right position. To make that positioning easier a concept of a steering device was developed. It contains two rails, which steer the stretcher into the right position. To minimize the friction, two wheels on each side help the stretcher to slide into the fixation points. The wheels are installed with bearings to make them rotate easier, shown in the Figure 100.

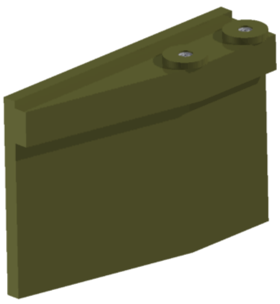

Figure 100. Steering device.

To make the steering device compatible with both direction of the stretcher it had to adjust the stretcher based on the two beams 0024 and 0025 in Appendix H. The reason is that the position of the wheels differed by 1.5 mm sideways. This is shown in Figure 101.

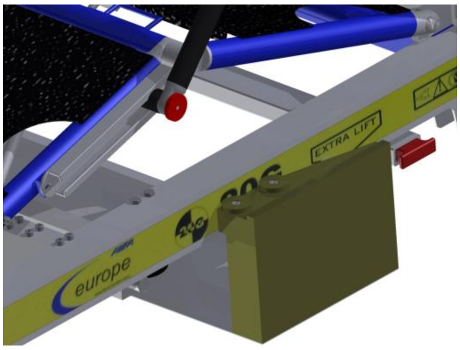

Figure 101. Steering device – in use.

5.6.4 Materials and Manufacturing

The density of the materials is critical when designing components for the helicopter industry. Three kilogram of extra mass results in one mile shorter range for the helicopter[16]. Therefore steel, which often is used in these types of construction, becomes too heavy. That is why all major parts of the fixation system concept are made of aluminium. This material was chosen based on its sufficient mechanical properties combined with its very low density. Another alternative for the material is titanium which has great mechanical properties as well but because aluminium is around 40% lighter than titanium, see Table 23 below, it was a beneficial material for this application. More information about the materials is presented in Appendix E. As seen in the LCA, Figure 102, a fixation system made of aluminium has a much lower effect on the environment than one made of titanium.

Table 23. Material data.

	Titanium	**Aluminum**
Price (SEK/kg)	170	16
Density (kg/m^3)	$4.5 \cdot 10^3$	$2.7 \cdot 10^3$
Young's modulus (GPa)	105	70

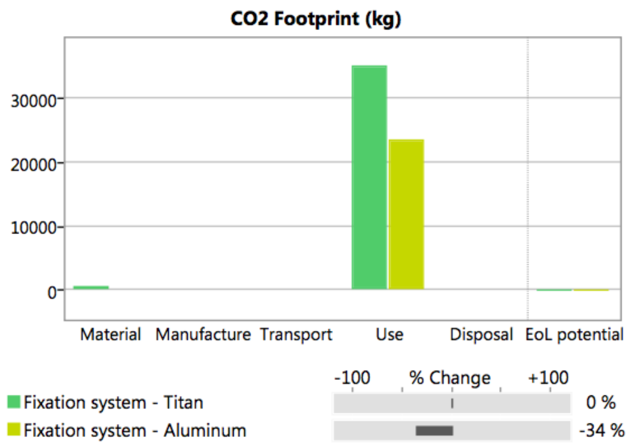

Figure 102. LCA.

[16] Pettersson, Anders. Design engineer. Heli-One. 2014-05-16.

5.6.5 Achieved Requirement Specification.

As seen in Table 24 most of the requests and requirements are met but a few have to be further investigated. Green means met and grey means further investigation needed.

Table 24. Achieved Requirement specification.

Achieved Requirement Specification				
Requirement/request	**Requested value**	**Met/Not met**	**Comment**	**Real value**
EASA				
Comply with certification requirement (EASA CS.29)	-	?	See chapter 5.7	
Size				
Weight	40 kg		According to 3D-model	12kg
Weight	20 kg		According to 3D-model	12kg
Time between service	1 year	?	See chapter 5.7	
Maximum height	200mm		According to 3D-model	140mm
Time				
Installation time for stretcher	15s		Estimated value	<5s
Installation time for stretcher	5s		Estimated value	<5s
Demount of stretcher	20s		Estimated value	<7s
Demount of stretcher	7s		Estimated value	<7s
Service life	10 years	?	See chapter 5.7	
Enviroment				
Ability to separate materials at disposal	95%		Estimated value according to 3D-model	>95%
Number of components	20		According to 3D-model	20
Maximum number of different materials	5		According to 3D-model	4
Features				
Possibility to strap cargo	-	?	See chapter 5.7	
Possibility to place the stretcher in two directions	-		According to 3D-model	
Possibility to place the stretcher in two locations in the helicopter	-		According to 3D-model	

Requirement/request	Requested value	Met/Not met	Comment	Real value
Number of people needed to locate the stretcher in right position	2		Estimated value according to 3D-model	2
Safety				
No risk of injury	-		No risk detected	

5.7 Discussion

In the development of the fixation system the concepts were eliminated despite inadequate information depending on lack of resources. With more resources it would have been appropriate to perform deeper analyses of the concepts in form of calculations and prototypes and a better and more complete concept could have been developed.

To minimize the error in the LCA, the same distance was used for both titanium and aluminium. If the traveling distance would change, a different result would be achieved but the relationship between the two materials would be intact. However it might be possible to, as described earlier, minimize the reinforcements when choosing titanium. In that case titanium probably would perform better in the LCA.

The manufacturing cost was not considered when the ideas of a fixation system were developed. This decision was based on the normally large cost for certification of equipment placed in a helicopter. Thereby the manufacturing cost is a minor cost in the project.

5.8 Further Development

Because of time limitation some analysis could not be performed. The following sections present a recommended further development process and a discussion of used methods.

Next step in the development process is to determine the optimal shape of the components as well as the exact function of the unlocking pedal. All requirements from EASA have to be considered to get the fixation system certified for use in helicopters. To do so a strength analysis among other things has to be done. An idea that has not been further investigated is to cover the outside of fixation point 1 with rubber to minimize the wear of both the stretcher and the fixation point. It might also help the stretcher to be in place without cause unwanted vibrations. An analysis of service life and time between services has to be done to see if the fixation system meets the requests and requirements earlier presented in the requirement specification.

Since it is of high importance due to lack of space in SAR helicopters, the possibility to strap cargo onto the fixation system needs to be examined more. One way to make that possible is to make holes in the fixation points. How that would affect the mechanical properties of the construction needs to be analysed.

The final material and manufacturing process also needs to be determined. By using titanium instead of aluminium the reinforcements of the fixation points could be minimized and thereby save weight. Titanium has a disadvantage compared to aluminium though; it is much more expensive, as seen in Table 23. According to all analyses that were made aluminium is a better choice than titanium but to be completely sure, further investigation is recommended.

To minimize the risk of problem when the fixation system is in use, feedback from the users is crucial to get knowledge about the problems as early as possible.

6 Discussion

After the visit at Heli-One in Stavanger, Norway, it turned out that the project was different and larger than expected, for example the importance of EASA requirements was not considered before the visit. In order to organise the project a project plan, see Appendix G, was made. Even though the project became wider, the project plan turned out to be reasonable because most of the tasks were done in right order and according to the time frame that was set for each task. Furthermore some additional tools were presented by Heli-One several weeks after set up of the project, for example Eurocode, caused some adjustments to the project plan. These tools were given as a help to deepen the study and make it more accurate but at the same time it also increased the workload. Furthermore some of the parts could have been more overlapped, for example the EASA study could have started earlier to gain greater understanding of the regulations before the strength analysis started, this to support the calculations with necessary information.

The project was divided into four parts since these differed considerable from each other. This allowed for the examination of each part to be more profound. This also applies to the report and its disposition since it was divided as well but they were still supposed to be linked together. Therefore it is important to reflect on how the different parts depend on each other's requirements and results. This implies that an error in one of the sections would affect the result in all the others and thereby alter the result of the whole project.

The error in measurements that occurred in the creating of the 3D-model could cause deviations between the results from the strength analysis and the real strength properties of the stretcher. Even the error from the adjustment in the assembly could cause deviation in the strength analysis. However this should not be a problem because the load bearing structure and the critical parts were measured more precise than the rest of the parts. This also means that the design of the 3D-model will differ from the reality. With respect to limited computer power some simplifications of the structure in the 3D-model had to be done. This could be the reason why such high stresses occur in some parts. It could also depend on the difficulties with mesh refinement caused by limitations in the software. The high stresses caused uncertainties when verifying the stretcher according to EASA but after discussions with the supervisors the conclusion was that these stresses would not occur in reality. In order to obtain a more reliable stress distribution from the numerical simulations a more accurate modelling and meshing would be required, such as definition of radii and contact conditions.

All the assumptions in the strength analysis section are based on knowledge from three years studying mechanical engineering. These assumptions were discussed with supervisors and Heli-One, although it is important to reflect how these assumptions would differ made by another perpetrator.

The paragraphs in EASA are very clear about the material specifications and the fabrication methods. It was very hard to find approved specifications but different sources have been compared and they showed similar properties. Therefore this should not affect the results of the calculations but the material specification is still not reliable enough to use in a certification. In the validation for certification an assumption was made that the stretcher would be installed within 15° of the longitudinal axis of the rotorcraft, see Table

1. This depends on the installation of the fixation system. If the system is slanted installed the stretcher will also be slanted and this paragraph in EASA needs to be reconsidered. The material and fabrication method of the fixation system will affect the verification; especially if casting is chosen as fabrication method, which it probably will be.

6.1 Reflection of Method

A requirement was that the software Autodesk Mechanical Simulations had to be used. This might have contributed to that various features that had been good to use in this case not were considered. If software for example ANSYS, which is a preselected program at Chalmers University of Technology, had been used some of these problems could have been eliminated. The computer did not have enough performance to run complex simulations with too many equations due to a high number of elements. An example was that the computer could not handle an increased number of elements with a further 30% from the last mesh level in the mesh analysis. Consequently this resulted in a delay in the project plan. Better computer capacity would have been desirable for the 3D-modelling as well because some dynamic functions were hard to demonstrate with the computers provided by the university.

The usage of reverse engineering and conventional was a good choice for both 3D-modelling and in the development of the fixation system. This is because they are well established methods both among companies and for education. For example the division of Product and Production development advocates reverse engineering for these kinds of projects. Therefore these methods could be considered as trustworthy. The usages of matrices, Pugh, Morphological and elimination, which can be found in Appendix F are not completely unprejudiced. Even if these kinds of matrices are great tools, they are still not entirely reliable. This depends on lack of information and resources for building prototypes for each concept.

The two theoretical methods used in the strength analysis for buckling are both well established. Grundläggande hållfasthetslära is used as course literature at many of the courses in solid mechanics at Chalmers University of Technology. Eurocode is produced by European Committee for Standardisation and is thereby a reliable working method.

7 Conclusion

As mentioned in chapter 1.2 the aim of this project was to produce a fully dynamic 3D-model and investigate whether the stretcher meets the requirements to be used in large rotorcrafts. A 3D-model was made to virtually demonstrate all the functions of the stretcher. Parts of the model were also used in finite element simulations. The strength analysis was made in accordance with EASA regulations and show that the stretcher would withstand required loads in CS 29.561b. To ensure the credibility of the strength analysis both handbook calculations and numerical simulations were performed. The stress results show good agreement with each other based on the fact that the results from the handbook calculations are of the same scale of magnitude as the results from the numerical simulations. The two buckling checks show similar results, which indicate that the theses results are reliable as well. The strength analysis did only consider the load bearing part and not the seat of the stretcher or fixation system and the interface between the helicopter and the fixation system. The project only resulted in a concept for the fixation system.

The project was successful in developing the 3D-model with all dynamic functions. A preliminary study of the requirements in EASA gives indication of the fact that the stretcher would fulfil certification requirements. All paragraphs that could not be fulfilled with simple calculations or tests were discussed with a compliance verification engineer at Heli-One until a conclusion was reached and therefore the results of the verification are considered reliable.

8 Recommendations

The results from the strength analysis and the discussed paragraphs indicate that the stretcher would be properly installed in the helicopter, but to be able to certify the stretcher the following list of tasks is recommended.

- Investigate the strength of the fixation system.
- Determine the optimal shape, material and fabrication method of the fixation system.
- Make calculations or suitable test on the seat of the stretcher to make sure that it will not come loose during a flight or in a crash.
- Find an approved material specification.
- Control the welded parts to ensure the strength.
- Fatigue analysis for stretcher and fixation system.
- Examine if drain holes are necessary and in that case analyse the strength of the new structure.
- Analyse the suitability of the belts and harnesses used on the stretcher, both with respect to strength and with respect to CS 29.785c which states that seat belts and harnesses should be connected with a single point release. The visit at Säve's ambulance helicopter showed they use an older version of the Allfa Europe but the belts and harness was replaced with a restraining system from the company Schroth racing[17], see Figure 103, who usually makes harnesses and other restraining systems to racing cars.

Figure 103. Seat belt and shoulder harness with single point release.

The stretcher has some optimisation potential, both in the design and in the manufacturing. The recommendations are listed below.

- Reduce the thicknesses of the main beams as mentioned in chapter 4.9. These reductions have to be controlled with respect to eventually manufacturing problems and user friendliness.

[17] Schroth Safety Products (1946)

- Investigate how other cross sections will withstand the required loads and how much weight that could be eliminated.
- Use more standardised components in especially the screws and nuts.

Bibliography

British Standards Institution, *Eurocode 9: Design of aluminium structure – Del 1-1: General rules – General rules and rules for building* (DD ENV 1999-1-1:2000), BSi, 2000, ICS 91.010.30; 91.080.10

European Aviation Safety Agency, *Certification Specifications for Large Rotorcraft: CS-29.* Amendment 3. European Aviation Safety Agency, 2012

Kaisarlis George J., *A Systematic Approach for Geometrical and Dimensional Tolerancing in Reverse Engineering*, Reverse Engineering - Recent Advances and Applications, Dr. A.C. Telea (Ed.), ISBN: 978-953- 51-0158-1, InTech, Available from: http://www.intechopen.com/books/reverse-engineering-recent-advances- and-applications/a-systematic-approach-for-geometrical-and-dimensional-tolerancing-in-reverse-engineering, 2012, (2014-05-07)

Lindstedt, Per and Burenius, Jan; *The Value Model*, Kullavik: Nimba AB, 2003.

Lundh Hans, *Grundläggande hållfasthetslära*. Ed. 2. Institutionen för hållfasthetslära, KTH Stockholm, 2000

Schroth Saftey Products, Restraint systems, http://english.schroth.com/, (2014-05-14)

Sundström Bengt, *Handbok och formelsamling i Hållfasthetslära*. Ed. 1. Institutionen för hållfasthetslära, KTH Stockholm, 1998

Söderberg, Rikard; Professor at the division of Product and Production Development, Chalmers University of Technology. *Produktarkitektur*, lecture 2013-10-28

Appendix A

The figures below show the stretcher in different angles and in different positions.






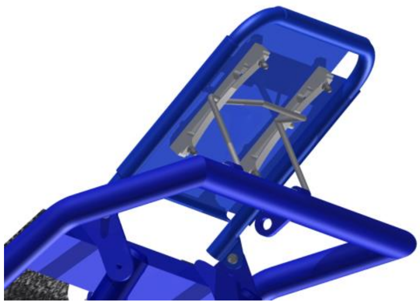


20G

20G

EXTRA LIFT
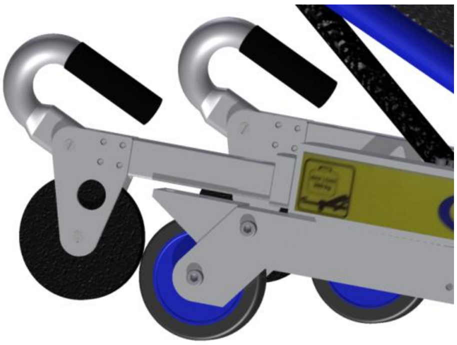

Appendix B

EASA Certification Specification 29

Subpart C – Strength Requirement

GENERAL

CS 29.301 Loads

(a) Strength requirements are specified in terms of limit loads (the maximum loads to be expected in service) and ultimate loads (limit loads multiplied by prescribed factors of safety). Unless otherwise provided, prescribed loads are limit loads.

(b) Unless otherwise provided, the specified air, ground, and water loads must be placed in equilibrium with inertia forces, considering each item of mass in the rotorcraft. These loads must be distributed to closely approximate or conservatively represent actual conditions.

(c) If deflections under load would significantly change the distribution of external or internal loads, this redistribution must be taken into account.

CS 29.303 Factor of safety

Unless otherwise provided, a factor of safety of 1.5 must be used. This factor applies to external and inertia loads unless its application to the resulting internal stresses is more conservative.

CS 29.305 Strength and deformation

(a) The structure must be able to support limit loads without detrimental or permanent deformation. At any load up to limit loads, the deformation may not interfere with safe operation.

(b) The structure must be able to support ultimate loads without failure. This must be shown by:

(1) Applying ultimate loads to the structure in a static test for at least 3 seconds; or

(2) Dynamic tests simulating actual load application.

CS 29.307 Proof of structure

(a) Compliance with the strength and deformation requirements of this Subpart must be shown for each critical loading condition accounting for the environment to which the structure will be exposed in operation. Structural analysis (static or fatigue) may be used only if the structure conforms to those for which experience has shown this method to be reliable. In other cases, substantiating load tests must be made.

(b) Proof of compliance with the strength requirements of this Subpart must include:

(1) Dynamic and endurance tests of rotors, rotor drives, and rotor controls;

(2) Limit load tests of the control system, including control surfaces;

(3) Operation tests of the control system;

(4) Flight stress measurement tests;

(5) Landing gear drop tests; and

(6) Any additional tests required for new or unusual design features.

FLIGHT LOADS

CS 29.321 General

(a) The flight load factor must be assumed to act normal to the longitudinal axis of the rotorcraft, and to be equal in magnitude and opposite in direction to the rotorcraft inertia load factor at the centre of gravity.

(b) Compliance with the flight load requirements of this Subpart must be shown:

(1) At each weight from the design minimum weight to the design maximum weight; and

(2) With any practical distribution of disposable load within the operating limitations in the rotorcraft flight manual.

CS 29.337 Limit manoeuvring load factor

The rotorcraft must be designed for –

(a) A limit manoeuvring load factor ranging from a positive limit of 3.5 to a negative limit of -1.0; or

(b) Any positive limit manoeuvring load factor not less than 2.0 and any negative limit manoeuvring load factor of not less than –0.5 for which:

(1) The probability of being exceeded is shown by analysis and flight tests to be extremely remote; and

(2) The selected values are appropriate to each weight condition between the design maximum and design minimum weights.

EMERGENCY LANDING CONDITIONS

CS 29.561 General

(a) The rotorcraft, although it may be damaged in emergency landing conditions on land or water, must be designed as prescribed in this paragraph to protect the occupants under those conditions.

(b) The structure must be designed to give each occupant every reasonable chance of escaping serious injury in a crash landing when:

(1) Proper use is made of seats, belts, and other safety design provisions;

(2) The wheels are retracted (where applicable); and

(3) Each occupant and each item of

mass inside the cabin that could injure an occupant is restrained when subjected to the following ultimate inertial load factors relative to the surrounding structure:

(i) Upward – 4 g
(ii) Forward – 16 g
(iii) Sideward – 8 g
(iv) Downward – 20g, after the intended displacement of the seat device
(v) Rearward – 1.5 g.

(c) The supporting structure must be designed to restrain under any ultimate inertial load factor up to those specified in this paragraph, any item of mass above and/or behind the crew and passenger compartment that could injure an occupant if it came loose in an emergency landing. Items of mass to be considered include, but are not limited to, rotors, transmission and engines. The items of mass must be restrained for the following ultimate inertial load factors:

(1) Upward – 1.5 g
(2) Forward – 12 g
(3) Sideward – 6 g
(4) Downward – 12 g
(5) Rearward – 1.5 g.

(d) Any fuselage structure in the area of internal fuel tanks below the passenger floor level must be designed to resist the following ultimate inertia factors and loads, and to protect the fuel tanks from rupture, if rupture is likely when those loads are applied to that area:

(1) Upward – 1.5 g
(2) Forward – 4.0 g
(3) Sideward – 2.0 g
(4) Downward – 4.0 g

Subpart D – Design and Construction

GENERAL

CS 29.601 Design

(a) The rotorcraft may have no design features or details that experience has shown to be hazardous or unreliable.
(b) The suitability of each questionable design detail and part must be established by tests.

CS 29.603 Materials

The suitability and durability of materials used for parts, the failure of which could adversely affect safety, must –
(a) Be established on the basis of experience or tests;
(b) Meet approved specifications that ensure their having the strength and other properties assumed in the design data; and
(c) Take into account the effects of environmental conditions, such as temperature and humidity, expected in service.

CS 29.605 Fabrication methods

(a) The methods of fabrication used must produce consistently sound structures. If a fabrication process (such as gluing, spot welding, or heattreating) requires close control to reach this objective, the process must be performed according to an approved process specification.
(b) Each new aircraft fabrication method must be substantiated by a test program.

CS 29.607 Fasteners

(a) Each removable bolt, screw, nut, pin or other fastener whose loss could jeopardise the safe operation of the rotorcraft must incorporate two separate locking devices. The fastener and its locking devices may not be adversely affected by the environmental conditions associated with the particular installation.
(b) No selflocking nut may be used on any bolt subject to rotation in operation unless a nonfriction locking device is used in addition to the selflocking device.

CS 29.609 Protection of structure

Each part of the structure must:
(a) Be suitably protected against deterioration or loss of strength in service due to any cause, including:

(1) Weathering;
(2) Corrosion; and
(3) Abrasion; and

(b) Have provisions for ventilation and drainage where necessary to prevent the accumulation of corrosive, flammable, or noxious fluids.

CS 29.613 Material strength properties and design values

(a) Material strength properties must be based on enough tests of material meeting specifications to establish design values on a statistical basis.
(b) Design values must be chosen to minimise the probability of structural failure due to material variability. Except as provided in subparagraphs (d) and (e), compliance with this paragraph must be shown by selecting design values that assure material strength with the following probability:

(1) Where applied loads are eventually distributed through a single member within an assembly, the failure of which would result in loss of structural integrity of the component, 99%

probability with 95% confidence; and

(2) For redundant structures, those in which the failure of individual elements would result in applied loads being safely distributed to other loadcarrying members, 90% probability with 95% confidence.

(c) The strength, detail design, and fabrication of the structure must minimise the probability of disastrous fatigue failure, particularly at points of stress concentration.

(d) Material specifications must be those contained in documents accepted by the Agency.

(e) Other design values may be used if a selection of the material is made in which a specimen of each individual item is tested before use and it is determined that the actual strength properties of that particular item will equal or exceed those used in design.

CS 29.619 Special factors

(a) The special factors prescribed in CS 29.621 to 29.625 apply to each part of the structure whose strength is:

(1) Uncertain;

(2) Likely to deteriorate in service before normal replacement; or

(3) Subject to appreciable variability due to:

(i) Uncertainties in manufacturing processes; or

(ii) Uncertainties in inspection methods.

(b) For each part of the rotorcraft to which CS 29.621 to 29.625 apply, the factor of safety prescribed in CS 29.303 must be multiplied by a special factor equal to:

(1) The applicable special factors prescribed in CS 29.621 to 29.625; or

(2) Any other factor great enough to ensure that the probability of the part being under strength because of the uncertainties specified in subparagraph (a) is extremely remote.

CS 29.621 Casting factors

(a) *General*. The factors, tests, and inspections specified in subparagraphs (b) and (c) must be applied in addition to those necessary to establish foundry quality control. The inspections must meet approved specifications. Subparagraphs (c) and (d) apply to structural castings except castings that are pressure tested as parts of hydraulic or other fluid systems and do not support structural loads.

(b) *Bearing stresses and surfaces*. The casting factors specified in subparagraphs (c) and (d):

(1) Need not exceed 1.25 with respect to bearing stresses regardless of the method of inspection used; and

(2) Need not be used with respect to the bearing surfaces of a part whose bearing factor is larger than the applicable casting factor.

(c) *Critical castings*. For each casting whose failure would preclude continued safe flight and landing of the rotorcraft or result in serious injury to any occupant, the following apply:

(1) Each critical casting must:

(i) Have a casting factor of not less than 1.25; and

(ii) Receive 100% inspection by visual, radiographic, and magnetic particle (for ferromagnetic materials) or penetrant (for non ferromagnetic materials) inspection methods or approved equivalent inspection methods.

(2) For each critical casting with a casting factor less than 1.50, three sample castings must be static tested and shown to meet:

(i) The strength requirements of CS 29.305 at an ultimate load corresponding to a casting factor of 1.25; and

(ii) The deformation requirements of CS 29.305 at a load of 1.15 times the limit load.

(d) *Non critical castings*. For each casting other than those specified in subparagraph (c), the following apply:

(1) Except as provided in subparagraphs (d)(2) and (3), the casting factors and corresponding inspections must meet the following table:

Casting factor	Inspection
2.0 or greater ……..	100% visual.
Less than 2.0 greater than 1.5	100% visual, and magnetic particle (ferromagnetic materials), penetrant (non ferromagnetic materials), or approved equivalent inspection methods.
1.25 through 1.50......	100% visual, and magnetic particle (ferromagnetic materials), penetrant (non ferromagnetic materials), and radiographic or approved equivalent inspection methods.

(2) The percentage of castings inspected by non visual methods may be reduced below that specified in subparagraph (d)(1) when an approved quality control procedure is established.

(3) For castings procured to a specification that guarantees the mechanical properties of the material in the casting and provides for demonstration of these properties by test of coupons cut from the castings on a

sampling basis:

(i) A casting factor of 1.0 may be used; and

(ii) The castings must be inspected as provided in subparagraph (d)(1) for casting factors of '1.25 to 1.50' and tested under subparagraph (c)(2).

CS 29.623 Bearing factors

(a) Except as provided in subparagraph (b), each part that has clearance (free fit), and that is subject to pounding or vibration, must have a bearing factor large enough to provide for the effects of normal relative motion.

(b) No bearing factor need be used on a part for which any larger special factor is prescribed.

CS 29.625 Fitting factors

For each fitting (part or terminal used to join one structural member to another) the following apply:

(a) For each fitting whose strength is not proven by limit and ultimate load tests in which actual stress conditions are simulated in the fitting and surrounding structures, a fitting factor of at least 1.15 must be applied to each part of:

(1) The fitting;

(2) The means of attachment; and

(3) The bearing on the joined members.

(b) No fitting factor need be used:

(1) For joints made under approved practices and based on comprehensive test data (such as continuous joints in metal plating, welded joints, and scarf joints in wood); and

(2) With respect to any bearing surface for which a larger special factor is used.

(c) For each integral fitting, the part must be treated as a fitting up to the point at which the section properties become typical of the member.

(d) Each seat, berth, litter, safety belt, and harness attachment to the structure must be shown by analysis, tests, or both, to be able to withstand the inertia forces prescribed in CS 29.561(b)(3) multiplied by a fitting factor of 1.33.

PERSONNEL AND CARGO ACCOMMODATIONS

CS 29.785 Seats, berths, safety belts, and harnesses

(a) Each seat, safety belt, harness, and adjacent part of the rotorcraft at each station designated for occupancy during takeoff and landing must be free of potentially injurious objects, sharp edges, protuberances, and hard surfaces and must be designed so that a person making proper use of these facilities will not suffer serious injury in an emergency landing as a result of the inertial factors specified in CS 29.561(b) and dynamic conditions specified in CS 29.562.

(b) Each occupant must be protected from serious head injury by a safety belt plus a shoulder harness that will prevent the head from contacting any injurious object except as provided for in CS 29.562(c)(5). A shoulder harness (upper torso restraint), in combination with the safety belt, constitutes a torso restraint system as described in ETSOC114.

(c) Each occupant's seat must have a combined safety belt and shoulder harness with a singlepoint release. Each pilot's combined safety belt and shoulder harness must allow each pilot when seated with safety belt and shoulder harness fastened to perform all functions necessary for flight operations. There must be a means to secure belts and harnesses, when not in use, to prevent interference with the operation of the rotorcraft and with rapid egress in an emergency.

(d) If seat backs do not have a firm handhold, there must be hand grips or rails along each aisle to let the occupants steady themselves while using the aisle in moderately rough air.

(e) Each projecting object that would injure persons seated or moving about in the rotorcraft in normal flight must be padded.

(f) Each seat and its supporting structure must be designed for an occupant weight of at least 77 kg (170 pounds) considering the maximum load factors, inertial forces, and reactions between the occupant, seat, and safety belt or harness corresponding with the applicable flight and ground load conditions, including the emergency landing conditions of CS 29.561(b). In addition:

(1) Each pilot seat must be designed for the reactions resulting from the application of the pilot forces prescribed in CS 29.397; and

(2) The inertial forces prescribed in CS 29.561(b) must be multiplied by a factor of 1.33 in determining the strength of the attachment of:

(i) Each seat to the structure; and

(ii) Each safety belt or harness to the seat or structure.

(g) When the safety belt and shoulder harness are combined, the rated strength of the safety belt and shoulder harness may not be less than that corresponding to the inertial forces specified in CS 29.561(b), considering the occupant weight of at least 77 kg (170 pounds), considering the dimensional characteristics of the restraint system installation, and using a distribution of at least a 60% load to the safety belt and at least a 40% load to the shoulder harness. If the safety belt is capable of being used without the shoulder harness, the inertial forces specified must be met by the safety belt alone.

(h) When a headrest is used, the headrest and its supporting structure must be designed to resist the inertia forces specified in CS 29.561, with a 1.33 fitting factor and a head weight of at least 5.9 kg (13 pounds).

(i) Each seating device system includes the device such as the seat, the cushions, the occupant restraint system, and attachment devices.

(j) Each seating device system may use design features such as crushing or separation of certain parts of the seat in the design to reduce occupant loads for the emergency landing dynamic conditions of CS 29.562; otherwise, the system must remain intact and must not interfere with rapid evacuation of the rotorcraft.

(k) For the purposes of this paragraph, a litter is defined as a device designed to carry a non ambulatory person, primarily in a recumbent position, into and on the rotorcraft. Each berth or litter must be designed to withstand the load reaction of an occupant weight of at least 77 kg (170 pounds) when the occupant is subjected to the forward inertial factors specified in CS 29.561(b). A berth or litter installed within 15fl or less of the longitudinal axis of the rotorcraft must be provided with a padded endboard, cloth diaphragm, or equivalent means that can withstand the forward load reaction. A berth or litter oriented greater than 15fl with the longitudinal axis of the rotorcraft must be equipped with appropriate restraints, such as straps or safety belts, to withstand the forward reaction. In addition:

(1) The berth or litter must have a restraint system and must not have corners or other protuberances likely to cause serious injury to a person occupying it during emergency landing conditions; and

(2) The berth or litter attachment and the occupant restraint system attachments to the structure must be designed to withstand the critical loads resulting from flight and ground load conditions and from the conditions prescribed in CS 29.561(b). The fitting factor required by CS 29.625(d) shall be applied.

Appendix C

References to Equations

(1)	eq (12-2)	Grundläggande hållfasthetslära – Hans Lundh, Stockholm, 2000
(2)	eq (12-4)	Grundläggande hållfasthetslära – Hans Lundh, Stockholm, 2000
(3)	eq (7-42)	Grundläggande hållfasthetslära – Hans Lundh, Stockholm, 2000
(4)	eq (7-35)	Grundläggande hållfasthetslära – Hans Lundh, Stockholm, 2000
(5)	eq (7-35)	Grundläggande hållfasthetslära – Hans Lundh, Stockholm, 2000
(6)		Assumption
(7)		Newton II
(8)	table 32.1	Formelsamling i hållfasthetslära – KTH, Stockholm, 1998
(9)	table 3	Grundläggande hållfasthetslära – Hans Lundh, Stockholm, 2000
(10)	eq (7-26)	Grundläggande hållfasthetslära – Hans Lundh, Stockholm, 2000
(11)	table 32.2	Formelsamling i hållfasthetslära – KTH, Stockholm, 1998
(12)	table 3	Grundläggande hållfasthetslära – Hans Lundh, Stockholm, 2000
(13)	table 32.2	Formelsamling i hållfasthetslära – KTH, Stockholm, 1998
(14)	table 3	Grundläggande hållfasthetslära – Hans Lundh, Stockholm, 2000
(15)		Newton II
(16)	table 4	Grundläggande hållfasthetslära – Hans Lundh, Stockholm, 2000
(17)	eq (8-78)	Grundläggande hållfasthetslära – Hans Lundh, Stockholm, 2000
(18)	eq (8-76)	Grundläggande hållfasthetslära – Hans Lundh, Stockholm, 2000
(19)	eq (8-79)	Grundläggande hållfasthetslära – Hans Lundh, Stockholm, 2000
(20)	eq (8-80)	Grundläggande hållfasthetslära – Hans Lundh, Stockholm, 2000
(21)	eq (8-78)	Grundläggande hållfasthetslära – Hans Lundh, Stockholm, 2000
(22)	pg. 144	Grundläggande hållfasthetslära – Hans Lundh, Stockholm, 2000
(23)	eq (5.46)	British Standards Institution, Eurocode 9, DD ENV 1999-1-1:2000
(24)		Definition of density
(25)		Assumption
(26)	5.3.5	British Standards Institution, Eurocode 9, DD ENV 1999-1-1:2000
(27)	5.3.5	British Standards Institution, Eurocode 9, DD ENV 1999-1-1:2000
(28)	5.1.1	British Standards Institution, Eurocode 9, DD ENV 1999-1-1:2000
(29)		Definition of area
(30)	eq (7-35)	Grundläggande hållfasthetslära – Hans Lundh, Stockholm, 2000
(31)	eq (7-35)	Grundläggande hållfasthetslära – Hans Lundh, Stockholm, 2000
(32)	eq (8-80)	Grundläggande hållfasthetslära – Hans Lundh, Stockholm, 2000
(33)	eq (8-80)	Grundläggande hållfasthetslära – Hans Lundh, Stockholm, 2000
(34)	eq (7-27)	Grundläggande hållfasthetslära – Hans Lundh, Stockholm, 2000
(35)	eq (7-27)	Grundläggande hållfasthetslära – Hans Lundh, Stockholm, 2000

(36)		Newton II
(37)		Definition of moment
(38)		Definition of moment
(39)	5.4.3	British Standards Institution, Eurocode 9, DD ENV 1999-1-1:2000
(40)	5.4.3	British Standards Institution, Eurocode 9, DD ENV 1999-1-1:2000
(41)	5.4.4	British Standards Institution, Eurocode 9, DD ENV 1999-1-1:2000
(42)	5.4.4	British Standards Institution, Eurocode 9, DD ENV 1999-1-1:2000
(43)	5.4.4	British Standards Institution, Eurocode 9, DD ENV 1999-1-1:2000
(44)	5.8.4.2	British Standards Institution, Eurocode 9, DD ENV 1999-1-1:2000
(45)	eq (8-77)	Grundläggande hållfasthetslära – Hans Lundh, Stockholm, 2000
(46)	5.8.5.2	British Standards Institution, Eurocode 9, DD ENV 1999-1-1:2000
(47)	5.8.4.1	British Standards Institution, Eurocode 9, DD ENV 1999-1-1:2000
(48)	5.8.4.1	British Standards Institution, Eurocode 9, DD ENV 1999-1-1:2000
(49)	5.8.4.1	British Standards Institution, Eurocode 9, DD ENV 1999-1-1:2000
(50)	5.8.5.3	British Standards Institution, Eurocode 9, DD ENV 1999-1-1:2000
(51)	5.8.4.1	British Standards Institution, Eurocode 9, DD ENV 1999-1-1:2000
(52)	5.6.6.3	British Standards Institution, Eurocode 9, DD ENV 1999-1-1:2000
(53)	5.6.6.3	British Standards Institution, Eurocode 9, DD ENV 1999-1-1:2000
(54)	5.6.6.3	British Standards Institution, Eurocode 9, DD ENV 1999-1-1:2000
(55)	5.6.6.3	British Standards Institution, Eurocode 9, DD ENV 1999-1-1:2000
(56)	5.6.6.3	British Standards Institution, Eurocode 9, DD ENV 1999-1-1:2000
(57)	5.6.6.3	British Standards Institution, Eurocode 9, DD ENV 1999-1-1:2000
(58)	5.9.4.2	British Standards Institution, Eurocode 9, DD ENV 1999-1-1:2000
(59)	5.9.4.2	British Standards Institution, Eurocode 9, DD ENV 1999-1-1:2000
(60)	5.9.4.2	British Standards Institution, Eurocode 9, DD ENV 1999-1-1:2000
(61)	5.9.4.2	British Standards Institution, Eurocode 9, DD ENV 1999-1-1:2000
(62)	5.9.4.2	British Standards Institution, Eurocode 9, DD ENV 1999-1-1:2000
(63)		Newton II

(T1)	table 3.2b	British Standards Institution, Eurocode 9, DD ENV 1999-1-1:2000
(T2)	table 3.2b	British Standards Institution, Eurocode 9, DD ENV 1999-1-1:2000
(T3)	table 5.1	British Standards Institution, Eurocode 9, DD ENV 1999-1-1:2000
(T4)	table 5.1	British Standards Institution, Eurocode 9, DD ENV 1999-1-1:2000
(T5)	table 5.1	British Standards Institution, Eurocode 9, DD ENV 1999-1-1:2000
(T6)	table 5.7	British Standards Institution, Eurocode 9, DD ENV 1999-1-1:2000
(T7)	table 5.6	British Standards Institution, Eurocode 9, DD ENV 1999-1-1:2000
(T8)	table 5.6	British Standards Institution, Eurocode 9, DD ENV 1999-1-1:2000

Appendix D

Calculations of Cross Section

$$I_{tot} = \sum I_{y,z,i} + {a_i}^2 A_i \quad (3)$$

$$I_{y,z} = \frac{bh^3}{12} \quad (4)$$

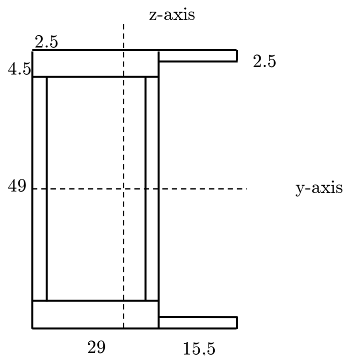

Figure 104. The cross section of the main beam divided in parts.

$a_i = distance\ from\ center\ of\ mass\ of\ part\ to\ center\ of\ mass\ of\ cross\ section$
$A_i = area\ of\ part$

$$I_y^{tot} = \sum I_y^i + a_i^2 A_i \quad (3)$$

$$I_y^1 = I_y^3 = \frac{29 \cdot 4.5^3}{12} = 220.2\ mm^4 \quad (4)$$

$$I_y^2 = I_y^4 = \frac{15.5 \cdot 2.5^3}{12} = 20.2\ mm^4 \quad (4)$$

$$I_y^5 = I_y^6 = \frac{2.5 \cdot 49^3}{12} = 2.45 \cdot 10^4\ mm^4 \quad (4)$$

$$a_{1z} = a_{3z} = 26.75\ mm$$

$$a_{2z} = a_{4z} = 27.7\ mm$$

$$a_{5z} = a_{6z} = 0\ mm$$

$$A_1 = A_3 = 130.5\ mm^2$$

$$A_2 = A_4 = 38.75\ mm^2$$

$$A_5 = A_6 = 122.5\ mm^2$$

$$I_y^{tot} = 2.9592 \cdot 10^5\ mm^4$$

$$I_z^{tot} = \sum I_z^i + a_i^2 A_i \quad (3)$$

$$I_z^1 = I_z^3 = \frac{4.5 \cdot 29^3}{12} = 9.1458 \cdot 10^3\ mm^4 \quad (4)$$

$$I_z^2 = I_z^4 = \frac{2.5 \cdot 15.5^3}{12} = 775.8\ mm^4 \quad (4)$$

$$I_z^5 = I_z^6 = \frac{49 \cdot 2.5^3}{12} = 63.8\ mm^4 \quad (4)$$

$$a_{1y} = a_{3y} = 2.96\ mm$$

$$a_{2y} = a_{4y} = 19.2\ mm$$

$a_{5y} = 16.21\, mm$

$a_{6y} = 10.29\, mm$

$I_z^{tot} = 9.5987 \cdot 10^4\, mm^4$

The cross-section of the joist is given in Figure 14.

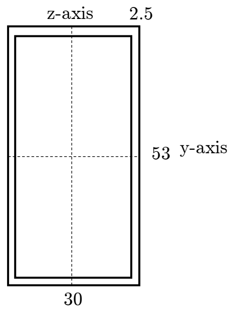

Figure 105. The cross section of the joist

$$I_y = I_z = \frac{bh^3 - b_{in}{h_{in}}^3}{12} \tag{5}$$

$$I_y = I_z = \frac{30 \cdot 53^3 - 25 \cdot 48^3}{12} = 7.7054 \cdot\ 10^4 mm^4$$

Eurocode 9

D.1 General Data

D.1.1 Material Properties

Material

Aluminium

Young's modulus

$$E = 70\,000\ {}^{N}\!/_{mm^2}$$

0.2% proof strength

$$f_{0.2} = 140\ {}^{N}\!/_{mm^2} \tag{T1}$$

Ultimate strength

$$f_u = 170\ {}^{N}\!/_{mm^2} \tag{T2}$$

f_0 is the characteristic strength for bending and overall yielding in tension and compression and can be defined as follows:

$$f_0 = f_{0.2} \tag{26}$$

f_a is the characteristic strength for the local capacity of a net section in tension or compression and can be defined as follows:

$$f_a = f_u \tag{27}$$

Partial safety factor:

$$\gamma_{M1} = 1.10 \tag{28}$$

D.1.2 Cross Section for Main Beam

A simplification was made for the cross section of the main beam that the two projecting flanges on the side were removed. The two projecting flanges increase the stiffness and strength of the system, which means conservative calculations. Instead the cross section became thin and hollow and it was therefore easier to perform the calculations, see Figure 106.

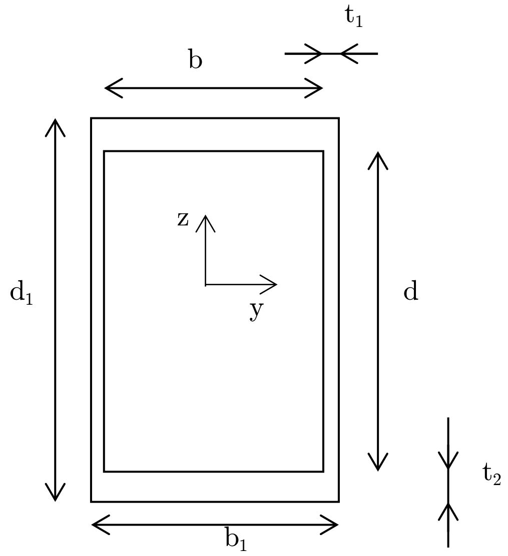

Figure 106. Simplified cross section for main beam, compare to Figure 13

Width of section

$$b_1 = 29\ mm$$
$$b = 24\ mm$$

Depth of section

$$d_1 = 58\ mm$$
$$d = 49\ mm$$

Wall thickness of the section

$$t_1 = 2.5\ mm$$
$$t_2 = 4.5\ mm$$

Gross area of the section

$$A = (b_1 \cdot d_1) - (d \cdot b) = 506\ mm^2 \tag{29}$$

Moment of Inertia

$$I_{yy} = \frac{b1^4 - b^4}{12} = \ 31\ 292\ mm^4 \tag{30}$$

$$I_{zz} = \frac{d1^4 - d^4}{12} = \ 462\ 641\ mm^4 \tag{31}$$

Radius of gyration

$$i_y = \sqrt{\frac{I_{yy}}{A}} = 7.86\ mm \tag{32}$$

$$i_z = \sqrt{\frac{I_{zz}}{A}} = 30.24\ mm \tag{33}$$

Shape factor

$$\alpha_y = 1.2$$

$$\alpha_z = 1.2$$

Section modulus about Y-axis

$$W_y = \frac{2 \cdot I_{yy}}{d1} = 0.1079 \cdot 10^4\ mm^3 \tag{34}$$

Section modulus about X-axis

$$W_z = \frac{2 \cdot I_{zz}}{b1} = 3.1906 \cdot 10^4\ mm^2 \tag{35}$$

D.1.3 Cross Section for Joist

A simplification was made that the cross section was square and that the thickness was consistent throughout. The smallest thickness was chosen, that is because if the beam would manage against buckling for the thinner cross section it would manage for the thicker as well, see Figure 107.

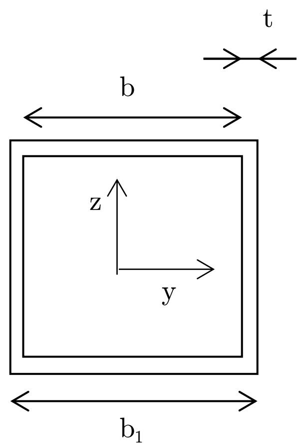

Figure 107. Simplified cross section for joist compared to *Figure 14.*

Width of section

$$b_1 = 30\ mm$$

$$b = 25\ mm$$

Depth of section

$$d_1 = 30\ mm$$

$$d = 25\ mm$$

Wall thickness of the section

$$t = 2.5\ mm$$

Gross area of the section

$$A = (b_1 \cdot d_1) - (d \cdot b) = 275\ mm^2 \tag{29}$$

Moment of Inertia

$$I_{yy} = \frac{b1^4 - b^4}{12} = 34\,947.9\ mm^4 \tag{30}$$

$$I_{zz} = \frac{d1^4 - d^4}{12} = 34\,947.9\ mm^4 \tag{31}$$

Radios of gyration

$$i_y = \sqrt{\frac{I_{yy}}{A}} = 11.27\ mm \tag{32}$$

$$i_z = \sqrt{\frac{I_{zz}}{A}} = 11.27\ mm \tag{33}$$

Shape factor

$$\alpha_y = 1.2$$

$$\alpha_z = 1.2$$

Section modulus about Y-axis

$$W_y = \frac{2 \cdot I_{yy}}{d1} = 2329.9\ mm^3 \tag{34}$$

Section modulus about X-axis

$$W_z = \frac{2 \cdot I_{zz}}{b1} = 2329.9\ mm^3 \tag{35}$$

D.2 Buckling Design of Main Beam

D.2.1 Design Cases

For these calculations only attachment 1 was considered. This was because the differences between attachment 1 and 2 are not enough to make any significant impact on the results. For the main beam there were three different cases that were studied, this was because the beam was separated into three parts as seen in Figure 19 with either dissimilar length or boundary conditions. The effective length factor depends on the boundary conditions and this would therefore result in different values of the effective length. The calculations were considering the worst case scenario, which implicates ultimate loads and added human body mass.

Cases

- Main beam – Euler 1
- Main beam – Euler 3
- Main beam – Euler 4

D.2.2 Loads and Moment Values

It is an empirical assumption that the moment about minor axis is taken as 10% of the moment about major axis.

Design value of the compressive force

$$N_{Ed} = 16 \cdot g \cdot \kappa_f \cdot m = 23.8\ kN \tag{36}$$

Since there is no predetermined point where the axial load affects, the assumptions is made that it comes into the centre of the cross section and the eccentricity therefore becomes zero.

$$ey = 0$$

$$ez = 0$$

Design value of the moment about YY axis

$$M_{y\_Ed} = N_{Ed} \cdot ez = 0 \tag{37}$$

Design value of the moment about ZZ axis

$$M_{z\_Ed} = N_{Ed} \cdot ey = 0 \tag{38}$$

D.2.3 Classification of Cross Section

This classification is performed according to 5.4 in Eurocode 9.

Slenderness parameter

$$\beta_A = \frac{b}{t1} = 9.6 \tag{39}$$

$$\beta_B = \frac{d}{t2} = 10.9 \tag{40}$$

$$\varepsilon = \sqrt{\frac{250}{f_0}} = 1.34 \tag{41}$$

Since this member is non heat treated and unwelded

$$\beta_1 = 9 \cdot \varepsilon = 12.06 \tag{T3}$$

$$\beta_2 = 13 \cdot \varepsilon = 17.42 \tag{T4}$$

$$\beta_3 = 18 \cdot \varepsilon = 24.12 \tag{T5}$$

Since

$\beta \leq \beta_1$	: class 1
$\beta_1 < \beta \leq \beta_2$	: class 2
$\beta_2 < \beta \leq \beta_3$	: class 3
$\beta_3 < \beta$	: class 4

Figure 108. Elements in beam.

$$\beta_A \leq \beta_1 \tag{42}$$

$$\beta_B \leq \beta_1 \tag{43}$$

Hence, the section is classified as class 1

D.2.4 Reduction Factor for Flexural Buckling - Euler 1

Length of beam

$$L_1 = 170\ mm$$

Effective length factor

$$K = 2.0 \tag{T6}$$

Effective length

$$L_{cr} = K \cdot L = 340\ mm \tag{44}$$

Elastic critical load

$$N_{cr} = \frac{\pi^2 \cdot E \cdot I_{yy}}{{L_{cr}}^2} = 187\ kN \tag{45}$$

$$\lambda = \pi \sqrt{\frac{E \cdot A}{N_{cr}}} = 43.24 \tag{46}$$

Since it is class 1

$$\eta = 1 \tag{47}$$

$$\lambda_1 = \pi \sqrt{\frac{E}{\eta \cdot f_0}} = 70.25 \tag{48}$$

$$\alpha = 0.32 \tag{T7}$$

$$\lambda b_0 = 0 \tag{T8}$$

$$\lambda b = \sqrt{\frac{A \cdot \eta \cdot f_0}{N_{cr}}} = 0.616 \tag{47}$$

$$\phi = 0.5(1 + \alpha(\lambda b - \lambda b_0) + \lambda b^2) = 0.789 \tag{50}$$

Reduction factor for flexural buckling

$$\chi = \frac{1}{\phi + \sqrt{(\phi^2 - \lambda b^2)}} = 0.78 \tag{51}$$

D.2.5 Reduction Factor for Flexural Buckling – Euler 3

$$L_3 = 230\ mm$$
$$K = 1.5 \tag{T6}$$
$$L_{cr} = 345\ mm \tag{44}$$
$$N_{cr} = 181.6\ kN \tag{45}$$
$$\eta = 1 \tag{47}$$
$$\lambda_1 = 70.25 \tag{48}$$
$$\alpha = 0.32 \tag{T7}$$
$$\lambda b_0 = 0 \tag{T8}$$
$$\lambda b = 0.625 \tag{49}$$
$$\phi = 0.795 \tag{50}$$

Reduction factor for flexural buckling

$$\chi = 0.78 \tag{51}$$

D.2.6 Reduction Factor for Flexural Buckling – Euler 4

$$L_2 = 785\ mm$$
$$K = 0.7 \tag{T6}$$
$$L_{cr} = 549.5\ mm \tag{44}$$
$$N_{cr} = 71.597\ kN \tag{45}$$
$$\eta = 1 \tag{47}$$
$$\lambda_1 = 70.25 \tag{48}$$
$$\alpha = 0.32 \tag{T7}$$
$$\lambda b_0 = 0 \tag{T8}$$
$$\lambda b = 0.995 \tag{49}$$
$$\phi = 1.15 \tag{50}$$

Reduction factor for flexural buckling

$$\chi = 0.58 \tag{49}$$

D.2.7 Reduction Factor for Lateral-Torsional Buckling – Euler 1

Length from pinned point to the point of load

$$L_{cr\_z} = L_1 = 170\ mm$$

Imperfection factor for lateral-torsional buckling

$$\alpha_{LT} = 0.1 \tag{52}$$

$$\lambda_{0LT} = 0.6 \tag{53}$$

$$\lambda_{LT} = \frac{L_{cr\_z}}{i_z} = 5.62 \tag{54}$$

Non-dimensional slenderness

$$\lambda_{LTb} = \lambda_{LT} \frac{1}{\pi} \sqrt{\frac{f_0}{E}} = 0.08 \tag{55}$$

$$\phi_{LT} = 0.5(1 + \alpha_{LT} \cdot (\lambda_{LTb} - \lambda_{0LT}) + \lambda_{LTb}^2) = 0.48 \tag{56}$$

Reduction factor for lateral-torsional buckling

$$\chi_{LT} = \frac{1}{\phi_{LT} + \sqrt{(\phi_{LT}^2 - \lambda_{LTb}^2)}} = 1.05 \tag{57}$$

D.2.8 Reduction Factor for Lateral-Torsional Buckling – Euler 3

$$L_{cr\_z} = 230\ mm$$

$$\alpha_{LT} = 0.1 \tag{52}$$

$$\lambda_{0LT} = 0.6 \tag{53}$$

$$\lambda_{LT} = 7.6 \tag{54}$$

$$\lambda_{LTb} = 0.11 \tag{55}$$

$$\phi_{LT} = 0.48 \tag{56}$$

Reduction factor for lateral-torsional buckling

$$\chi_{LT} = 1.06 \tag{57}$$

D.2.9 Reduction Factor for Lateral-Torsional Buckling – Euler 4

$$L_{cr\_z} = 785\ mm$$

$$\alpha_{LT} = 0.1 \tag{52}$$

$$\lambda_{0LT} = 0.6 \tag{53}$$

$$\lambda_{LT} = 25.96 \tag{54}$$

$$\lambda_{LTb} = 0.37 \tag{55}$$

$$\phi_{LT} = 0.56 \tag{56}$$

Reduction factor for lateral-torsional buckling

$$\chi_{LT} = 1.02 \tag{57}$$

D.2.10 Buckling Check – Euler 1

$$N_{Rd} = \frac{A \cdot f_0}{\gamma_{M1}} = 64.4\ kN \tag{58}$$

Since no welds

$$\omega_0 = \omega_x = 1 \tag{59}$$

Bending moment capacity about the y-axis

$$M_{y,Rd} = \frac{\alpha_y \cdot W_y \cdot f_0}{\gamma_{M1}} = 164.8\ Nmm \tag{60}$$

Bending moment capacity about the z-axis

$$M_{z,Rd} = \frac{\alpha_z \cdot W_z \cdot f_0}{\gamma_{M1}} = 4872.92\ Nmm \tag{61}$$

$$\psi_c = 0.8 \tag{62}$$

Show that

$$\left(\frac{N_{Ed}}{\chi_{min} \cdot \omega_x \cdot N_{Rd}}\right)^{\psi_c} + \frac{1}{\omega_0}\left(\left(\frac{M_{y,Ed}}{M_{y,Rd}}\right)^{1.7} + \left(\frac{M_{z,Ed}}{M_{z,Rd}}\right)^{1.7}\right)^{0.6} \leq 1.00 \tag{23}$$

Since the design value of the moment is zero in equation (23) it shows that

$$\frac{1}{\omega_0}\left(\left(\frac{M_{y,Ed}}{M_{y,Rd}}\right)^{1.7} + \left(\frac{M_{z,Ed}}{M_{z,Rd}}\right)^{1.7}\right)^{0.6} = 0$$

$$N_{Ed} = 23.8\ kN \tag{36}$$

The minimum value for the reduction factor of flexural buckling and lateral-torsional buckling

$$\chi_{min} = 0.78$$

$$\left(\frac{N_{Ed}}{\chi_{min} \cdot \omega_x \cdot N_{Rd}}\right)^{\psi_c} = 0.55$$

D.2.11 Buckling Check – Euler 3

$$N_{Rd} = 64.4\ kN \tag{58}$$
$$\omega_0 = \omega_x = 1 \tag{59}$$
$$M_{y,Rd} = 164.8\ Nmm \tag{60}$$
$$M_{z,Rd} = 4872.92\ Nmm \tag{61}$$
$$\psi_c = 0.8 \tag{62}$$

Show that

$$\left(\frac{N_{Ed}}{\chi_{min} \cdot \omega_x \cdot N_{Rd}}\right)^{\psi_c} + \frac{1}{\omega_0}\left(\left(\frac{M_{y,Ed}}{M_{y,Rd}}\right)^{1.7} + \left(\frac{M_{z,Ed}}{M_{z,Rd}}\right)^{1.7}\right)^{0.6} \leq 1.00 \tag{23}$$

$$N_{Ed} = 23.8\ kN \tag{36}$$

The minimum value for the reduction factor of flexural buckling and lateral-torsional buckling

$$\chi_{min} = 0.78$$

$$\left(\frac{N_{Ed}}{\chi_{min} \cdot \omega_x \cdot N_{Rd}}\right)^{\psi_c} = 0.55$$

D.2.12 Buckling Check – Euler 4

$$N_{Rd} = 64.4\ kN \tag{58}$$
$$\omega_0 = \omega_x = 1 \tag{59}$$
$$M_{y,Rd} = 164.8\ Nmm \tag{60}$$
$$M_{z,Rd} = 4872.92\ Nmm \tag{61}$$
$$\psi_c = 0.8 \tag{62}$$

Show that

$$\left(\frac{N_{Ed}}{\chi_{min} \cdot \omega_x \cdot N_{Rd}}\right)^{\psi_c} + \frac{1}{\omega_0}\left(\left(\frac{M_{y,Ed}}{M_{y,Rd}}\right)^{1.7} + \left(\frac{M_{z,Ed}}{M_{z,Rd}}\right)^{1.7}\right)^{0.6} \leq 1.00 \tag{23}$$

$$N_{Ed} = 23.8\ kN \tag{36}$$

The minimum value for the reduction factor of flexural buckling and lateral-torsional buckling

$$\chi_{min} = 0.58$$

$$\left(\frac{N_{Ed}}{\chi_{min} \cdot \omega_x \cdot N_{Rd}}\right)^{\psi_c} = 0.7$$

D.3 Buckling Design of Joist

D.3.1 Design Cases

The joists have only one case that is necessary to study.

Case

- Joist beam – Euler 4

D.3.2 Loads and Moment Values

It is an empirical assumption that the moment about minor axis is taken as 10% of the moment about major axis.

Design value of the compressive force

$$N_{Ed} = 8 \cdot g \cdot \kappa_f \cdot m = 11.9\ kN \tag{63}$$

Since there is no predetermined point where the axial load affects, the assumptions was made that it comes into the centre of the cross section and the eccentricity therefore becomes zero.

$$ey = 0$$
$$ez = 0$$

Design value of the moment about YY axis

$$M_{y\_Ed} = N_{Ed} \cdot ez = 0 \tag{37}$$

Design value of the moment about ZZ axis

$$M_{z\_Ed} = N_{Ed} \cdot ey = 0 \tag{38}$$

D.3.3 Classification of Cross Section

Slenderness parameter

$$\beta_A = \frac{b}{t} = 10 \tag{39}$$

$$\beta_B = \frac{d}{t} = 10 \tag{40}$$

$$\varepsilon = \sqrt{\frac{250}{f_a}} = 1.3 \tag{41}$$

Since this member is non heat treated and unwelded

$$\beta_1 = 9 \cdot \varepsilon = 12.06 \tag{T3}$$

$$\beta_2 = 13 \cdot \varepsilon = 17.42 \tag{T4}$$

$$\beta_3 = 18 \cdot \varepsilon = 24.12 \tag{T5}$$

Since, as in Figure 108

$$\beta_A \leq \beta_1 \tag{42}$$

$$\beta_B \leq \beta_1 \tag{43}$$

Hence, the section is classified as class 1

D.3.4 Reduction Factor for Flexural Buckling – Euler 4

Length of beam

$$L = 495\ mm$$

Effective length factor

$$K = 0.7 \tag{T6}$$

Effective length

$$L_{cr} = K \cdot L = 346.5\ mm \tag{44}$$

Elastic critical load

$$N_{cr} = \frac{\pi^2 \cdot E \cdot I_{yy}}{{L_{cr}}^2} = 201.1\ kN \tag{45}$$

The torsional buckling slenderness parameter

$$\lambda = \pi \sqrt{\frac{E \cdot A}{N_{cr}}} = 30.74 \tag{46}$$

Since it is class 1

$$\eta = 1 \tag{47}$$

$$\lambda_1 = \pi\sqrt{\frac{E}{\eta \cdot f_0}} = 70.25 \tag{48}$$

Imperfection factors

$$\alpha = 0.32 \tag{T7}$$

$$\lambda b_0 = 0 \tag{T8}$$

Slenderness parameter for buckling

$$\lambda b = \sqrt{\frac{A \cdot \eta \cdot f_0}{N_{cr}}} = 0.438 \tag{49}$$

$$\phi = 0.5(1 + \alpha(\lambda b - \lambda b_0) + \lambda b^2) = 0.67 \tag{50}$$

Reduction factor for flexural buckling

$$\chi = \frac{1}{\phi + \sqrt{(\phi^2 - \lambda b^2)}} = 0.85 \tag{51}$$

D.3.5 Reduction Factor for Lateral-Torsional Buckling – Euler 4

Length from pinned point to the point of load

$$L_{cr\_z} = L = 495\ mm$$

Imperfection factor for lateral-torsional buckling

$$\alpha_{LT} = 0.1 \tag{52}$$

$$\lambda_{0LT} = 0.6 \tag{53}$$

$$\lambda_{LT} = \frac{L_{cr\_z}}{i_z} = 43.9 \tag{54}$$

Non-dimensional slenderness

$$\lambda_{LTb} = \lambda_{LT}\frac{1}{\pi}\sqrt{\frac{f_0}{E}} = 0.625 \tag{55}$$

$$\phi_{LT} = 0.5(1 + \alpha_{LT} \cdot (\lambda_{LTb} - \lambda_{0LT}) + \lambda_{LTb}^2) = 0.697 \tag{56}$$

$$\chi_{LT} = \frac{1}{\phi_{LT} + \sqrt{(\phi_{LT}^2 - \lambda_{LTb}^2)}} = 0.995 \tag{57}$$

D.3.6 Buckling Check – Euler 4

$$N_{Rd} = \frac{A \cdot f_0}{\gamma_{M1}} = 35\ kN \tag{58}$$

Since no welds

$$\omega_0 = \omega_x = 1 \tag{59}$$

Bending moment capacity about the y-axis

$$M_{y,Rd} = \frac{\alpha_y \cdot W_y \cdot f_0}{\gamma_{M1}} = 355\ kNmm \tag{60}$$

Bending moment capacity about the z-axis

$$M_{z,Rd} = \frac{\alpha_z \cdot W_z \cdot f_0}{\gamma_{M1}} = 355\ kNmm \tag{61}$$

$$\psi_c = 0.8 \tag{62}$$

$$\left(\frac{N_{Ed}}{\chi_{min} \cdot \omega_x \cdot N_{Rd}}\right)^{\psi_c} + \frac{1}{\omega_0}\left(\left(\frac{M_{y,Ed}}{M_{y,Rd}}\right)^{1.7} + \left(\frac{M_{z,Ed}}{M_{z,Rd}}\right)^{1.7}\right)^{0.6} \leq 1.00 \tag{23}$$

$$N_{Ed} = 11.9\ kN \tag{36}$$

The minimum value for the reduction factor of flexural buckling and lateral-torsional buckling

$$\chi_{min} = 0.85$$

$$\left(\frac{N_{Ed}}{\chi_{min} \cdot \omega_x \cdot N_{Rd}}\right)^{\psi_c} = 0.48$$

Appendix E

Material Information

E.1 Aluminum EN AW 6060F22 T6 Main Beams

Material Model	Standard
Material Source	Not Applicable
Material Source File	
Date Last Updated	2014-04-13-22:35:36
Material Description	Customer defined material properties
Mass Density	0.0000000027 $N \cdot s^2/mm/mm^3$
Modulus of Elasticity	70000 N/mm^2
Poisson's Ratio	0.33
Thermal Coefficient of Expansion	0.000023 1/°C
Yield Strength	170 N/mm^2
Ultimate Strength	215 N/mm^2

E.2 Aluminum 6061 Bricks & assistant wheel

Material Model	Standard
Material Source	Not Applicable
Material Source File	
Date Last Updated	2014-04-13-22:35:36
Material Description	Customer defined material properties
Mass Density	0.00000000271 $N \cdot s^2/mm/mm^3$
Modulus of Elasticity	68900 N/mm^2
Poisson's Ratio	0.33
Thermal Coefficient of Expansion	0.0000236 1/°C
Yield Strength	275 N/mm^2
Ultimate Strength	310 N/mm^2

E.3 Aluminum 6060 Joists

Material Model	Standard
Material Source	Not Applicable
Material Source File	
Date Last Updated	2014-04-13-22:35:36
Material Description	Customer defined material properties
Mass Density	0.0000000027 N·s²/mm/mm³
Modulus of Elasticity	70000 N/mm²
Poisson's Ratio	0.33
Thermal Coefficient of Expansion	0 1/°C
Yield Strength	170 N/mm²
Ultimate Strength	190 N/mm²

E.4 Plastic - PVC (Molded) Wheels

Material Model	Standard
Material Source	Autodesk Simulation Material Library
Material Source File	C:\Program Files\Autodesk\Simulation 2014\matlibs\algormat.mlb
Date Last Updated	2012-07-12-16:45:12
Material Description	Polyvinyl Chloride
Mass Density	1.3E-0.9 N·s²/mm/mm³
Modulus of Elasticity	2757 N/mm²
Poisson's Ratio	0.36
Thermal Coefficient of Expansion	7 1/°C
Yield Strength	31 N/mm²
Ultimate Strength	51 N/mm²

E.5 Steel mild - Joints

Material Model	Standard
Material Source	Not Applicable
Material Source File	
Date Last Updated	2014-04-13-22:35:36
Material Description	Customer defined material properties
Mass Density	0.00000000786 $N \cdot s^2/mm/mm^3$
Modulus of Elasticity	220000 N/mm^2
Poisson's Ratio	0.275
Thermal Coefficient of Expansion	0 1/°C
Yield Strength	207 N/mm^2
Ultimate Strength	345 N/mm^2

Motsvarande beteckningar	Sapa 6060		Sapa 6060 F22[4]		Sapa 6063			Sapa 6063A		Sapa 6005	
Europanormer:											
numerisk beteckning	EN-AW-6060		EN-AW-6060		EN-AW-6063			EN-AW-6063A		EN-AW-6005	
kemiska symboler[1]	AlMgSi		AlMgSi		AlMg0,7Si			AlMg0,7Si(A)		AlSiMg	
USA: Aluminum Association	AA 6060		AA 6060		AA 6063			AA 6063A		AA 6005	
Svenska normer:	SS-EN-AW-6060		SS-EN-AW-6060		SS-EN-AW-6063			SS-EN-AW-6063A		SS-EN-AW-6005	
Tekniska data											
Tillstånd	T4[2]	T6	T4[2]	T6	T4[2]	T6	T66 F25	T4[2]	T6	T6 Massiv profil	T6 Hål-profil
Draghållfasthet[3] t – godstjocklek, mm											
Sträckgräns $R_{p0,2}$, MPa, min.	t ≤ 25 60	t ≤ 3 150 3< t ≤ 25 140	t ≤ 25 65	t ≤ 10 170 10 < t ≤ 25 160	t ≤ 25 65	t ≤ 10 170 10 < t ≤ 25 160	t ≤ 10 200 10 < t ≤ 25 180	t ≤ 25 90	t ≤ 10 190 10 < t ≤ 25 180	t ≤ 5 225 5 < t ≤ 10 215 10 < t ≤ 25 200	t ≤ 5 215 5 < t ≤ 15 200
Brottgräns R_m, MPa, min.	t ≤ 25 120	t ≤ 3 190 3< t ≤ 25 170	t ≤ 25 130	t ≤ 10 215 10 < t ≤ 25 195	t ≤ 25 130	t ≤ 10 215 10 < t ≤ 25 195	t ≤ 10 245 10 < t ≤ 25 225	t ≤ 25 150	t ≤ 10 230 10 < t ≤ 25 220	t ≤ 5 270 5 < t ≤ 10 260 10 < t ≤ 25 250	t ≤ 5 255 5 < t ≤ 15 250
Förlängning A, % min.	t ≤ 25 16	t ≤ 25 8	t ≤ 25 14	t ≤ 25 8	t ≤ 25 14	t ≤ 25 8	t ≤ 25 8	t ≤ 25 12	t ≤ 25 7 10 < t ≤ 25 5	t ≤ 25 8	t ≤ 15 8
Hårdhet (upplysningsvärde)											
Webster B, approx.	5	10	5	12	5	12	13	7	13	14	14
Vickers, approx.	40	60	45	70	45	70	80	50	80	85	85
Värmeledningsförmåga Vid 20°, W/m,°C	190	190	190	190	190	190	190	190	190	170	170
Densitet, kg/dm³	2,7	2,7	2,7	2,7	2,7	2,7	2,7	2,7	2,7	2,7	2,7
	Lämpliga legeringar för **dekorativ anodisering**										
Samtliga legeringar: Längdutvidgnings-koefficient: 23×10^{-6}/°C Elasticitetsmodul: 70 000 MPa Skjuvmodul: 27 000 MPa Poissons tal: 0,33	Alla användningsområden där högsta ytkvalitet är ett önskemål och där styrkan inte är den kritiska faktorn. T.ex. tavelramar, exklusiva möbler.				Alla användningsområden. I denna legering förenas de flesta goda egenskaper. T.ex. möbler, dekorlister.			Vissa bärande konstruktioner såsom segelbåtsmaster, stegar.		Vid krav på hög hållfasthet. T.ex. balkonger, portar, stegar, segelbåtsmaster.	

1) Beteckningarna ska föregås av EN-AW, t.ex. EN-AW-AlMgSi.
2) Draghållfastheten nås efter minst 3 dygns kallåldring efter pressning.
3) Draghållfastheten gäller för sektioner upp till 25 mm godstjocklek. För ytterligare information kontakta Sapa.
4) Legeringsdata enligt Sapa-norm.

Utgåva 2010:1

Aluminum alloys

Description

The material

Aluminum was once so rare and precious that the Emperor Napoleon III of France had a set of cutlery made from it that cost him more than silver. But that was 1860; today, nearly 150 years later, aluminum spoons are things you throw away - a testament to our ability to be both technically creative and wasteful. Aluminum, the first of the 'light alloys' (with magnesium and titanium), is the third most abundant metal in the earth's crust (after iron and silicon) but extracting it costs much energy. It has grown to be the second most important metal in the economy (steel comes first), and the mainstay of the aerospace industry.

Composition (summary)

Al + alloying elements, e.g. Mg, Mn, Cr, Cu, Zn, Zr, Li

Image

Caption

Aluminum can formed both by casting and by deformation.

General properties

Density	2.5e3	-	2.9e3	kg/m^3
Price	* 15.9	-	17.4	SEK/kg

Mechanical properties

Young's modulus	68	-	82	GPa
Yield strength (elastic limit)	30	-	500	MPa
Tensile strength	58	-	550	MPa
Elongation	1	-	44	% strain
Hardness - Vickers	12	-	151	HV
Fatigue strength at 10^7 cycles	21.6	-	157	MPa
Fracture toughness	22	-	35	MPa.m^0.5

Thermal properties

Melting point	475	-	677	°C
Maximum service temperature	120	-	210	°C
Thermal conductor or insulator?	Good conductor			
Thermal conductivity	76	-	235	W/m.°C
Specific heat capacity	857	-	990	J/kg.°C
Thermal expansion coefficient	21	-	24	µstrain/°C

Electrical properties

Electrical conductor or insulator?	Good conductor

Optical properties

Transparency	Opaque

Values marked * are estimates.
No warranty is given for the accuracy of this data

Titanium alloys

Description

The material

Titanium is the seventh most abundant metal in the Earth's crust, but extracting the metal from the oxide in which it occurs naturally is unusually difficult. This makes titanium, third member of the light alloy trio, by far the most expensive of the three (more than ten times the price of aluminum). Despite this, the use of titanium is growing, propelled by its remarkable properties. It has a high melting point (1677 C), it is light, and - although reactive - its resists corrosion in most chemicals, protected by a thin film of oxide on its surface. Titanium alloys are exceptionally strong for their weight, and can be used at temperatures up to 500 C - compressor blades of aircraft turbines are made of them. They have unusually low thermal and electrical conductivity, and low expansion coefficients.

Composition (summary)

Ti + alloying elements, e.g. Al, Zr, Mo, Si, Sn, Ni, Fe, V

Image

Caption

The strength of titanium is exploited in eyeglass frames.

General properties

Density		4.4e3	-	4.8e3	kg/m^3
Price	*	169	-	185	SEK/kg

Mechanical properties

Young's modulus		90	-	120	GPa
Yield strength (elastic limit)		250	-	1.25e3	MPa
Tensile strength		300	-	1.63e3	MPa
Elongation		1	-	40	% strain
Hardness - Vickers		60	-	380	HV
Fatigue strength at 10^7 cycles	*	175	-	600	MPa
Fracture toughness		14	-	120	MPa.m^0.5

Thermal properties

Melting point		1.48e3	-	1.68e3	°C
Maximum service temperature		300	-	500	°C
Thermal conductor or insulator?		Poor conductor			
Thermal conductivity		7	-	14	W/m.°C
Specific heat capacity		520	-	600	J/kg.°C
Thermal expansion coefficient		7.9	-	11	µstrain/°C

Electrical properties

Electrical conductor or insulator?		Good conductor			

Appendix F

Matrices

COMBINATION OF CONCEPTS							
	A	**B**	**C**	**D**	**E**	**F**	**G**
1		x	x	x			
2	x	x	x	x	x	x	x
3	x	x	x	x	x	x	x
4	x	x	x	x	x	x	x

Elimination Matrix

(+) Yes

(-) No

(?) More information is required

CONCEPTS	Meet all requirements	Realizable	Safe	Ergonomic	Easy to use	Comments	Decision
A2	+	+	+	+	+		Keep
A3	+	-				Liquid container	
A4	-					Two directions not possible	
B1	+	+	+	+	+		Keep
B2	+	+	+	+	+		Keep
B3	?	-				Height, Liquid container	
B4	-					Two directions not possible	
C1	+	+	+	+	+		Keep
C2	+	+	+	+	+		Keep
C3	+	-				Liquid container	
C4	-					Two directions not possible	
D1	+	+	+	+	+		Keep
D2	+	+	+	+	+		Keep
D3	+	-				Liquid container	
D4	-					Two directions not possible	
E2	+	+	+	+	+		Keep
E3	+	-				Liquid container	
E4	-					Two directions not possible	
F2	+	+	+	+	+		Keep
F3	+	-				Liquid container	
F4	-					Two directions not possible	
G2	+	+	+	+	+		Keep
G3	+	-				Liquid container	
G4	-					Two directions not possible	

Pugh 1		**Concepts**									
Criteria	Weight	Ref: A2	B1	B2	C1	C2	D1	D2	E2	F2	G2
Ergonomics	5	0	-	0	-	0	-	0	0	0	0
Height	4	0	0	0	0	0	-	-	0	0	0
Risk of Injury	3	0	-	-	-	0	-	+	0	0	0
Weight	4	0	0	0	+	-	0	-	-	0	0
Easy to use	4	0	-	0	-	0	-	-	0	0	0
+		0	0	0	4	0	0	3	0	4	4
0		20	8	17	4	16	4	0	16	16	16
-		0	12	3	12	4	16	12	4	0	0
Sum		0	-12	-3	-8	-4	-16	-9	-4	4	4

Pugh 2		**Concepts**									
Criteria	Weight	Ref: F2	A2	B1	B2	C1	C2	D1	D2	E2	G2
Ergonomics	5	0	0	-	0	-	0	-	0	0	0
Height	4	0	0	-	-	-	-	-	-	0	0
Risk of Injury	3	0	0	-	-	0	0	-	0	0	0
Weight	4	0	0	0	0	0	0	0	0	-	0
Easy to use	4	0	0	-	-	-	-	-	-	0	0
+		0	0	0	0	0	0	0	0	0	0
0		20	20	4	9	7	12	16	12	16	20
-		0	0	16	11	13	8	4	8	4	0
Sum		0	0	-16	-11	-13	-8	-4	-8	-4	0

Appendix G

Project Plan

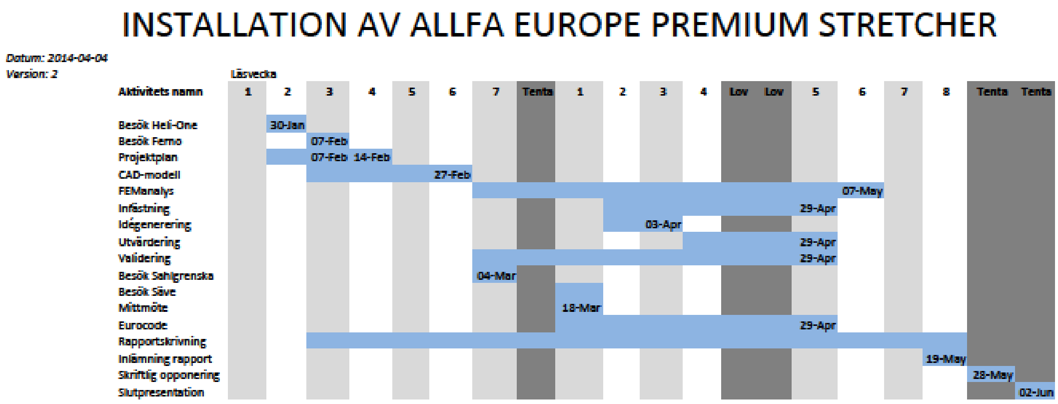

Appendix H

Bill of material

The following pages contain the bill of material.

Appendix I

Drawings

The following pages contain drawings of significant parts of the stretcher.